MASTERARBEIT | MASTER'S THESIS

Titel | Title

Metabolic and Lipidomic Effects of Supplementation with Linseed Oil from Germinated Seeds in C57BL/6 wild-type mice

verfasst von | submitted by

Raphael Brandl BSc

angestrebter akademischer Grad | in partial fulfilment of the requirements for the degree of

Master of Science (MSc)

Wien | Vienna, 2025

Studienkennzahl lt. Studienblatt | Degree programme code as it appears on the student record sheet:	UA 066 838
Studienrichtung lt. Studienblatt | Degree programme as it appears on the student record sheet:	Masterstudium Ernährungswissenschaften
Betreut von | Supervisor:	Univ.-Prof. Mag. Dr. Marc Pignitter

EIDESSTATTLICHE ERKLÄRUNG

Hiermit erkläre ich eidesstattlich, dass ich die vorliegende Masterarbeit selbstständig verfasst und keine anderen als die angegebenen Hilfsmittel verwendet habe. Alle aus ungedruckten Quellen, gedruckter Literatur oder aus dem Internet im Wortlaut oder im wesentlichen Inhalt übernommenen Formulierungen und Gedanken wurden gemäß den wissenschaftlichen Richtlinien zitiert und durch genaue Quellenangabe kenntlich gemacht.

Raphael Brandl

Table of contents

List of illustrations

List of tables

List of abbreviations

ABTS	2,2’-azino-bis-3-ethylbenzthiazoline-6-sulphonic acid
AdipoR1	Adiponectin receptor 1
AJS	Agilent Jet Stream
ALA	α-linolenic acid
APCI	Atmospheric pressure chemical ionization
APPI	Atmospheric pressure photoionization
BAT	Brown adipose tissue
BUME	Butanol/Methanol
cAMP	Cyclic adenosine monophosphat
CID	Collision induced dissociation
CoA	Co-enzym A
CPT	Carnitine palmitoyl transferase 1
DAG	Diacylglycerol
DESI	Desorption electrospray ionization
DPPH	1,1-diphenyl-2-picrylhydrazyl
ESI	Electrospray ionization
FADH	Flavin adenine dinucleotide
GLO	Germinated linseed oil
GP	Glycerophospholipid
HDL	High-density lipoprotein
HFD	High fat diet
HILIC	Hydrophilic interaction liquid chromatography
HSL	Hormone-sensitive lipase
IL-4/10	Interleukin 4/10
IS	Internal Standard
LC	Liquid-Chromatography
LDL	Low-density lipoprotein
LDI	Laser desorption/ionization
LO	Linseed oil
Lys-PC	Lysophosphatidylcholine
Lys-PE	Lysophosphatidylethanolamine
Lys-PI	Lysophosphatidylinositol
Lys-PS	Lysophosphatidylserine
MAG	Monoacylglycerol
MALDI	Matrix-assisted laser desorption/ionization
MAS	Magic angle spinning
M-CPT I	Carnitine palmitoyltransferase I
MSC	Mass Spec Center
MRM	Multiple reaction monitoring
MS	Mass spectrometry
MTBE	Methyl tert-butyl ether
mTORC1	mechanistic Target of Rapamycin Complex 1
NADH	Nicotinamide adenine dinucleotide

NFD	Normal fat diet
NLS	Neutral loss scan
NMR	Nuclear magnetic resonance
P70S6K	ribosomal protein S6 kinase beta-1
PA	Phosphatidic acid
PCA	Principal component analysis
PC	Phosphatidylcholine
PE	Phosphatidylethanolamine
PI	Phosphatidylinositol
PS	Phosphatidylserine
PIS	Precursor ion scan
PKA	Protein kinase A
PLS-DA	Partial least squares discriminant analysis
PUFA	Polyunsaturated fatty acid
QC	Quality control
QQ-Plot	Quantile-quantile plot
QTOF	Quadrupole Time-of-Flight
RPM	Revolutions per minute
SEM	Standard error of mean
SRM	Selected reaction monitoring
SREBP-1	Sterol Regulatory Element-Binding Protein 1
SIMS	Secondary ion MS
S/N	Signal to noise ratio
Sn-3	Stereospecific number
TAG	Triacylglycerol
TIC	Total Ion Chromatogram
TIMSTOF	Trapped Ion Mobility Spectrometry-Time-of-Flight
UCP-1	Uncoupling protein 1
UHPLC	Ultra-high performance liquid chromatography
WAT	White adipose tissue
XIC	Extracted Ion Chromatogram

1 Introduction

Lipid metabolism plays a fundamental role in cellular energy homeostasis, with β-oxidation serving as an essential pathway for the breakdown of fatty acids (Hisanaga et al., 2004). Lipids contain a broad number of individual species, each involved in different metabolic pathways that play essential roles in biological processes such as membrane synthesis, thermoregulation, energy storage, immunoregulatory responses and many more (Cannon & Nedergaard, 2004; Yoon et al., 2021). Fatty acids, originating from the breakdown of stored triacyclglycerols (TAG) via lipolysis, are crucial as they serve as the main structural component in several important membrane lipids like glycerophospholipids (GP) and sphingolipids (SL). In addition, fatty acids serve as an important energy source, as they can be taken up from the circulating plasma by all cells that contain mitochondria. Once inside, they may get degraded into acetyl-CoA, which enters the citric acid cycle providing nicotinamide adenine dinucleotide (NADH) and flavin adenine dinucleotide ($FADH_2$) (E. Xu et al., 2021; Yoon et al., 2021).

Due to the composition of linseed, containing essential linoleic and α-linolenic fatty acids (ALA), dietary fibers and lignans, it is beneficial for the overall health as it decreases the risk of cardiovascular diseases, levels of cholesterol and cancer. Furthermore, it increases blood flow by relaxing smooth muscle cells in arteries. Fatty acids from linseed oil not only serve as storage lipids but also participate in several metabolic mechanisms as structural compounds of cell membranes (Campos et al., 2019). Alterations in diets lead to different lipid profiles and compositions of metabolites. To increase the quality of nutrition, seed germination has been proposed as a cost-effective pretreatment method (Cáceres et al., 2017). Due to its high content of bioactive compounds, germinated linseed oil (GLO) represents a promising area of research, as the germination results in a notable increase in antioxidant activity, total polyphenol and tocopherol content, as well as free fatty acids, causing positive effects to the oxidative stability and shelf-life of linseed oil (LO) (Pointner et al., 2024). The containing polyunsaturated fatty acids (PUFAs) are vital for risk reduction of diabetes, cardiovascular diseases, cancer, depression and other mental health disorders (Shahidi & Ambigaipalan, 2018). However, while the benefits of LO and GLO are known regarding their nutritional profile and antioxidant potential, the specific impact of GLO on metabolic and lipidomic pathways remains

largely unexplored. In particular, less is known about the influence of supplementation with GLO on β-oxidation and its modulation in lipid and metabolite profiles. To gain a comprehensive understanding of these metabolic effects, a combination of lipidomic and metabolomic approaches was applied. Untargeted methods were used to capture a broad range of metabolic changes, while targeted analyses provided precise quantification of key metabolites involved in lipid metabolism. These techniques enabled the identification of several metabolic alterations in mice tissues such as BAT, WAT and liver, offering new insights into how GLO influenced β-oxidation as well as broader changes in lipid and metabolite profiles. Moreover, understanding these metabolic shifts may provide valuable information on how dietary interventions can contribute to nutritional strategies for metabolic disorders. This study aims to investigate these effects and their broader relevance for energy metabolism.

2 Theoretical background

Linseeds are rich in linoleic and α-linolenic acids, as well as dietary fibers and lignans, all of which contribute to various health benefits. These compounds have been associated with risk reduction of cardiovascular diseases and cancer. In addition, they promote vasodilation by relaxing smooth muscle cells, thereby enhancing blood flow (Duarte et al., 2025). Moreover, they serve as structural elements of cellular membranes, function as storage lipids and play essential roles in metabolic processes (Campos et al., 2019). The nutritional value of linseed (*Linum usitatissimum*) is not only due to its high content of essential fatty acids but also because of its vitamins, minerals, proteins and fiber. These seeds consist of approximately 45% oils, 30% fiber and 25% protein, highlighting their diverse nutritional composition and versatility (Pointner et al., 2024). Furthermore, it is widely used as animal fodder and in textiles such as paints, bio-fibers and linoleum flooring. Cold-pressed LO is primarily made up of the PUFA ALA, which plays a noteworthy role in maintaining the balance of the omega-6 to omega-3 ratio, therefore contributing to improved cognitive function, lower cholesterol and the regulation of blood pressure (Farag et al., 2021). Moreover, it enhances the storage stability and shows further health benefits due to the containing tocopherols and phenolic compounds (Li et al., 2018; J. Yang et al., 2021). GLO is used for research, as it has a higher content of bioactive components, after germination (Herchi et al., 2015; Lenihan-Geels et al., 2013).

PUFAs have been extensively recognized for their wide-ranging health benefits, particularly in the prevention and management of various conditions, including cardiovascular diseases such as atherosclerosis, thrombosis, inflammation and sudden cardiac death. Furthermore, they are vital for risk reduction of diabetes, depression, cancer and various other metal health disorders (Shahidi & Ambigaipalan, 2018). A major concern in the food industry is the susceptibility of unsaturated oils, especially those rich in PUFAs, to autooxidation, thus resulting in a relative short shelf life. The oxidative stability is influenced by various factors and their interplay, such as the fatty acid composition and presence of antioxidants (Pignitter et al., 2019; Prescha et al., 2014). To increase the nutritional content and quality of oils, seed germination has been suggested as an economical and environmentally friendly pretreatment method (Cáceres et al., 2017). Germination led to a significant increase in antioxidant activity, as determined by 2,2'-azino-bis-3-ethylbenzthiazoline-6-sulphonic acid (ABTS) and 1,1-diphenyl-2-picrylhydrazyl (DPPH). These changes were accompanied by higher levels of tocopherols and free fatty acids, causing positive effects on the oxidative stability and shelf-life of linseed oil (Pointner et al., 2024). Furthermore, it initiates a metabolic cascade characterized by hydrolysis and energy production, resulting in the degradation of the endosperm and seed coat, which subsequently facilitates the release of bioactive compounds with potential health-promoting properties (Pointner et al., 2024). Studies by Herchi et al., (2014, 2015) have demonstrated that germination can increase the levels of important vitamins, minerals and their associated compounds as well as carotenoids and chlorophyll concentrations in oils. However, it is not yet fully understood whether germination impacts the synthesis of antioxidants, especially specific phenolic compounds, which might also be present in higher concentrations in cold-pressed oils. To address the knowledge gap of the impact of GLO on metabolic and lipidomic pathways, in particular their influence on β-oxidation and the modulation of lipid and metabolite profiles, this study enables a comprehensive analysis of metabolic alterations and allows for detailed assessment.

Modern 'omics' technologies, including lipidomics and metabolomics, are used to explain various processes and their effects in more detail. These enable precise analysis of lipids and metabolic products to capture complex biochemical changes and relationships in the body. Multiomics approaches can provide a more comprehensive

understanding of the data stream compared to single omics studies, from disease origin, genetic, environmental or developmental nature, to consequences and significant interactions (Hasin et al., 2017). In the context of this study, integrating multiomics allows a comprehensive characterization of metabolic pathways within BAT, WAT and liver. Given the rich content of bioactive compounds, it is essential to understand their effects on a biochemical level. Therefore, both untargeted and targeted approaches were applied, whereby untargeted metabolomics and lipidomics provide a broad overview of substances. Targeted methods allowed for the precise quantification of specific compounds, which are also involved in β-oxidation. In addition, general changes in lipid and metabolite profiles can be seen. Understanding how bioactive compounds or rather diets, especially linseed oil from germinated seeds, influence lipid composition and metabolic regulations is crucial for elucidating their potential health advantages.

2.1 Metabolomics

Metabolomics, a subfield of systeomics, is a scientific discipline capable of analyzing thousands of metabolites, their profiles and metabolic phenotypes in biological samples. Due to ongoing developments in bioinformatics and analytical methods, metabolomics has emerged as an innovative diagnostic tool in biomedical and clinical research. Dynamic equilibrium, meaning that biological organisms are changing over time due to several exogenous impacts, which could be environmental influences or treatment of diseases by using pharmacological medicine, is a hallmark of every living system. Imbalances can lead to disturbances of the biological system including tissue and organs, and to understand those impacts and changes regarding the complex living systems a holistic approach, referred to systeomics, consisting of proteomics, transcriptomics, genomics and metabolomics, is utilized, whereby priority is given to behavior prediction based on structural and dynamical factors as well as biological components and their interaction. Genome sequencing is a result of genomics, which further initializes the progress of transcriptomics and proteomics, whereby the first focuses on the determination of mRNA transcription and the second on protein abundance. Research in the latter led to development in metabolomics. As a result, biological information within a living system progresses from genes to transcripts and transitions through proteins to metabolites (Bujak et al., 2015). The metabolome is a chemical

representation of a molecular phenotype, as observed changes affect alterations of the system biology subfields. In addition, the metabolic profile composition mirrors the current organism status as well as the predisposition to specific behaviors. Complementary, the biochemical spectrum might be a promising key point between the phenotype-genotype gap and therefore it is a dominant technique in systeomics and biomedical as well as toxicological and pharmaceutical research (Gowda et al., 2008). Initializing a new era in metabolomics, Horning & Horning, and Pauling et al., were pioneers in 1971 with their studies, which were about determining a specific set of metabolites in biological liquids instead of detecting a single metabolite. Ongoing research and continuous improvement of technologies led to development in biostatistics and analytics providing a more attainable metabolite identification and detection in blood and tissue or rather general sophisticated biological extracts (Gowda et al., 2008). Over the last decades modern approaches were developed, among other things metabonomics, which was defined by Nicholson et al., 1999, as a quantitative assessment of the dynamic, multiparametric metabolic effects in biological organisms in response to genetic alterations and pathophysiological triggers. Moreover, in 2001 Fiehn O. described metabolomics as metabolites in a system which undergo a comprehensive and quantitative analysis. In addition, it's worth to note that the subtle difference between these two "omics" is more linguistic than technical. Although there are limitations in metabolomics, it is still a useful tool in laboratory diagnostics as metabolic changes occur earlier than other specific symptoms, which leads to better understanding of complex pathomechanisms for instance in cancer, diabetes and cardiovascular diseases. In addition, metabolomics might be mandatory for the identification of prognostic and diagnostic disease biomarkers (Gowda et al., 2008). Metabolic profiling, fingerprinting and footprinting are established research techniques in metabolome analysis. The first method is a targeted strategy with emphasis on detection and quantification of predefined metabolites sharing comparable properties or pathways, such as amino and organic acids or rather β-oxidation and citric acid cycle. The metabolic fingerprinting as a unique pattern is an untargeted method unbiased by any preselected assumptions and previous knowledge of determined metabolites, which defines metabolome changes at certain state of an organism in cell or tissue. Therefore, this method, which is mainly used to compare two subject groups (healthy/non healthy),

primarily seeks to identify and qualify a maximum number of metabolites in biological fluids, whereby there is no universal analytical option to determine the whole ratio of metabolites due to the physicochemical diversity and complexity (Beckonert et al., 2007; Ellis et al., 2007). The metabolic footprint or exo-metabolome, often used in microbiological studies, which offers an integrative interpretation of the metabolic network within a living system, is a slightly different approach as it does not focus on intracellular metabolites but on compounds released or unutilized by cells within defined media (Mapelli et al., 2008). Due to the mentioned complexity and diversity, it is common that in both untargeted and targeted more than one analytical platform is used, whereby nuclear magnetic resonance (NMR), suitable for all detected compounds with hydrogen atoms, and MS are the predominate techniques in metabolomics. NMR is a rapid, unbiased, nondestructive approach with a high throughput, which requires barely any sample pretreatment and when used with magic angle spinning (MAS) it is also suitable for tissue analysis. Unfortunately, NMR lacks sensitivity and has some difficulties with signal noises and overlapping. In comparison the MS, which could be coupled to several separation techniques like LC, GC or capillary electrophoresis (CE), has a high sensitivity and wide identification range. Furthermore, detected metabolites can easily be identified through various databases. Drawbacks are low quantification and reproducibility (Lindon & Nicholson, 2008). Nonetheless MS found a wider utilization in metabolome research than the NMR, although it requires a higher sample volume. LC-MS, which is primarily dependent on the stationary phase's chemistry within a chromatographic column, is often used to analyze biological fluids like urine, blood or extracts from tissue, as it is suitable for thermally unstable, non-volatile compounds, that can be high or low in their molecule weight (Becker et al., 2012). In addition, those compounds have a wide range of polarity. Ensuring a broader coverage of the metabolome during LC-MS, a reverse phase column and ESI are utilized to separate metabolites, both in positive and negative mode, whereby it is not fitting for hydrophilic metabolites as the reverse phase separation is meant for compounds with low or medium polarity (Spagou et al., 2010). Furthermore, the separation power and sensitivity are impacted due to the column's dimensions and particle sizes, which are normally 4.6mmx150mm and 5 µm. These limiting factors can be compensated by using a hydrophilic interaction liquid chromatography (HILIC) column and ultra-high

performance liquid chromatography (UHPLC) with a dimension of 2.1mm inner diameter and a particle size of 2 µm (Kind et al., 2009). Metabolomics works also with tissue samples instead of biological fluids although it is not common due to difficult sample collection and pretreatment, as they need to be homogenized additionally before centrifuging (Bujak et al., 2015). Normally, there is a higher detection of proteins than metabolites but nevertheless there are lots of studies in the metabolomics area, like the publication by Huang et al., (2013), who conducted untargeted metabolomics research to determine metabolites out of 50 hepatocellular carcinoma patients. Hereby carcinoma tissue, non-carcinoma tissue and adjacent noncancerous tissue were analyzed. The measurement was performed in negative and positive mode using UHPLC coupled with linear ion trap quadrupole Orbitrap MS. The samples were prepared via homogenization and deproteinization. To identify substances, MS/MS spectra as well as spiked authentic standards were analyzed, and several databases were combed through, resulting in 109 identified compounds, among other things amino acids or substances like malate and fumarate which are part of the tricarboxylic acid cycle. In summary, the authors linked the alterations in concentration of the determined compounds with the biochemical pathways, therefore explaining the biochemical reactions occurring during hepatocellular carcinoma. In conclusion, metabolomics provides detailed insights into the biochemical complexity of living organisms and therefore offers significant potential for advanced biomedical research. Considering the physicochemical diversity of metabolites and complexity of biological systems, adopting a multiplatform metabolomics method is highly advisable. To provide a holistic view and taking into account the sensitivity of analytical techniques a multivariate data analysis is required to examine all identified metabolites comprehensively. Future techniques and advancements enhance the way for specific pathways and the ability to comprehensively analyze metabolic profiles. The present study aims to investigate the metabolomic effects of GLO, with a special focus on its influence on β-oxidation, offering new insights into lipid metabolism and its modulation.

2.2 Lipidomics

Lipids are highly complex, important components of cellular membranes and lipid-based particles. These include micelles or lipoproteins such as high-density lipoprotein (HDL) and low-density lipoprotein (LDL). They also serve as cell barriers, signal stores and are an integral component of membrane structures. Furthermore, lipids play a central role in energy storage, particularly in the form of TAG. A typical analysis of lipids contains several steps, such as proper sample preparation and storage, lipid extraction via Bligh and Dyer, Folch, butanol/methanol (BUME), or the methyl tert-butyl ether (MTBE) method, mass spectrometry (MS) data acquisition, and the processing of the data. For proper quantitative lipidomics analysis, the addition of internal standards is crucial (K. Yang & Han, 2016). Originally introduced by Eugene G. Bligh and William J. Dyer through studies of lipid degradation in frozen fish, the Bligh and Dyer method is a very effective, consistent and rapid option to extract and purify lipids from biological substances. Further it does not involve any harmful procedures. The mixture of chloroform and methanol is homogenized with tissue and MS grade water so that a combinable system is formed. Subsequently, the homogenate is formed into a chloroform and a methanolic layer, whereby the first one contains all the lipids and the second one all the non-lipid components, such as carnitines. For purification only the chloroform layer is isolated. Although the method was applied to fish muscle, it is still applicable to other tissues (Bligh & Dyer, 1959). The individual steps can be seen in the subsequent flowchart.

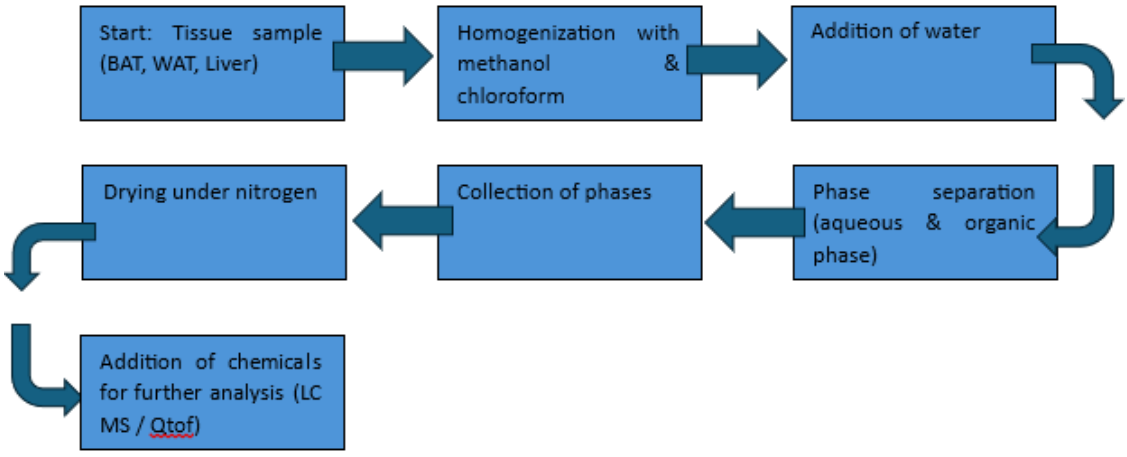

Figure 1: Schematic overview of the extraction procedure (Bligh & Dyer, 1959).

Before there was the Bligh and Dyer extraction Jordi Folch-Pi created a method for the lipid-isolation and purification from animal tissue, which was named after him (Folch et

al., 1957). It also uses a solvent system consisting of chloroform, methanol and water v/v/v (8:4:3). This major contribution to lipidomics changed the standard for lipid biochemistry as there only was the method after Bloor, which was very time consuming and not as effective as Folch's method since lipid extracts still contained non lipid components after several successive steps. Furthermore a higher amount of chemicals were mandatory as this procedure used ethanol, ether, petrolether and chloroform (Eggers & Schwudke, 2016). Lipid extraction methods vary in efficiency and selectivity, with MTBE offering high throughput due to its phase separation behavior, where lipids predominantly accumulate in the top layer. On the other hand, the solution houses a notable number of liquid-based components that might transfer water soluble impurities. Following lipid extraction, various preparatory steps can enhance MS analysis. For instance, derivatization is particularly beneficial when lipids lack distinct fragmentation patterns in tandem MS, which can otherwise limit the specificity and sensitivity of shotgun lipidomics. Hereby important functional groups of the substances are chemically tagged.

The second optional procedure is important for a directly infused shotgun practice as there is no need for chromatography to separate or enrich the substance before the MS analysis. This can be accomplished through chemical approaches, such as base hydrolysis or physical techniques like liquid-liquid partitioning. While the hydrolysis is to concentrate sphingolipids which are low in their abundance from complex, high-abundance glycero- or phospholipids, the partitioning is to separate organic from polar fractions. In modern MS several ionization techniques are frequently used. Those are: Electrospray ionization (ESI), Desorption electrospray ionization (DESI), Matrix-assisted laser desorption/ionization (MALDI), Atmospheric pressure chemical ionization (APCI), Atmospheric pressure photoionization (APPI) and secondary ion MS with gold or silver ions as primary ions (SIMS) (K. Yang & Han, 2016). ESI gained more and more significance as it is a tool for structural investigations of biochemical compounds. Furthermore, it can be used for quantitative data points, screening amino and fatty acid errors and malfunctions in the metabolism of purine and pyrimidine (Ho et al., 2003). While ESI generates ions from solutions, DESI, which was originally introduced in 2004, produces ions from objects. Those ions can be directly sprayed on any surface without vacuum requirements. Additionally, barely any sample preparation is needed (Morato & Cooks,

2023). MALDI is a great tool in lipid biochemistry, enabling simultaneous identification and detection of biomolecules. Notably, MALDI-imaging MS (MALDI-IMS) provides spatial visualization of biological substances without the need for extraction or labeling (Zaima et al., 2010). Another widely utilized ionization technique is APCI, known for its simplicity and effectiveness in analyzing diverse lipid classes, especially neutral molecules like carotenoids and TAGs (Byrdwell, 2001). In lipidomics, several tandem MS mechanisms exist, such as product ion scan, precursor ion scan (PIS) and neutral loss scan (NLS), all contributing to the targeted identification of lipid species (Plumb, 2023; K. Yang & Han, 2016). Tandem MS or MS2 allows the fragmentation of selected m/z features through gas-phase ion activation. The resulting fragment ions support metabolite structure analysis (Heiles, 2021). A different but also practical method used in targeted analysis is the non-scanning selected or multiple reaction monitoring (SRM/MRM). This technique utilizes two static mass detectors to focus on a specific fragment ion, which applies to devices such as triple quadrupole (QQQ) MS. The union of the mass to charge ratio (m/z) from precursor and fragment is named “transition”. MRM refers to the process where several parallel transitions are acquired (Junot et al., 2014). Unless there is an internal standard (IS) the spectral data needs to be deisotoped after the data is captured to adjust the impact of the isotopic cluster presence on monoisotopic peak intensities. LC-based lipidomics also need a calibration curve for individual lipids. Depending on the approach which might be LC-MS, shotgun or imaging, the characterization and quantitative analysis of solely species is the next step. The outcome of this data is further used for bioinformatic purposes to understand the crucial role of fat metabolism, its health regulations, and the resulting advancements in biomedical science (K. Yang & Han, 2016). Due to the high complexity of biological fatty extracts and the big variation of lipid classes and subclasses, it is important to reduce the intricacy of those extracts for a better characterization and quantification to obtain a certain reliance and accountability. While shotgun lipidomics is a high throughput method, missing a pre-chromatographic differentiation at the cost of the lipid complexity, which is normally reduced during analytical preparation or during MS analysis, LC-MS uses separation techniques and further enhances the concentration of low abundance species (X. Han et al., 2012; Y.-Y. Zhao et al., 2014). Besides the difference on how the complexity of lipids is decreased, LC and Shotgun also differ in their data

result and analysis. The former includes not only Total Ion and Extracted Ion Chromatograms (TIC / XIC) but also mass spectra like MS/MS data involving SRM or rather MRM. An important variable in chromatograms is the retention time, which is often used to identify the investigated lipids. To quantify the substances LC mostly examines peak areas, whereas shotgun utilizes ion peak intensities. The temporal limitations induced by the “on the fly” nature of chromatographic analysis significantly restrict the amount of chosen precursor ions that can be exposed to fragmentation during a single LC throughput unlike the shotgun technique. Lipids are identified through product ion spectra or building block-related NLS/PIS whereby the latter is way more efficient as there is only a small need of NLS/PIS spectra but a high amount of product ion spectra to identify numerous lipid classes (K. Yang & Han, 2016). Even though the two approaches differ in many features, they also share mainly 3 aspects. The first one is that ESI as well as MALDI-MS are suitable, although the second one is not that often used as ESI and further utilized off-line, which means that the LC and MALDI-MS are used separately and not connectively, as would be the case with ESI. The second common feature is the compatibility to ion mobility MS (Paglia et al., 2015). Last but not least after the lipids are identified and quantified the same bioinformatic tools can be implemented (Checa et al., 2015). In the context of this study LC-MS/MS analysis was performed using a Shimadzu LCMS-8040 (QQQ) system with ESI and an LCMS 6546 (QTOF) from Agilent. A combination of the following bioinformatic tools was applied: Skyline, for quantitative analysis and MZmine for feature detection and annotation.

2.3 Lipid metabolism

2.3.1 Lipid absorption and digestion

The absorption and digestion of lipids play an essential role in maintaining energy homeostasis. Moreover, lipids play a crucial role in cellular and structural integrity, enabling membrane stability and functionality. Efficient digestion is vital for overall health as it ensures the absorption of numerous nutrients like fat-soluble vitamins (Omer & Chiodi, 2024). Fatty acids can be sorted into 3 divisions: short-chain fatty acids (SCFA) with less than 6 carbons attached, middle-chain fatty acids (MCFA) with aliphatic tails of 6-12 carbons and long-chain fatty acids (LCFA) with more than 12 carbons. Together with their corresponding ligands they regulate various functions and contribute to cholesterol transport and biosynthesis, thermoregulation and inflammatory responses. The digestive process occurs in three main phases, starting in the oral cavity with mastication. Lingual lipase is secreted in the oral cavity but is not active until it reaches the acidic environment of the stomach. The food bolus travels down the esophagus into the stomach, where it triggers the release of gastric lipase from chief cells in the fundus, initiating the partial hydrolysis of TAG into DAG and free fatty acids. After the pre-digestion the main breakdown appears in the small intestine via the pancreatic lipase and colipase, which further cleave lipids into fatty acids and monoacylglycerides (MAG) (E. Xu et al., 2021). As a reaction to the hormone cholecystokinin, micelles are formed, by combining fatty acids with bile salts, released from gallbladder to transport lipids across the intestinal membrane. Nutrients can be absorbed across the apical membrane of enterocytes either through passive diffusion or via protein-mediated transport in the distal duodenum and jejunum (see figure 2) (Iqbal & Hussain, 2009). After absorption, lipids are carried as chylomicrons into the lymphatic system before entering the bloodstream, where they provide energy for several cellular functions, like the construction and maintenance of cell membranes, bile acid synthesis, steroid hormone synthesis, and lipoprotein transport, whereby any excess fat serves as a reserve in cytoplasmic lipid droplets (Omer & Chiodi, 2024). Depending on the efficiency of luminal mixing, the uptake of substances in the gut is determined by the amount that reaches the brush-border membrane. The unstirred water layer, a permeability barrier between the digesta and brush border, plays a significant role in membrane transport because of

its regulating functions, which is about the rate at which rapidly penetrating solutes cross the membrane (E. Xu et al., 2021).

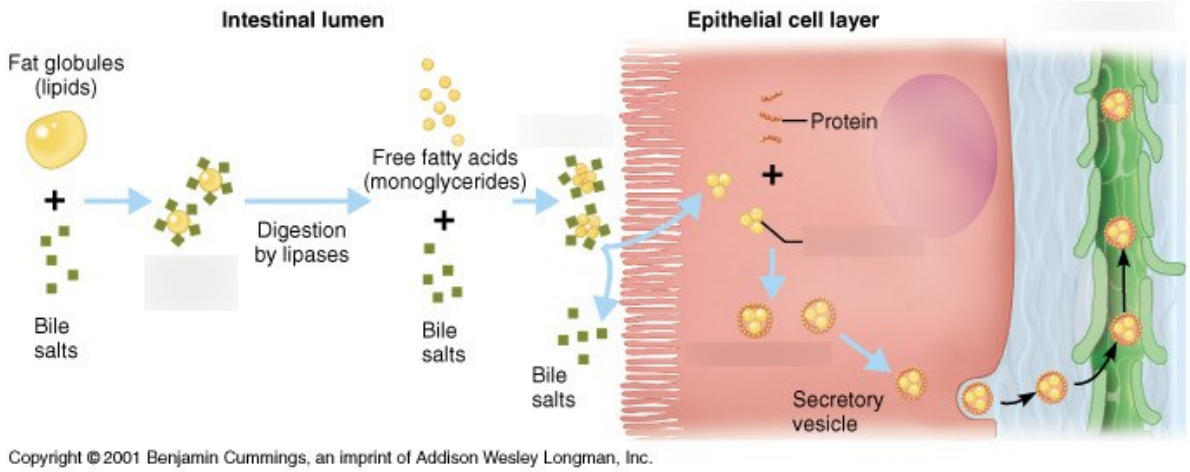

Figure 2: Steps of the intestinal lipid absorption. From: Cummings B., 2001, an imprint of Addison Wesley Longman, Inc.

2.3.2 Lipid metabolism

A crucial step in the *de novo* synthesis is the transformation of carbohydrates into pyruvate through glycolysis. Afterwards, acetyl-CoA is formed in the mitochondria due to the decarboxylation of pyruvate (E. Xu et al., 2021). Nearly all naturally occurring fatty acids indicate an even number of carbon atoms, as the malonyl-CoA, which is generated by the acetyl-CoA carboxylase, is prolonged by 2 carbons at a time (E. Xu et al., 2021). It is important that acetyl-CoA must be carried to the cytosol, where the fatty acid synthesis takes place. To generate cytosolic acetyl-CoA, citrate is extracted from the citric acid cycle. Of note, citrate is formed by the condensation of acetyl-CoA with oxaloacetic acid, which in the end is taken back as malic acid to the mitochondria. It continues with the transport of acetyl-CoA through the inner mitochondria membrane into the cytosol, where it is separated into oxaloacetate and acetyl-CoA via the ATP-citrate lyase (Ferré & Foufelle, 2007). The main storage form and therefore the main energy source are TAGs, which are generated during lipogenesis. They are also an important part of phospholipids as they enhance cell membranes by creating phospholipid bilayers. Fatty acids originate from the breakdown of stored TAGs through lipolysis. Because of the natural hydrophobic chemistry of lipids, they rely on the binding to plasma albumin. However, the number of binding sites of albumin is restricted by the concentration of fatty acids in the plasma. Fatty acids can be taken up from the circulating plasma by all

cells that contain mitochondria. Once inside, they serve as an energy producing factor, because of their degradation into acetyl-CoA, which enters the citric acid cycle, generating NADH and $FADH_2$. These electron carriers then feed into the electron transport chain, leading to the production of ATP, water and CO_2 (E. Xu et al., 2021). The first step in this process is mitochondrial β-oxidation, initiated by long chain-acyl-CoA synthetase, which activates fatty acids for further metabolic breakdown. To enter metabolic pathways, acyl-CoA synthetase initiates the thio-esterification of fatty acyl-CoA esters in the presence of adenosin triphosphate (ATP) and magnesium ions. This catalyzation is split into two steps with an adenylation in the first half, where inorganic pyrophosphate is released while fatty acyl-AMP is formed. The subsequent step is about the replacement of AMP through CoA and the resulting generation of a thioester bond and fatty acyl-CoA (Hisanaga et al., 2004). In humans, long-chain acyl-CoA synthetases have been found in several cellular compartments like in the plasma and mitochondrial membranes, peroxisomes and endoplasmic reticulum (Mashek et al., 2004). Acyl-carnitine esters, formed by L-carnitine enable the passage of long and medium-chain fatty acyl-CoA esters across the mitochondrial membrane, catalyzed by L-carnitine acyltransferases, which facilitate the reversible transfer of acyl groups to L-carnitine. Palmitoyltransferase 1 (responsible for the transport through the outer mitochondrial membrane) and 2 (responsible for the transport back into the inner part) as well as carnitine-acylcarnitine translocase play a crucial role in the L-carnitine system, whereby the latter helps maintaining the cytosolic pool of free L-carnitine by exchanging acyl-carnitine esters for free L-carnitine. Generally, mitochondrial β-oxidation involves four key reactions, whereby the first step is catalyzed by a very long-chain acyl-CoA dehydrogenase and the last three steps are initiated by the mitochondrial trifunctional protein complex. Therefore, the degradation of fatty acids is hierarchical, starting with the initial catalyzation of fatty acyl-CoA dehydrogenase, leading to an oxidation of the saturated chain and production of 2-enoyl-CoA ester. This oxidation also facilitates the production of $FADH_2$ from FAD. The second step in the mitochondrial β-oxidation is the formation of 3-hydroxy-acyl-CoA ester, which is initiated by the enoyl-CoA hydratase. 3-hydroxyacyl-CoA dehydrogenase catalyzes the third step, which is the production of NADH from NAD^+. In the end, acetyl-CoA and an acyl-CoA ester are generated by the β-ketothiolase catalyzing the thiolytic breakdown of 3-ketoacyl-CoA. The resulting acetyl-

CoA molecules feed into the citric acid cycle, and NADH and $FADH_2$ produced during β-oxidation contribute to ATP synthesis via the electron transport chain, highlighting the critical role of β-oxidation in cellular energy metabolism (Adeva-Andany et al., 2019). While β-oxidation is essential for the catabolic cleavage of fatty acids to produce energy, the transport and synthesis of these acids are equally important for maintaining cellular homeostasis. While the transport of fatty acids from plasma to brain across the blood-brain barrier is dependent on the carbon chain length, the synthesis occurs in central nervous cells, supporting the maintenance and production of phospholipids that are necessary for organelles and cell membrane integrity (Tsuji, 2005). For example, fatty acids derived from TAGs released in adipose tissue or from dietary fat intake are distributed to various cells, functioning as an energy source for muscle contraction and further for systemic metabolism (E. Xu et al., 2021). In conclusion, the dynamic interactions between synthesis, transport, storage and degradation set the foundation of cellular energy metabolism, supporting structural integrity and proper physiological function. Table 1 roughly summarizes the individual steps, their functions and the individual area where it takes place.

Table 1: Key processes during the fatty acid metabolism

Process	Function	Area
De novo synthesis	Metabolic processing of carbohydrates into fatty acids	Adipose tissue / liver (E. Xu et al., 2021)
Lipogenesis	Storage of TAGs	Adipose tissue / liver (E. Xu et al., 2021)
Lipolysis	Degradation of TAGs within circulating plasma	Adipose tissue (E. Xu et al., 2021)
β-oxidation	Breakdown of fatty acids	Mitochondria (E. Xu et al., 2021)
Citric acid cycle	ATP production from acetyl CoA	Mitochondria (Adeva-Andany et al., 2019)
Transport to brain	Supply of fatty acids for membrane synthesis	Central nervous cells and blood brain barrier (Tsuji, 2005)

2.3.3 Physiological roles of carnitines

Carnitine, a low-molecular-weight compound, present in nearly all animal species and plants, can be endogenously synthesized from lysine and methionine, as well as acquired from dietary intake (Hoppel, 2003). Carnitine (3-hydroxy-4-N-trimethylaminobutyrate) commonly found as free carnitine (80-90%) or bound to several acyl groups (10-20% short-chain acylcarnitines/ <5% long-chain acylcarnitines) has been shown to be distributed across various mammalian tissues such as heart, kidney, skeletal muscle and liver, which is also part of the tissues investigated in this thesis. The main role of carnitine, respectively the biological active form L-carnitine is the transport of long-chain fatty acids from the cytosol to the mitochondria, where β-oxidation takes place (Gnoni et al., 2020). Further important functions of the amino acid derivative are the regulation of the acyl-CoA to free CoA ratio, facilitation of branched-chain amino acid metabolism, peroxisomal fatty acid oxidation, elimination of excess acyl groups, reduction of lactate production and the maintenance of the membrane integrity (Gnoni et al., 2020; Hoppel, 2003). Carnitine remains metabolically unchanged and is therefore excreted in its free form in urine, although parts of it might not be absorbed in the small intestine but completely degraded by bacteria in the large intestine leading to the production of trimethylamine, which subsequently undergoes oxidation in the liver after it is absorbed by enterocytes, resulting in the generation of trimethylamine-N-oxide (Koeth et al., 2013). L-carnitine, found in red meat, fish, poultry and milk, has been proposed as a treatment for heart failure, weight loss and angina due to its help in reduction of oxidative stress (Pekala et al., 2011). The biosynthesis of L-carnitine begins with a post-translational methylation of a lysine residue bound to specific proteins. Catalyzed by the methyltransferase methyl groups are transferred from S-adenosylmethionine to form 6-N-trimethyllysine with S-adenosylhomocysteine as a byproduct. After lysosomal proteolytic release of free 6-N-trimethyllysine it is hydroxylated by the dioxygenase producing 3-hydroxy-6-N-trimethylysine. Enzyme 3 (see figure 3) then breaks down this metabolite into glycine and 4-N-trimethylaminobutyraldehyde, which follows dehydrogenation by the 4th enzyme, resulting in 4-N-trimethylaminobutyrate, also known as γ-butyrobetaine. Through hydroxylation via the γ-butyrobetaine dioxygenase, which is strictly limited to kidney, liver and brain, L-carnitine is produced (see figure 3) (Ferreira & McKenna, 2017).

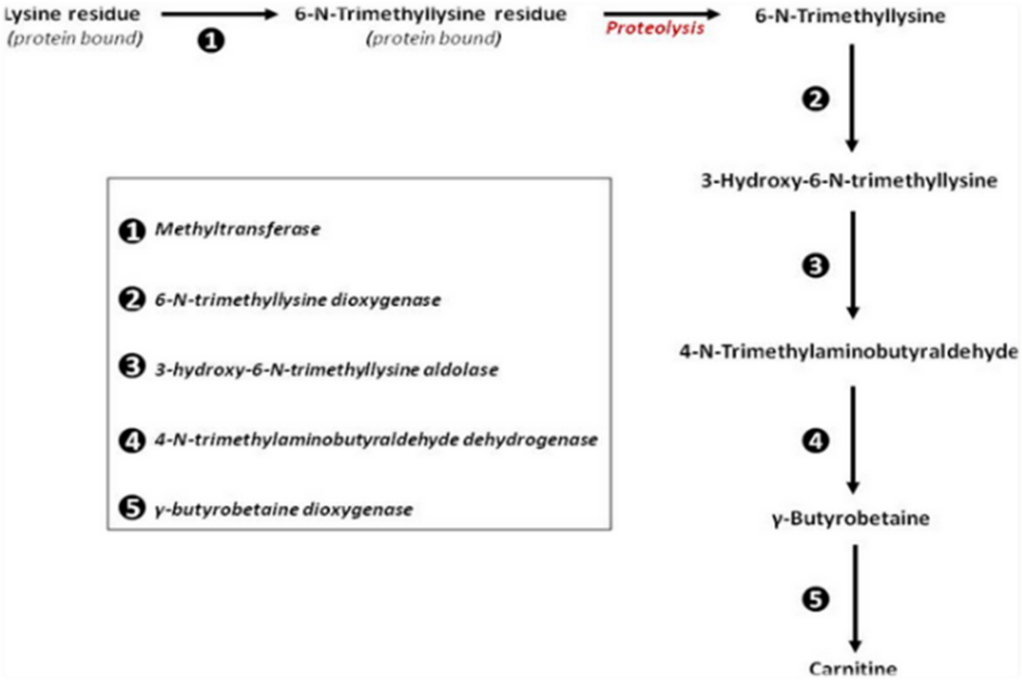

Figure 3: L-Carnitine biosynthesis. From: (Ferreira & McKenna, 2017)

2.3.4 Physiological roles of BAT and WAT

BAT serves the critical function of transferring energy derived from food into heat. Therefore, regarding the thermogenesis, which is centrally modulated through a pathway originating in the hypothalamus, it is indispensable for non-shivering and cold acclimation, norepinephrine-induced thermoregulation. Both the thermogenic activity and the resulting reduction in metabolic efficiency are physiologically significant, as the heat producing mechanism does not occur in the absence of BAT. Norepinephrine, released from sympathetic nerves, regulates the recruitment procedure that leads to an upregulated thermogenic capacity, as well as the acute heat production, which is activated as soon as the organism requires extra warmth, e.g. postnatally, during the onset of fever and during the awakening from hibernation. In addition, feeding per se also stimulates BAT activity, especially through various diets that share the characteristic of being low in protein quantity, leading to a leptin-dependent, hypothalamic controlled, activation. This process can also be described as metaboloregulatory thermogenesis resulting in oxidation of significant quantities of glucose and lipids. Marked by its characteristic uncoupling protein-1 (UCP-1) the evolutionary emergence of BAT was a fundamental factor in the adaptive success of mammals, as the thermogenic capacity plays a vital role in neonatal survival. Moreover, it facilitates prolonged activity in frigid

conditions (Cannon & Nedergaard, 2004). When the organism is exposed to cold temperatures, norepinephrine-induced stimulation of thermogenesis takes place. The messenger then activates cyclic adenosine monophosphate (cAMP) involving an enzyme cascade, consequently inducing protein kinase A (PKA), ensuing the stimulation of the key enzyme hormone-sensitive lipase (HSL). This enzyme facilitates the degradation of TAG droplets, causing a release of free fatty acids, which are converted by the acyl-CoA synthetase to the active form acyl-CoA, and further into acyl-carnitine by the highly expressed enzyme in BAT and WAT, carnitine palmitoyltransferase I (M-CPT I) (muscle isoform) (Esser et al., 1996). With the help of the carnitine transporter, acyl-carnitine is transferred into the mitochondria and with the help of CPT II reconverted to acyl-CoA. Once inside, the β-oxidation breaks down fatty acids, generating acetyl-CoA, that enters the citric acid cycle enabling the production of FADH and NADH. These two electron carriers are later oxidized within the electron transport chain, eventually via oxygen utilization, facilitating the pumping out of protons and formation of a proton-motive force across the mitochondrial membrane, driving the protons back into the matrix through the UCP I. Therefore, the energy is directly released as heat driving the thermogenesis, rather than producing ATP (see figure 4) (Cannon & Nedergaard, 2004). WAT, one of the largest organs in human body, plays a crucial role in fat metabolism and energy homeostasis, as it not only secrets hormones and metabolites but also deposits excess energy and releases fatty acids when energy is required. Furthermore it is involved in inflammatory processes and essential for maintaining glucose homeostasis (Heinonen et al., 2020; Trayhurn & Beattie, 2001). To prevent TAG accumulation in other organs and for metabolic well-being a healthy adipose tissue that can expand in a healthy manner is important. As mentioned before, mitochondria are central to key functions in adipose tissue. Therefore, a reduction in mitochondrial activity within WAT contributes to obesity-related metabolic diseases. Dysfunctions of mitochondrial activities in an obesity state involve oxidative processes as well as the reformation and enlargement of adipose tissue through enlistment and progression of adipocyte progenitor cells, leading to a long term negative impact on the whole body metabolic health (Heinonen et al., 2020). The discovery of leptin, a key hormone in energy regulation, mainly produced by WAT, marked a fundamental shift as it has endocrine functions. The proteohormone is just one of many bioactive compounds produced by white fat tissue, such as

angiotensinogen, adipsin, adiponectin, retinol binding protein, acylation stimulating protein, tumor necrosis factor α, interleukin 6, plasminogen activator inhibitor 1 and tissue factor. While some of those are linked to vascular hemostasis, others participate in lipid metabolism or act as inflammatory cytokines. Overall, WAT is increasingly acknowledged as an active secretory and endocrine organ, functioning as regulating role that extend well beyond its traditional function of lipid storage (Trayhurn & Beattie, 2001). In comparison to BAT which has multilocular adipocytes, WAT primarily consists of densely packed, spherical, large adipocytes, also referred to as unilocular fat cells, whereby their size varies typically in a range of approximately 30 to 130 µm, depending on their lipid content. Larger adipocytes generally correlate to greater metabolic activity and higher secretion of chemo attractants for immune cells (Skurk et al., 2007). In fully differentiated adipocytes, a large lipid droplet occupies nearly the whole cell volume, bounded solely by a lipid monolayer, enriched with several structural proteins. Therefore, for maintaining an intact fat cell and tissue structure, a robust extracellular connective tissue framework is mandatory (Ohsaki et al., 2009; Wronska & Kmiec, 2012).

To sum up, BAT and WAT have distinct but complimentary metabolic functions. While the first one is essential for thermogenesis, converting energy into heat via the carnitine-dependent fatty acid metabolism involving the mitochondrial UCP-1, white fat tissue plays a vital endocrine role, not only highlighting important functions such as energy storage, lipid metabolism regulation or balancing the glucose and energy status, it also secretes key hormones like leptin. In addition, dysfunctional mitochondria in WAT contributes to the development of obesity-related metabolic disorders.

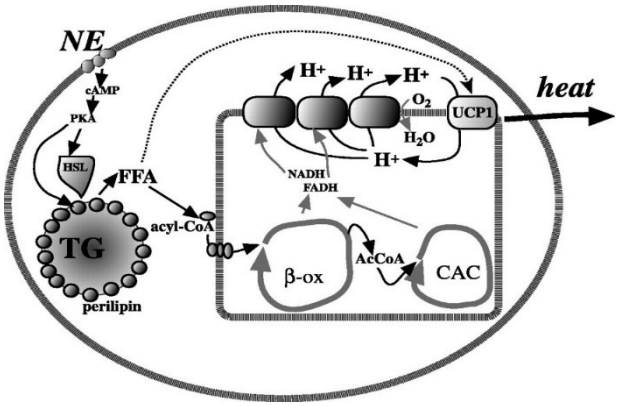

Figure 4: Molecular mechanisms of thermogenesis in BAT (Cannon & Nedergaard, 2004))

2.4 Lipids of interest

Among the various lipids identified in this study, a particular focus lays on both well characterized and less known lipid species. Supplementation with linseed oil from germinated seeds is likely to result in the presence of additional bioactive compounds beyond those found in conventional linseed oil. The germination process activates pathways that can modify the seed's biochemical composition. The application of an untargeted approach acknowledges the possibility of identifying expected as well as less extensively recognized compounds, providing deeper insights into metabolic pathways and processes. This strategy ensures that the analysis is not limited to predefined targets. To provide structured analysis, several lipid species (see chapter 2.4.1 – 2.4.3) have been chosen for detailed exploration due to their established roles in metabolic regulation.

2.4.1 Triacylglycerol & Diacylglycerol

TAGs are a diverse class of lipids with a glycerol backbone and three fatty acids attached to the hydroxyl groups via ester bonds. Depending on the chain length and degree of unsaturation of the fatty acids, their physical and chemical characteristics can vary, leading to different purposes, such as energy production through the storage of fatty acids, or membrane lipid synthesis. TAGs are a significant component of seed oils, which are a valuable resource for dietary and industrial applications (Yen et al., 2008). These oils represent the most abundant energy-rich storage molecules in eukaryotes, contributing to overall maintenance, cellular energy balance and lipid homeostasis. Even though vegetative plant tissue does not accumulate a great amount of TAGs, it is of major importance for their synthesis and metabolism (C. Xu & Shanklin, 2016). Moreover, in mammals they are primarily stored in adipocytes, as well as myocytes, enterocytes, hepatocytes and mammary epithelial cells. Besides energy storage, TAG synthesis contributes to mitigating toxic effects of surplus fatty acids in cells. In most mammals, enterocytes and hepatocytes synthesize TAGs to produce and secrete lipoproteins, facilitating transportation of dietary and endogenous fatty acids between tissues. Moreover, they are a part of the skins surface water barrier and by accumulation of TAGs in adipose tissue, they provide thermal insulation (Yen et al., 2008). In the mid-20th century two major pathways for biosynthesis were discovered. Both, Kennedy or glycerol phosphate as well as the MAG pathway use fatty acyl-CoAs as acyl donors (Kennedy,

1957; Lehner & Kuksis, 1996). While the first takes places in nearly all cells, the MAG one is present in specific cell types, like enterocytes, adipocytes and hepatocytes, where it serves the purpose of aiding the re-esterification of cleaved TAGs (Xia et al., 1993). Facilitated by the acyl-CoA diacylglycerol acyltransferase, TAG is formed via the covalent linkage of acyl-CoA and diacylglycerol (DAG) and consequently released into the lipid bilayer (Yen et al., 2008).

DAG, a lipid intermediate of TAG hydrolysis, consists of a glycerol backbone linked to two fatty acids through ester bonds. Due to its small and simple structure, DAG aids as a second messenger as well as a part of biological membranes. Further it is a key component in lipid-mediated signaling (Carrasco & Mérida, 2007). DAG makes about 10% of glycerides in plant-based oils and fats and it is not only an ideal platform for the attachment of new components in lipid synthesis, but also a source of free fatty acids. Several organisms, including plants and mammals have the ability to metabolize DAG and thus aiding in cell growth and development (Carrasco & Mérida, 2007; Tada & Yoshida, 2003). Besides the two main pathways in the *de novo* DAG synthesis, there are three alternative pathways involving sphingomyelin synthase, phospholipase D and phospholipase C, whereby DAG, generated through those ways, usually is not utilized for metabolic purposes (Huitema et al., 2004). In the two main mechanisms DAG is generated from glycerol-3-phosphate and dihydroxacetone-3-phosphate, whereby the first one is a result of the TAG synthesis. As a result of the multiple modifications that the two precursors need to complete, including two acylation steps, lysophosphatidic acid and phosphatidic acid (PA) is formed and subsequently converted into DAG via the phosphohydrolase (Nanjundan & Possmayer, 2003). Dysregulated DAG metabolism has been linked to the development of human diseases including diabetes and cancer. In a diabetic rat model, vascular cells display a principal metabolic alteration characterized by an imbalance of the synthesis of glycerophospholipids (GP), due to less DAG kinase activity, triggering the activation of DAG dependent effectors like protein kinase C, whose phosphorylation rate serves as a prognostic indicator for diabetes (Verrier et al., 2004).

2.4.2 Glycerophospholipids

GPs are a class of phospholipids consisting of a glycerol backbone with a polar headgroup at the stereospecific number three (sn-3) position. While this counts for eukaryotes and eubacteria, the polar headgroup regarding archaebacteria is at position sn-1. GPs represent a widely found group in nature, as they serve as fundamental parts of lipid bilayers, therefore forming a primary framework of cellular membranes. Furthermore, they function as essential binding sites for intra- and intercellular proteins as well as membrane derived second messengers. GPs that only consist of one fatty acid moiety, normally at the sn-1 position, get the prefix “lyso” to the corresponding GP, like lysophosphatidylcholine (Lys-PC) and lysophosphatidylinositol (Lys-PI) (Donato et al., 2013). While Lys-PC is important regarding DNA methylation and rheumatoid arthritis, Lys-PI might be suggested as a biomarker in cancer patients. Further lysophosphatidylserine (Lys-PS) has anti-inflammatory functions and takes part in the signal transduction of neutrophil activation (Castro-Gómez et al., 2015). A wide range of lipids can be categorized as GPs, such as phosphatidylcholine (PC) and sphingomyelin (SM), providing the majority of the lipid content in the outer plasma membrane monolayer in animal tissues. Moreover, phosphatidylethanolamine (PE), phosphatidylserine (PS) and phosphatidylinositol (PI), which can all be seen in figure 5 fall into this category of phospholipids. While PE is accumulated the most in microorganisms, it is the second most abundant in plant and animal tissue. Additionally, PI contributes to the regulation of vital processes (Donato et al., 2013). The synthesis of GPs starts with the glycerol-3-phosphate acyltransferase connecting a fatty acid-CoA with glycerol-3-phosphate, resulting in the generation of lysophosphatidic acid, which subsequently leads to the formation of PA in the endoplasmic reticulum through the acylglycerol-3-acyltransferase that bonds another fatty acid-CoA to glycerol. Consequently, PA serves as the substrate for two essential metabolic pathways, whereby the first one takes place in the endoplasmic reticulum and is regulated by PA phosphatase, which removes the phosphate group from the sn-3 position, resulting in the creation of DAG. Thereafter TAG can be synthesized through esterification at the same position. Another relevant pathway that includes PA is the formation of PC and PE, two essential phospholipids in context of cellular functions, which happens through the addition of ethanolamine and choline (Castro-Gómez et al., 2015).

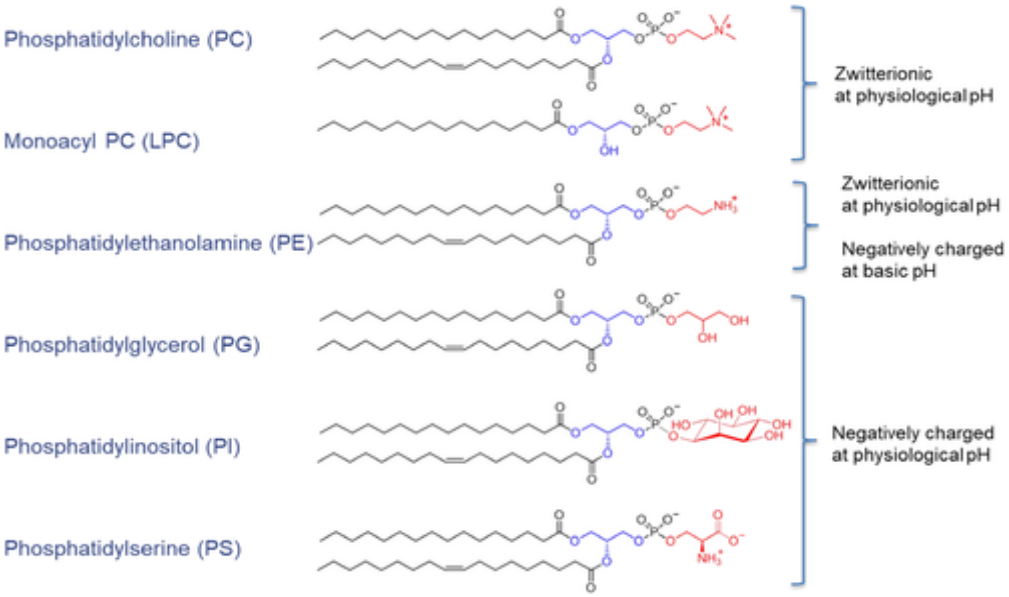

Figure 5: Structural representation of several glycerophospholipids (Van Hoogevest et al., 2021))

2.4.3 Sphingomyelin

Sphingomyelin (SM), categorized as a sphingolipid, consists of a phosphorylcholine attached to ceramide, and while it is unique to eukaryotic cells, its plant version is ceramide phosphorylinositol (Buré et al., 2014). Its low degree of unsaturation results in a tightly packed hydrophobic chain structure that attracts cholesterol, aiding in the maintenance of a liquid ordered state (Slotte, 2013). Catalyzed by the enzymes, sphingomyelin synthase 1 and 2 using ceramide and PC as substrates, SM is synthesized in the plasma membrane and Golgi apparatus. The same substrate is used to produce DAG. The synthesis starts in the endoplasmic reticulum where ceramide is converted to ceramide phosphorylethanolamine after obtaining its polar head from methylated PE. SMs provide and maintain stability as well as chemical resistance in the outer membrane layer and myelin sheaths. Due to the regulatory effects, like the interaction with specific proteins and the function of a receptor for the transferrin internalization, iron can be easier transported into the cells (Castro-Gómez et al., 2015). Lipidomic analyses of human fibroblasts revealed that SM consisted of at least 18 different molecular species, with d18:1/16:0 SM being the dominant form, followed by significantly lower levels of d18:1/24:1 and d18:1/24:0 (Valsecchi et al., 2007). Overall SM plays a fundamental role in maintaining membrane structure, protein recruitment, lipid metabolism and cellular processes like endocytosis and cytokinesis, but although the positive effects might be

predominate, SM secures cholesterol in arterial walls, thereby reducing reverse cholesterol transport, which further promotes lesion formation (Slotte, 2013).

2.5 Metabolites of interest

The following section provides a more detailed specification of a selected subset of carnitines identified in this study. While a broader range of metabolites like amino acids, carnitines or several derivates was detected, various acetylated forms of carnitines have been specifically chosen for further examination due to their significance and relevance across different tissues and metabolic processes. These selected carnitines may influence essential physiological processes, potentially affecting lipid metabolism, mitochondrial function and energy homeostasis.

2.5.1 Acetylcarnitine

Acetylcarnitine, naturally occurring in tissues like brain, heart and liver, as an endogenous metabolic intermediate, is an acetylated form of carnitine. It is involved in the transfer of acetyl groups across the mitochondrial membrane for anabolic and catabolic processes (Scafidi et al., 2010). These mechanisms include oxidation for energy production, the function as a precursor for acetylcholine synthesis and integration into neurotransmitters, like glutamate, glutamine and gamma-aminobutyric acid. In addition, acetylcarnitine has shown that it has neuroprotective characteristics regarding several neurological disorders like traumatic brain injury or hypoxia-ischemia as well as Alzheimer's disease and general conditions associated with central and peripheral nervous system damage. It also reduces oxidative stress and prevents neuronal cell death (Ferreira & McKenna, 2017b). Furthermore, rat studies have shown that acetylcarnitine influences metabolic pathways e.g., by increasing levels of phosphocreatine in rat brains and counteracting the age-related decline in cardiolipin levels within rat heart mitochondria. Depending on the cell's bioenergetic demands, the acetyl group can be formed into acetyl-CoA via the carnitine acetyltransferase without requiring ATP, which enables acetylcarnitine to provide acetyls moieties for essential metabolic mechanisms when cellular energy levels are reduced (Lligona-Trulla et al., 1997).

2.5.2 Lauroylcarnitine

Lauroylcarnitine is an acylcarnitine ester featuring a hydrophilic head group and a hydrophobic alkyl chain with 12 carbon atoms. Due to its amphiphilic structure, it is capable of self-aggregation and adsorption at interfaces in aqueous solutions (Liu et al., 2021). Currently LC-MS/MS is the most widely used application for metabolomic profiling. It allows the precise differentiation of acylcarnitine isomers while enhancing detection sensitivity and specificity. Acylcarnitines including CAR 12:0 are involved in several pathways, such as detoxification or processes related to the metabolism of branched chain amino acids (Brejchova et al., 2024). But they are also implicated in other metabolic disorders, like diabetes and cancer. Several studies investigated the effects of acylcarnitines. For instance Schooneman et al., (2013) examined the functions of medium-and long chain acylcarnitines, highlighting that the levels of these metabolites are closely associated with various metabolic diseases, suggesting that accumulations or alterations in their concentration might function as a potential biomarker for metabolic dysfunction. Lauroylcarnitine is considered as a medium chain acylcarnitine. Due to the potential physiological significance of these carnitines, lauroylcarnitine may exert beneficial effects on metabolic health. Furthermore, it has been suggested that medium chain acylcarnitines play a crucial role in cellular energy metabolism and mitochondrial function. Therefore, lauroylcarnitine could contribute to these effects (Dambrova et al., 2022). Another study from Zhou et al., (2024) identified lauroylcarnitine as a potential biomarker for acute myocardial infarction. While acylcarnitines enhance the transport of fatty acids into the mitochondria for energy metabolism under normal conditions, impaired β-oxidation in affected patients due to accumulation might lead to metabolic stress and inefficient ATP production in cardiomyocytes. Moreover, the disrupted carnitine shuttle could lead to mitochondrial dysfunction and energy deficits, making lauroylcarnitine an early diagnostic marker for myocardial infarct (Zhou et al., 2024).

2.5.3 Propionylcarnitine

Propionylcarnitine is a short-chain fatty acid with 3 carbon atoms. As the propionyl ester of carnitine, it raises the intracellular pool of it. Furthermore, propionylcarnitine shows a high affinity for the carnitine acetyltransferase as well as the sarcolemmal transporter and therefore it can easily be metabolized to propionyl CoA and free carnitine.

Additionally, it contributes to the citric acid cycle through its propionyl-CoA units. It also facilitates peripheral vasodilation and a more rapid uptake into myocytes (Malaguarnera, 2012; Vanella et al., 2000). Supplementing with the derivative of carnitine has demonstrated promising results in enhancing energy production in oxygen deprived muscles, which is possible due to the metabolic transformation to succinyl-CoA and subsequently to succinate. This intermediate enters the citric cycle as an energy generating metabolite, providing additional fuel to ischemic muscle tissue. In addition, propionylcarnitine has shown that it can restore ATP and phosphocreatine in rats with peripheral arterial disease. Moreover it enhances the coagulative fibrinolytic homeostasis in vascular endothelium, while also improving the blood fluidity (Wiseman & Brogden, 1998).

As metabolomics advances, the importance of intermediary metabolites like propionylcarnitine in understanding and optimizing metabolic pathways becomes increasingly evident, as it offers significant potential for both research and clinical applications. Future research may further cast light on the carnitine derivative, forging the path for novel therapeutic strategies in cardiovascular diseases, mitochondrial dysfunctions as well as metabolic disorders. Given its ability to influence cellular energy metabolism and vascular functions, propionylcarnitine represents a promising target for metabolic interventions, with potential implications for precise medicine and therapies.

2.6 Thesis aims

The presented thesis aims to investigate the metabolic and lipidomic effects of supplementation with linseed oil from germinated seeds (GLO), with special attention on its impact on β-oxidation. The study focuses on lipidomics and metabolomics in order to analyze related pathways. Key metabolites of this research are carnitines profiles and lipid classes, as e.g. glycerolipids (DAG, TAG), GPs (PC, PE, PI) and SLs (SM, Cer) in different tissue types. Several core objectives were closely examined, which led to various assessments. The main goal was to analyze the effects of 1% GLO and 10% GLO supplementation on lipid classes and metabolite profiles, as well as their impact on β-oxidation. Because of its nutrient composition, GLO has a higher content of bioactive substances, leading to the assumption that it improves metabolic health and effects on the β-oxidation. Carnitines enable the transport of fatty acids into the mitochondria for

β-oxidation by forming acylcarnitine complexes. Given this function, changes in carnitine levels could potentially impact mitochondrial fat oxidation and energy production (Lenihan-Geels et al., 2013; Longo et al., 2016). We hypothesize that GLO will show higher beneficial effects compared to conventional linseed oil (LO) supplementation, as well as normal fat diet (NFD) and high fat diet (HFD) due to its higher bioactive compound content. These effects might influence metabolic efficiency, improve lipid transportation and increase lipid storage capacity. While treatments with 1% oil might lead to smaller effects, observed for individual metabolites, more significant shifts are expected for key metabolic pathways in β-oxidation for 10% treatment groups, particularly in response to supplementation with GLO.

Given their distinct but complementary roles in energy metabolism and thermoregulation, both BAT and WAT are of particular interest for this thesis. While BAT is essential for non-shivering thermogenesis and cold adaptation, WAT is crucial for fat storage and energy homeostasis. It stores excess energy, releases fatty acids when needed, secretes hormones, supports glucose regulation and plays a role in inflammation (Cannon & Nedergaard, 2004; Heinonen et al., 2020; Trayhurn & Beattie, 2001). Furthermore, liver is important in context of this thesis as it interacts with adipose tissue by packaging excess lipids for secretion and transport to storage sites. In addition, liver regulates the balance of lipid and cholesterol as well as blood volume and the macronutrient metabolism (Trefts et al., 2017). Due to the distinct roles in and metabolic capacities of each tissue, uniform effects across all analyzed tissues are not anticipated. Rather, tissue specific responses reflecting their individual functions in energy and lipid metabolism are expected.

Key markers of interest are not only several lipid classes, but also acylcarnitine profiles – substances involved in storage and membrane function as well as mitochondrial function markers, such as increased ATP production. While the polar metabolite profile primarily revealed shifts in carnitine concentrations, the inclusion of the organic phase was essential to capture broader lipidomic alterations. Thus, we also expect distinct adaptations in storage and membrane lipids across the dietary treatments. These lipid species including glycerolipids, GPs and SMs serve as critical indicators of metabolic

health, cellular signaling, fat storage, cell differentiation, immune response and membrane composition. Therefore, the following hypothesis were developed:

1. Germinated linseed oil enhances β-oxidation by modulating carnitine metabolism and increasing mitochondrial fatty acid transport efficiency.
2. Germinated linseed oil influences changes in lipidomic profiles by modulating lipid storage and metabolic pathway activity, leading to enhanced lipid homeostasis and mitochondrial function.

Although linseed oil has been studied in various contexts, there is a lack of research on GLO and its impact on β-oxidation and metabolic regulation. Germination is known for increasing the nutritional content and quality of oils, but its direct effects on lipid metabolism and mitochondrial function remain largely unrecognized (Pointner et al., 2024). This study provides a comprehensive metabolic and lipidomic analysis using untargeted and targeted approaches, highlighting the influence on fatty acid oxidation. Furthermore, by investigating lipid metabolites we aim to analyze specific lipidomic shifts associated with membrane integrity and energy metabolism. Moreover, this study provides an innovative approach in regard to the effects of the different supplementation levels in combination with metabolomics and lipidomics. These approaches will help to determine whether higher concentrations of GLO lead to more significant improvements in lipid metabolism and β-oxidation.

This research fills a critical gap in the current understanding of several lipids and metabolites at the level of metabolomics and lipidomics, offering new perspectives on dietary interventions, metabolic health and the potential applications of GLO in nutritional sciences.

3 Methods and materials

This chapter outlines the research methods and procedures as well as the animal study design, data collection and analysis techniques. Furthermore, it provides detailed information on how the samples are prepared and which chemicals and instruments are used in this thesis. All laboratory rules were strictly followed, and careful handling of equipment and substances was ensured.

3.1 Animal study design and numbered samples

The study was conducted in cooperation with the German Institute of Human Nutrition (DIfE) and received ethical approval under TVA-Nr: 2347-21-2021. This study is represented by 6 different groups with 11 female C57BL/6J wild-type mice each. Every group had specific treatments, which are the following ones in ascending group numbering: Normal-fat diet (NFD) | High-fat diet (HFD) | High-fat 1% conventional linseed oil diet (LO 1%) | High-fat 10% conventional linseed oil diet (LO 10%) | High-fat 1% linseed oil from germinated seeds diet (GLO 1%) | High-fat 10% linseed oil from germinated seeds diet (GLO 10%). The intervention lasted 12 weeks, from week 12 until week 24 of the mice's age, the daily feed intake as well as the body weight and the composition of their body fat were regularly controlled. To minimize any influences the animals were euthanized on closely spaced days, in this case it was September 25th, 26th and 28th of 2023. Tissues of interest were BAT, WAT and liver. To sum up the study, figure 5 shows the animal study design.

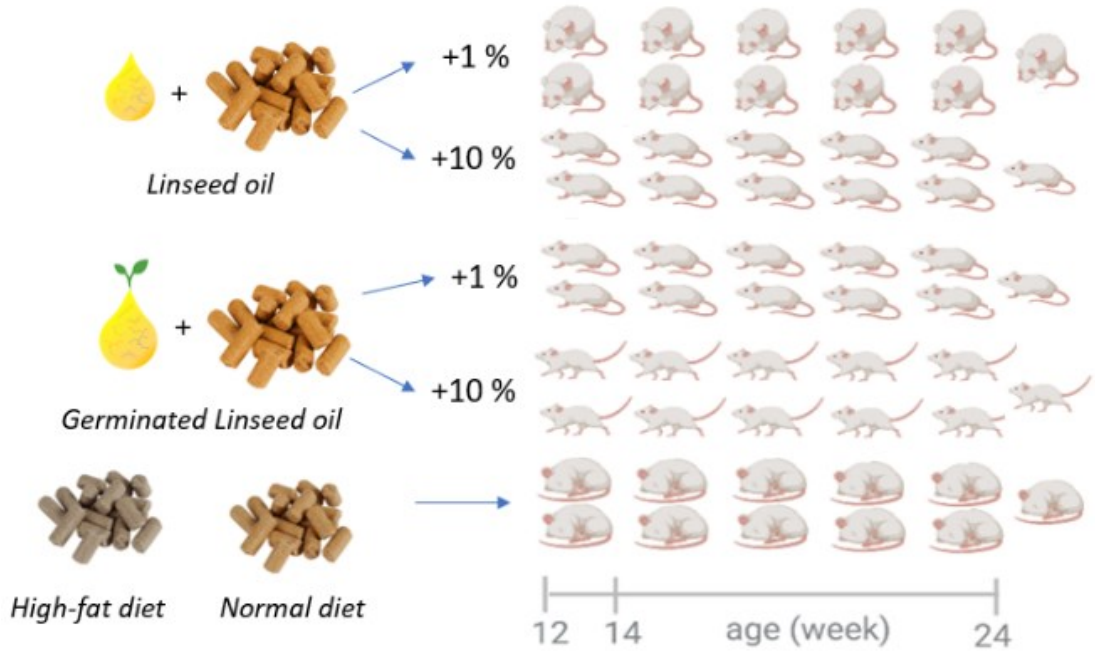

Figure 6: Animal study design: Effects of conventional LO and LO from germinated seeds supplementation on mice under different dietary conditions.

After the organs were kindly provided by the DIFE, they were carefully cut into appropriate pieces, ranging from 12.7 – 35.7 mg. However, an effort was made to ensure a consistent tissue weight between 20 and 28 mg. The organs were deployed in tubes at

-80°C. In 2 x 50 ml centrifuge tubes methanol and chloroform were stored to ensure that the chemicals are ice cold when used. Next, acetonitrile, acetyl chloride, butanol, MS-grade water and toluene were filled into fitting tubes and stored in the fridge. Sorted by group the examples were taken out and put into liquid nitrogen when starting the cutting and weighing process. The required cuts were then put in other appropriately labeled tubes with safety locks to fit the requirements for homogenizing and centrifuging. General information regarding the tubes and their content: Tissues of 768 and 817 were mixed up but corrected in this work again. 834 WAT and 834 BAT were also mixed up but correctly adjusted in this study. Mouse 718 died. After every usage, the balances and instruments were cleaned with 90% ethanol to avoid any contamination and appropriate safety equipment was worn at every step. The exact masses of all pieces relevant for this work can be found in the appendix.

3.2 List of chemicals and instruments

This section is about the chemicals used including their hazard pictogram, purity and the supplier as well as a table containing information about the devices and their software.

Table 2: Chemicals used for extraction, measurement, derivatization and preparation

Chemical	Purity	Supplier	Hazard Pictogram
Acetonitrile	MS grade	VWR	
Acetylchloride	≥99%	Fluka analyticals	
Acetylcarnitine-d3 (0.2427 µg/mL)	Analytical standard	Cayman	×
Ammonium acetate	Lichropur	Merck Millipore	×
Ammonium formate	≥99%	Sigma Aldrich	×
Formic acid	≥99%	VWR	
Isopropanol	MS grade	Merck Millipore	
L-Carnitine-d3 (0.2007 µg/mL)	Analytical standard	Cayman	×

Chemical	Purity	Supplier	Hazard Pictogram
Methanol	MS grade	Merck Millipore	
Myristoylcarnitine-d3 (0.411 µg/mL)	Analytical standard	Cayman	×
n-butanol	≥99%	VWR	
Oleoylcarnitine-d3 (0.4651 µg/mL)	Analytical standard	Cayman	×
SPLASH Lipidomix: •15:0–18:1 (d7) PC 100 µM •15:0–18:1 (d7) PE 7 µM •15:0–18:1 (d7) PS 20 µM •15:0–18:1 (d7) PG 5 µM •15:0-18:1 (d7) PI 20 µM •15:0–18:1 (d7) PA 10 µM •18:1-(d7) Lyso PC 45 µM •18:1-(d7) Lyso PE 2 µM •18:1-(d7) Cholesterolester 250 µM •C18(Plasma)-18:1(d9) PC 20 µM •15:0-18:1-(d7) DAG 15 µM •15:0-18:1-(d7) 15:0 TAG 35 µM •d18:1-18:1-(d9) SM 20 µM •C18(Plasma)-18:1(d9) PE 5 µM	Analytical standard	Avanti Polar Lipids	
Toluene	≥99.8%	CarlRoth	
Water	MS grade	VWR	×

Table 3: Devices and Software

Devices and Software	Supplier
Balance Pioneer	Ohaus
Ceramic beads 1.4mm	VWR
Centrifuge	Thermo scientific
Centrifuge Tubes 0.5ml, 1.5ml, 50ml	Eppendorf, pluriMate II
Dryer 60°C	
Filter Tips	
GraphPad Prism 10 Version 10.5.0	GraphPad Software
Homogenizer Precellys 24	VWR
Micro inserts for vials	VWR
MzMine Version 4.4.3	MzMine Software
Needles	
Office 365 students	Microsoft
Pipette tips: 10µL, 100µL, 200µL, 1000µL, 1250µL	Eppendorf
Pipettes 2.5µL, 10µL, 100µL, 1000µL	Eppendorf
LC vials	Shimadzu
LCMS-8040 (QQQ)	Shimadzu
Nitrogen dryer	
PTFE septum caps	Rotilabo
LCMS-6546 (QTOF)	Agilent
CompassXport	Bruker

Devices and Software	Supplier
Skyline Version 24.1	MacCoss Lab Software
Syringes 1ml, 5ml	
Ultrasonic cleaner USC500 TH	VWR
Vortex RS-VA10	Phoenix Instrument

3.3 Sample preparation

For sample preparation a biphasic solvent system, namely Bligh & Dyer extraction was used. This method was chosen for its efficiency in separating lipids and polar metabolites (Bligh & Dyer, 1959). Firstly, samples of each treatment group were taken out and put on ice for further processing. To ensure consistent grinding, homogenizing and breaking down the tissue, 10-15 units of 1.5 ml ceramic beads were added. After transferring the organs from 0.5 ml into 1.5 ml tubes, 1 ml of methanol and chloroform in a ratio of 2:1 (v/v), leading to 666,6 µL MeOH and 333.3 µL $CHCl_3$ were added to the samples. To correct certain variations and improve the accuracy in the analytical process internal standards (IS) were added to the samples. Hereby a mixture was made for the 18 samples containing 45 µL of each of the following carnitines: Acetylcarnitine-d3, L-carnitine-d3, Myristoylcarnitine-d3, Oleoylcarnitine-d3, leading to a total of 10 µL carnitine standard mix for each tube. Furthermore 2.5 µL of SPLASH Lipidomix was added to every sample. After vortexing for 10 s, liver, WAT and BAT needed to be homogenized to break down the organs and facilitate solvent extraction. The Precellys 24 homogenizer (VWR) was used with the following settings: Rotational speed of 4000 U/min, 2 rounds à 60 s and a pause of 5 s. Hereby it is important to note that the exemplars must not overlap, nor should they be directed in various directions, as this could lead to cracking, even with safety lock caps like it was the case with the following samples: 732B, 728L, 745W, 732W, 706W, 727W, 817W and 817L. To allow an efficient extraction, working on ice or incubating for 15-30 min is indispensable. To induce phase separation, after unifying the organic substances, 300 µL of MS grade water was added to each microcentrifuge tube. Subsequently the samples needed to be vortexed for around 10 s as this helps enhance the differentiation. Next, the content was centrifuged with the

following settings: 13.200 revolutions per minute (rpm), duration of 5 min and at 4°C. When this step was completed, the mixture separated into two layers, an upper, aqueous, polar phase and a lower, non-polar, organic phase. While the upper level was recovered in a new Eppendorf tube with 1.5 ml filling quantity, the bottom layer was carefully transferred into another one. Ensuring that the materials are replaced after each use to avoid any cross contamination, syringes were the best choice to go. In addition, appropriate filters were necessary to maximize the purity of the liquid layers, without any solid components. Under the nitrogen dryer both phases were evaporated until dryness, whereby the aqueous one took around 1 h 30 min and organic 30 min. As this is done step by step, the polar samples were put in the -80°C until the resuspension of the organic ones with 60 µL methanol/toluene in a ratio of 9:1 was completed. Again, the samples were vortexed for 10 s before centrifuging them with the same settings for 5 min. Before placing them in the -80°C freezer until measurement, these samples were transferred into correctly labeled LC vials with glass micro inserts, sealed with PTFE septum caps.

3.3.1 Derivatization of the polar phase

To determine relevant butylated compounds, especially carnitines, the dried substances underwent the process of derivatization, which was described by Giesbertz et al., (2015) and Gucciardi et al., (2012). Before vortexing the tubes for 10 seconds, a freshly prepared solution with 100 µL butanol and 5% v/v acetyl chloride was added. After incubating the mixtures for 20 minutes at a temperature of 60°C, the samples were again completely dried with the help of nitrogen. The microcentrifuge tubes were resuspended with 40 µL acetonitrile and 10 µL MS grade water to get a total of 50 µL liquid, which was vortexed for the same time duration as always and moreover refilled in correctly labeled LC vials with glass micro inserts, sealed with PTFE septum caps. Those were then stored at -80°C until they were needed for further steps.

3.3.2 Untargeted Lipidomics

To identify certain lipid substances of interest in the organic phase untargeted lipidomics was applied. This is useful as variations in their individual concentrations can be found, whereby a mass range of m/z 50 – 1700 for the quadrupole time-of-flight (QTOF) mass-spec technology was applied. The gradient being used for separation can be seen in table

5. The measurement was done with an LCMS-6546 device (QTOF) from Agilent including its respective ion source. Here the samples were analyzed in positive and negative mode, whereby in the end only positive mode results were considered due to better outcomes. For this device newer columns were used, namely Zorbax SB-C18 Rapid Resolution HT 2.1 x 50 mm 1.8 µm 600 bar with a UHPLC Guard 3 PK Zorbax Eclipse Plus C18 2.1 x 5 mm 1.8 µm. The temperature was set to 40°C and the injection volume was 10 µL, while the flow rate was set to 0.6 mL/min. The solvent preparation involved mixing acetonitrile: H_2O 6:4 (v/v) as solvent A and isopropanol: acetonitrile 9:1 (v/v) as solvent B. Furthermore, each solution was supplemented with 0.1% formic acid and 10 mM ammonium formate before they were sonicated for at least 15 minutes twice with a short break in between. This was done as it is important to avoid any bubbles in the mobile phases for better device care and results.

3.3.3 Untargeted Metabolomics

For the analysis of the polar phase, a separate setup was used. The gradient being used for separation can be seen in table 4. The solvents for these measurements consisted of MS grade water completed with 0.2% formic acid and 10 mM ammonium acetate as solvent A, while solvent B contained 0.1% formic acid added to acetonitrile. This time a Kinetex 2.6 µm HILIC 100 Å LC column (150 x 2.1 mm) together with the pre column SecurityGuard ULTRA UHPLC HILIC 2.1 mm cartridge were used. While for the organic phase a temperature of 40°C was used, the settings for polar were 50°C coupled with a flow rate of 0.5 mL/min. Again, 10 µL was the injection volume. Careful solvent preparation and temperature control were essential to ensure optimal separation and detection of metabolites. This allowed for high resolution analysis of metabolites present in the polar phase, complementing the previously conducted lipidomics analysis. The following tables contain the gradients used for separation, on the one hand organic and on the other hand polar.

Table 4: Gradient being used for separation (polar)

Time	% B
0.00	90
5.00	80
10.00	80
12.10	90

Table 5: Gradient being used for separation (organic)

Time	% B
0.01	Start
1.00	5
4.00	95
11.50	100
12.50	5
14.00	End

3.3.4 MZmine

To begin with, the untargeted analysis was performed using MZmine as well as the two libraries, Mona and GNPS, to match the results. After measuring, the raw data files were generated and imported into MZmine. First, the raw data files were converted into a mzML format using the Bruker software “CompassXport”. In the preprocessing stage, to reduce the amount of data and emphasize relevant peaks and spectra and further facilitate data preparation and feature extraction, the MS1 and MS2 filter were adjusted, with centroided mass detectors, all scan types and an automatically set retention time. To concentrate on molecules that were better detected in positive polarity the criterion was set to this method as the samples were also analyzed in positive ion mode. Noise levels can also be adapted directly in the crop filter and mass detection itself. In the next step, several factors in the ADAP chromatogram builder were adjusted to create MS chromatograms. Minimum consecutive scans, meaning how many scans, containing a signal are necessary to get a chromatogram, were set to 5. Minimum intensity for consecutive scans, which defines the intensity threshold, was set to 2.0E5 and the minimum absolute height was 5.0E5. Subsequently, some settings in the local minimum feature resolver were changed to ensure that only significant features are retained, like the chromatographic threshold which was set to 85% and the minimum ratio of peak top/edge to 1.70. Further 5 data points were chosen with a peak duration range of 0.00 – 1.00, which means that peaks with a duration of more than 1 minute were filtered out. As it allows differentiation between the primary ion and its natural variants the 13C isotope filter is important to identify features that belong to the same compound based on their isotopic pattern. Following this, a maximum charge of two, retention time

tolerance of 0.02 and the most intense representative isotope were selected. Features with MS2 data were retained regardless of filtering. In addition to this setting the isotopic pattern (peaks) finder was also adapted a little although the presets were already fitting well. As the process continued, the join aligner was applied to align all features from multiple samples into one list, whereby the m/z value was weighted three times heavier than other factors, to assure that even with small changes in retention time, peaks with highly similar m/z are more likely to be aligned. The alignment was now modified via feature list rows filter. Once again, the presetting was already in good condition. Finally, before exporting the complete molecular networking files, gap filling via peak finder (multithreaded) was performed to address gaps in feature detection when peaks are absent due to limited sensitivity or high noise levels. Intensity tolerance was set to 20% and this time three data points instead of five were utilized. After that, a table with the most abundant substances greater than cosine similarity 0.7, and filtered by the highest area was then created and later used for targeted LC-MS. The cosine similarity reflects the spectral match between experimentally obtained MS/MS spectra and those in reference libraries, with values above 0.7 indicating a high-reliable annotation. Among the annotated features, several carnitine species were identified. The list of metabolites and their respective MRM-transitions were completed and confirmed based on the comprehensive dataset provided by Giesbertz et al., 2015. (see appendix, table 8, 9, 13 and 14)

3.3.5 Targeted Metabolomics

The targeted LC-MS/MS measurement was performed utilizing a Shimadzu LCMS-8040 (QQQ) system, including a SIL-20AC autosampler maintaining a temperature of 4°C, a LC-20AD pump and a CTO-20AC oven. Both organic and polar columns and their security guard columns as well as each solvent were the same as in the untargeted approaches when executing the task of measuring. The injection volume was once again 10 µL. For metabolomics the temperature was set to 30°C. Furthermore, a flow rate of 0.5 mL/min was conducted. Each sample was analyzed via a 12.10 min polar method. The solvents for these measurements consisted of MS grade water completed with 0.2% formic acid and 10 mM ammonium acetate as solvent A, while solvent B contained 0.1% formic acid added to acetonitrile. After adapting the MRM-transitions (see table 14) by their product

m/z and compound names the respective lists including standards and each sample result sorted by BAT, WAT and liver, were imported into Skyline. Nearly all substances met the expected criteria: Fine signals with sufficient peak intensity and quality, which fell into the intended retention times, good signal to noise ratio (S/N), positive matches with databases and reliable quantification. Sometimes not all fragments were found. Rarely, there were also no detected peaks/matches. Based on the most presumable peak, every substance in each sample was then adapted by its retention time to get a unified result by synchronizing the integration and applying peak to all. The molecule transition results were then exported and quantified based on the corresponding deuterated IS (ISTD d3) (see table 14). Quantification was performed by calculating the area ratio between each analyte and its respective IS, multiplied by the IS concentration. Subsequently, the resulting values were multiplied with the solvent volume of which the dried carnitines were resuspended and finally normalized to the sample weight and expressed in (µg/g).

3.3.6 Targeted Lipidomics

For Lipidomics, a 45 min LC-MS/MS method was used with 40°C, and a flow rate of 0.3 mL/min. The same Shimadzu LCMS-8040 (QQQ) instrument was used. The solvent preparation involved mixing acetonitrile:H_2O 6:4 (v/v) as solvent A and isopropanol: acetonitrile 9:1 (v/v) as solvent B. Furthermore, each solution was supplemented with 0.1% formic acid and 10 mM ammonium formate. The solvents were always sonicated for at least 15min to avoid any bubbles, which could damage the instruments or distort the results. For targeted lipidomics a Zorbax SB-C18 Rapid Resolution HT 2.1 x 50 mm 1.8 µm, 600 bar column with a UHPLC Guard 3 PK Zorbax Eclipse Plus C18 2.1 x 5 mm 1.8 µm was used. Similar to metabolomics, the MRM-transitions (see table 13) were adapted based on product m/z and compound names. The results, including standards and sample data sorted by BAT, WAT, liver were imported into Skyline.

3.3.7 Statistical evaluation

For statistical analysis, the processed data underwent a procedure in GraphPad Prism 10, whereby one-way ANOVA (and nonparametric or mixed) was applied. First, a diagnostic for residuals was done by normality tests of Anderson-Darling, Shapiro-Wilk, D'Agostino and Kolmogorov-Smirnov as well as tests for clustering and heteroskedasticity by Brown-

Forsythe and Barlett. A quantile-quantile (QQ) plot was shown to see whether the data follow a normal distribution or not. In addition, a multiple comparison test for comparing each mean-value of the groups was done with an alpha threshold (p-value <0.05). As the data was normally distributed, the correction was then performed by a post-hoc Tukey test. After statistical preparation was done, the column graph type was set to a bar graph and mean with standard error of mean (SEM). Blanks were used as quality control (QC) samples, and each group was measured in triplicates.

4 Results and discussion

The following chapter presents the metabolic and lipidomic responses resulting from the different supplementation groups, focusing on their impact on β-oxidation across BAT, WAT and liver. Particular attention is paid to the comparison between conventional LO and GLO groups to NFD and HFD as well as the difference between 1% LO / 1% GLO and 10% LO / 10% GLO. The results include both untargeted and targeted metabolomic and lipidomic analyses within BAT, WAT and liver. The untargeted analysis primarily functioned as a broad overview of metabolites and lipids, providing insights into which compound classes were present the most and how they were distributed. This approach was particularly helpful for detecting both known and previously less-characterized substances. In comparison, the targeted analysis focused on specific metabolite and lipid classes, enabling a more detailed and quantitative examination of individual compounds of interest. We expected not only the detection of well-known carnitines and lipids, but also the presence of less studied or unexpected substances.

4.1 Untargeted Metabolomics

To provide an all-encompassing vision of the metabolic activity captured in this untargeted analysis, all MS2 confirmed metabolites detected across BAT, WAT, and liver were compiled. The identification was done using spectral databases such as GNPS and MoNA and only features with MS2 coverage were included. This summary offers insights into the metabolic profile and forms the rough basis for interpreting various tissue specific effects. Despite the broad range of metabolites identified through untargeted analysis, carnitines were the only group selected for further untargeted and targeted analysis, due to their well-established functional importance in mitochondrial fatty acid

oxidation, their role as important shuttle molecules for long-chain fatty acid transport into the mitochondria and their critical contribution to energy homeostasis (Cannon & Nedergaard, 2004; Longo et al., 2016). In addition to their biological relevance, carnitines demonstrated the highest annotation confidence among all detected metabolites, along with robust detection and stable area across all three tissues. Taken together, these points strongly supported the decision to concentrate targeted quantification efforts specifically on carnitines.

Table 6: Overview of all metabolites detected by untargeted metabolomics, across BAT, WAT, liver. The MS2 confirmed data was annotated with GNPS and MoNA spectral databases.

Metabolites	All Detected Σ (349)	All detected features %	BAT	WAT	Liver	Mean cosine similarity	MS2	Databank
Primary nitrogen metabolites:								
Carnitines	86	24.64	34	30	22	0.88	MS2	GNPS/MoNA
Amino acid derviatives	59	16.91	22	18	19	0.72	MS2	GNPS/MoNA
Amine/Amide	32	9.17	14	10	8	0.77	MS2	GNPS/MoNA
Nucleotides	35	10.03	11	7	17	0.69	MS2	GNPS/MoNA
Secondary Metabolites:								
Terpenoids	31	8.88	10	14	7	0.78	MS2	GNPS/MoNA
Glycosides	11	3.15	4	3	4	0.73	MS2	GNPS/MoNA
Alkaloids	25	7.16	9	9	7	0.71	MS2	GNPS/MoNA
Bioactive & Xenobiotics								
Vitamins	22	6.03	6	5	11	0.73	MS2	GNPS/MoNA
Phenols	22	6.03	8	7	7	0.76	MS2	GNPS/MoNA
Drug-like substances	26	7.45	9	7	10	0.68	MS2	GNPS/MoNA

Table 6 illustrates the broad range of metabolites detected through untargeted metabolomics. The table lists the number of identified compounds, alongside the mean cosine similarity, which reflects the spectral confidence based on MS/MS library matching with GNPS and MoNA. This numerical overview gives a precise summary of the detection frequency across all annotated metabolites. The most dominant classes were carnitines, followed by amino acid derivatives and nucleotides, whereby the latter did not reach the threshold of 0.7 for the mean cosine similarity. In comparison, the mean cosine similarity for carnitines, which was about 0.88, further strengthens their reliability and makes them an ideal candidate for further analysis. Although some secondary metabolites such as terpenoids and alkaloids were also detected in modest numbers,

their biological relevance in the context of mitochondrial metabolism and β-oxidation was considered less important. These secondary plant metabolites may be present in linseeds, especially within the unsaponifiable fraction (terpenoids). Nevertheless, the concentrations of these substances can vary depending on processing conditions. Therefore, the results should be interpreted with care (Shim et al., 2014; Tang et al., 2021). Similarly, vitamins and glycosides were found in smaller amounts, highlighting the diversity, but falling outside the primary target of this thesis. Interestingly, a small percentage of drugs or drug-like substances was possibly identified, among other metronidazole and azithromycin, which are not endogenously produced and may have originated from exogenous sources. However, some matches showed low similarity scores, indicating limited confidence in the identification. These compounds should therefore be interpreted with caution.

Overall, the provided table highlights the analytical reach of the untargeted approach, further offering a clear focus on carnitines. Moreover, their consistently high detection rate across BAT, WAT, and liver, biological importance in β-oxidation and annotation quality strengthens the prioritization.

To visually support the statistical analysis of the carnitines, which are marked with a red rectangle, and to further show the abundance of several metabolites like terpenoids or vitamins, heatmaps were created. These visualizations show the Log_2 fold changes of detected metabolites across BAT (I), WAT (II), liver (III).

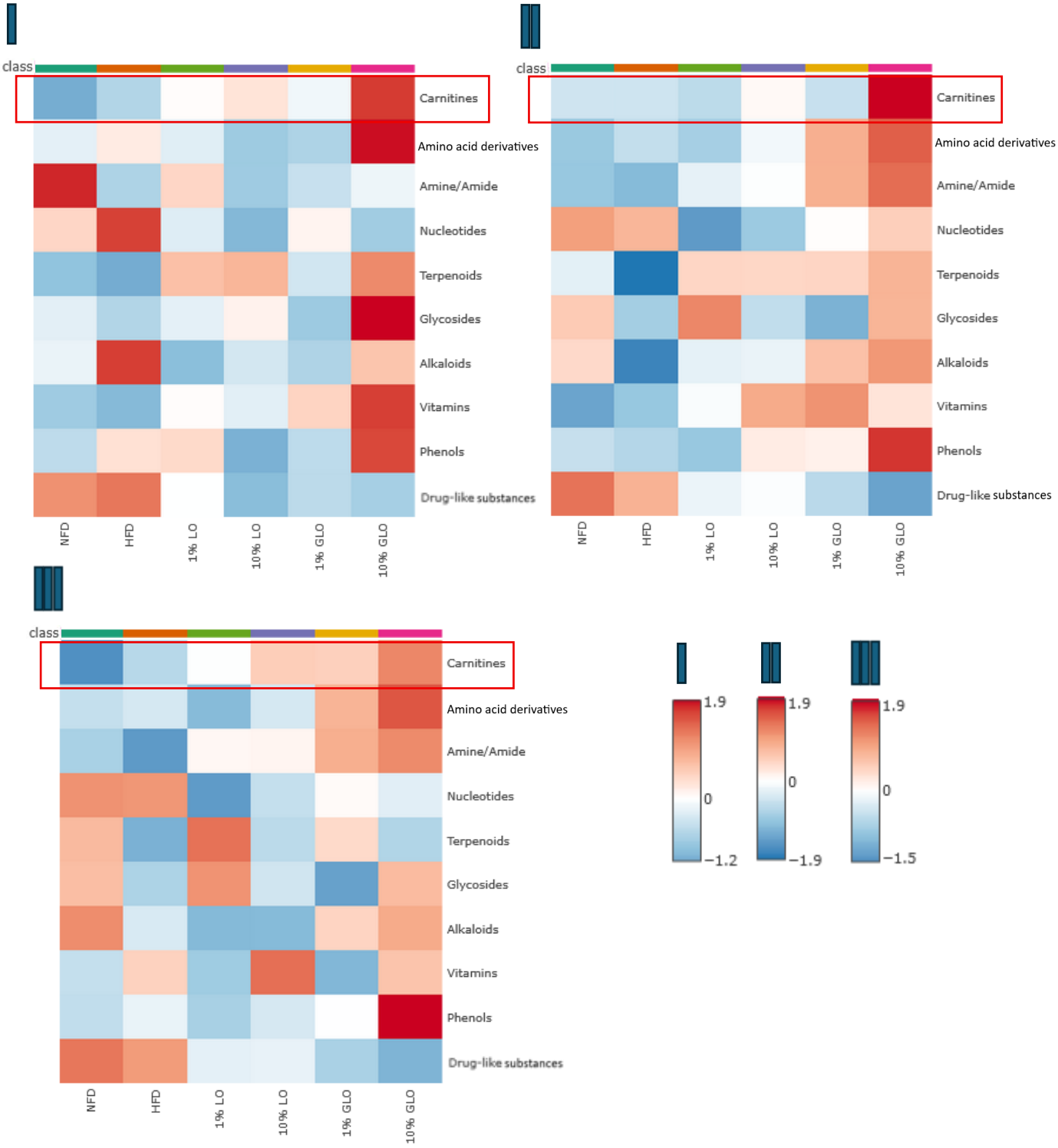

Figure 7: Hierarchical clustered heatmaps of detected metabolite classes in BAT (I), WAT (II), liver (III). Log_2 fold changes are between -1.2 and +1.9 across the treatment groups. Carnitines marked with a red rectangle.

Heatmaps allow for a comprehensive and simultaneous representation of trends and clustering patterns. Carnitines showed a clear increase in BAT, WAT, and liver in the 10% GLO group, followed by 1% GLO or rather 10% LO. This distribution highlights a favorable impact on β-oxidation and metabolic activity. Due to the crucial biological function and high annotation confidence, carnitines were exclusively selected for further analysis. Nonetheless, also vitamins showed a positive accumulation, especially in BAT and WAT, which might be due to the germination process and the general positive nutritional composition of linseeds. Higher vitamin content suggests that tocopherol is also increased, which is beneficial due to its antioxidant capacity (Pointner et al., 2024). Moreover, Terpenoids indicate a favorable profile, as they were increased in the LO group, particularly in GLO. These compounds have several positive characteristics like their antibacterial, anti-allergic, antioxidant and anticancer profile (Masyita et al., 2022).

The pie charts visualize the relative distribution of carnitines within BAT, WAT and liver, whereby each segment shows the proportion of the metabolites attributed to the specific treatment, therefore representing how dietary intervention influences the carnitine profile throughout several tissues.

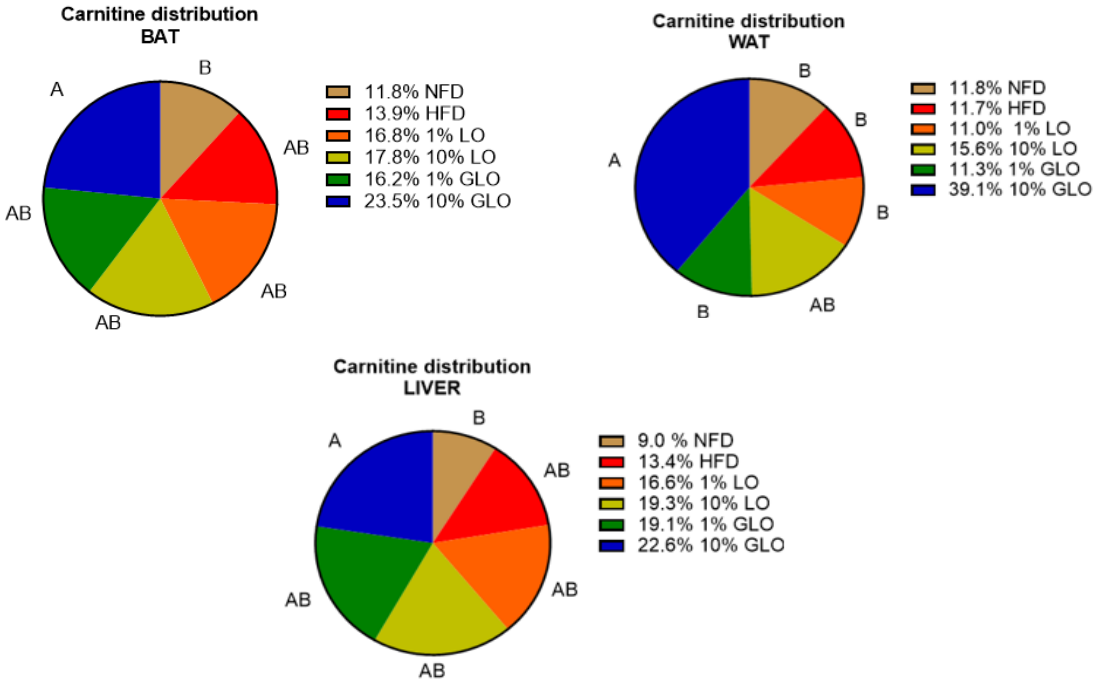

Figure 8: Relative distribution (%) of total detected carnitines in WAT, BAT, & liver of C57BL/6 wild-type mice. Data are presented as mean ± SEM (n>9). Statistical significance was determined using one-way ANOVA followed by Tukey's multiple comparison test. Groups labeled with different letters are significantly different ($p < 0.05$).

In BAT it can clearly be seen that carnitines are increased up to 23.5% in the 10% GLO diet, compared to lower percentages in all other groups with a range of 11.8% to 17.8%. The increase suggests a pronounced activation of β-oxidation pathways, as carnitines play a central role in shuttling fatty acids into the mitochondria (Cannon & Nedergaard, 2004). NFD differs significantly from 10% GLO, whereas other groups are not significantly different. In comparison, carnitine levels in WAT were distributed slightly differently with a significantly predominating accumulation of 39.1% in the 10% GLO treatment. Notably the 10% LO treatment does not show any significance compared to the 10% GLO and the other 4 groups. In liver, carnitines were again highly abundant in the 10% GLO group with a percentage of 22.6%. The distribution of the significances is similar to those in BAT, with a percentage of 9.0% in NFD. Table 8 in the appendix represents the most abundant polar metabolites detected in the untargeted analysis using QTOF LC-MS. The compounds were annotated based on their m/z, retention time, area, fragments, spectral matches to the GNPS and MONA compound databases, and most importantly by their cosine similarity, whereby a threshold of 0.7 was chosen. The list features several carnitines and acylcarnitine species, such as L-carnitine, lauroylcarnitine and acetylcarnitine. The presence of less well-known metabolites like deoxycarnitine and O-malonylcarnitine highlights the value of untargeted approaches in revealing subtle but potentially biologically relevant metabolic shifts.

The increased proportion of carnitines in BAT, WAT and liver within the 10% GLO group indicates a tissue specific metabolic response with an enhanced mitochondrial activity (Cannon & Nedergaard, 2004). Due to the fact that BAT is essential for non-shivering thermogenesis, a process that heavily relies on mitochondrial β-oxidation, higher carnitine levels in BAT point towards increased thermogenic capacity and energy expenditure (Esser et al., 1996). Therefore, these findings suggest an enhanced oxidative capacity of BAT within GLO, contributing to a more balanced energy metabolism.

Higher amounts of carnitines, especially L-carnitine found in liver might have beneficial effects due to the counteracting functions to the increased serum levels of alanine aminotransferase and aspartate aminotransferase in chronic liver diseases. A study from Oh et al., (2022) found that a supplementation with L-carnitine and carnitine-orotate has the potential to normalize liver enzymes in patients with chronic liver diseases such as

non-alcoholic fatty liver disease. Furthermore, a study from Madsen et al., (2018) has shown that L-carnitine treatment in patients with primary carnitine deficiency prevents cardiac complications and enhances skeletal muscle fat metabolism during exercise. One of the most interesting findings was the drastic carnitine increase in WAT in the 10% GLO group, as it usually has less free carnitine because it oxidizes only small numbers of fat. The most plausible interpretation is induction of adipose browning and enhanced fatty acid oxidation. The 10% GLO treatment group most likely experienced a conversion of WAT towards more brown fat, also called beige fat. Browning is characterized by a higher number of mitochondria in adipocytes and an upregulation of β-oxidation and UCP-1. These processes require more carnitine and therefore the body may respond by transporting more carnitine into adipose tissue. Evidence shows that omega-3 fatty acids can stimulate the appearance of brown adipocytes and boost thermogenesis. In addition, secoisolariciresinol diglucoside, the main phytoestrogen component of linseed, which is highly increased in GLO, can trigger browning via the activation of AMP-activated protein kinase (Kang et al., 2020; Pointner et al., 2024; Universidad de Barcelona, 2016).

Overall, the untargeted metabolomics approach yielded a broad range of metabolite identifications, with high spectral matching scores across treatment groups, particularly indicating potential differences in carnitine-related metabolism. While these results suggest metabolic shifts, particularly in β-oxidation, they require further confirmation. Therefore, a targeted approach using reference standards was performed to quantify and confirm these preliminary insights. In conclusion, supplementing GLO might contribute to improved metabolic health. Overall, untargeted metabolomics provide strong indications of diet-specific metabolic shifts, particularly highlighting mitochondrial β-oxidation and carnitine related functions such as transporting fatty acids or the regeneration of CoA. The composition of the carnitines visualized in the pie charts, combined with the range of detected metabolites listed via QTOF measurements provide a comprehensive metabolic imprint of dietary interventions and therefore help to gain a deeper understanding of metabolic adaptions (Cannon & Nedergaard, 2004).

4.2 Untargeted Lipidomics

Adipose tissue fulfills multiple essential functions that are central to maintaining systemic energy homeostasis, such as the storage of lipids and the mobilization of energy, as well as the secretion of bioactive components that influence the lipid metabolism (Fernández-Galilea et al., 2020; Leiria & Tseng, 2020). As lipids are the majority of adipocyte`s cellular content, their composition is fundamentally linked to adipose tissue function and its interaction with other organs. The specific lipid profile of adipocytes not only influences intracellular metabolic processes, but also interorgan communication (Leiria & Tseng, 2020). Untargeted lipidomics was performed in order to evaluate the tissue specific lipid profiles and how the identified lipid classes are related to each other throughout the six treatments. QTOF LC-MS analysis again was used to get a broad overview of lipid species across the three metabolically relevant tissues. To provide an all-encompassing vision of the lipidome captured in this untargeted analysis, all MS2 confirmed lipid classes detected across BAT, WAT, and liver were compiled. The identification was done using spectral databases such as GNPS and MoNA and only features with MS2 coverage were included. This summary offers insights into the lipidomic profile and forms the basis for interpreting metabolic effects.

Table 7: Overview of all lipid classes detected by untargeted lipidomics, across BAT, WAT, liver. The MS2 confirmed data is annotated with GNPS and MoNA spectral databases.

Lipidclasses	**All Detected Σ (811)**	**All detected features %**	**BAT**	**WAT**	**Liver**	**Mean cosine similarity**	**MS2**	**Databank**
Glycerolipids:								
TAG	323	39.83	107	123	93	0.81	MS2	GNPS/MoNA
DAG	112	13.81	31	50	31	0.79	MS2	GNPS/MoNA
MAG	3	0.37	1	1	1	0.69	MS2	GNPS/MoNA
Glycero phospholipids:								
PC	168	20.72	64	46	58	0.88	MS2	GNPS/MoNA
PE	103	12.70	48	28	27	0.86	MS2	GNPS/MoNA
PI	15	1.85	6	6	3	0.78	MS2	GNPS/MoNA
PS	18	2.22	8	5	5	0.70	MS2	GNPS/MoNA
Sphingolipids:								
SM	39	4.81	19	4	16	0.82	MS2	GNPS/MoNA
Ceramide	30	3.70	11	8	11	0.83	MS2	GNPS/MoNA

To illustrate the broad range of lipid classes detected through untargeted lipidomics, a quantitative table was created. The table lists the number of identified compounds within each lipid class, alongside the cosine similarity presented as mean, which reflects the spectral confidence based on MS/MS library matching with GNPS and MoNA. This numerical overview gives a precise summary of the analytical identification quality and detection frequency across all annotated lipid species.

Among all detected lipids, TAGs were the most abundant class, followed by PC, DAG and PE, reflecting a typical lipid storing and metabolically active status (Cannon & Nedergaard, 2004; Heinonen et al., 2020). Additionally, classes like SMs, including ceramides, and PIs were present in smaller quantities. All together they underline the inclusion of bioactive and signaling lipids in the dataset. However, table 7 provides a base for a comprehensive overview of the lipidomic composition and analytical depth of the untargeted measurements.

Heatmaps were created to visually support the results of the statistical analyses. These visualizations show the Log_2 fold changes of detected lipid classes across BAT (I), WAT (II), liver (III). Unlike column or pie charts, heatmaps allow for a comprehensive and simultaneous representation of trends and clustering patterns.

Figure 9: Hierarchical clustered heatmaps of detected lipid classes in BAT (I), WAT (II), liver (III). Log_2 fold changes are between -1.4 and +1.9 across the treatment groups.

By highlighting grouped specific lipid shifts, the inclusion of this type of graphs enhances the interpretability of untargeted lipidomics data. For instance, GLO supplementation resulted in an increased abundance of glycerolipids, whereby most of the time 10% GLO supplementation reached a higher accumulation than 1% GLO. In contrast, ceramide levels were the highest throughout all groups in HFD, representing a favorable distribution as they are commonly associated with metabolic stress, insulin resistance and pro-inflammatory effects (Kolak et al., 2007). In addition, LO supplementation mostly represents a neutral color, leading to the suggestion that they enhance lipid levels slightly more than NFD and HFD but less than GLO, although sometimes 10% LO reached a higher accumulation than 1% GLO. In conclusion, heatmaps serve as a valuable graph tool to identify tissue specific effects and potential targets for further investigation, visually supporting statistical analysis.

An untargeted lipidomics approach was done to evaluate the tissue specific shifts in lipid profiles and how the identified lipid classes are correlated to each other throughout the dietary treatments.

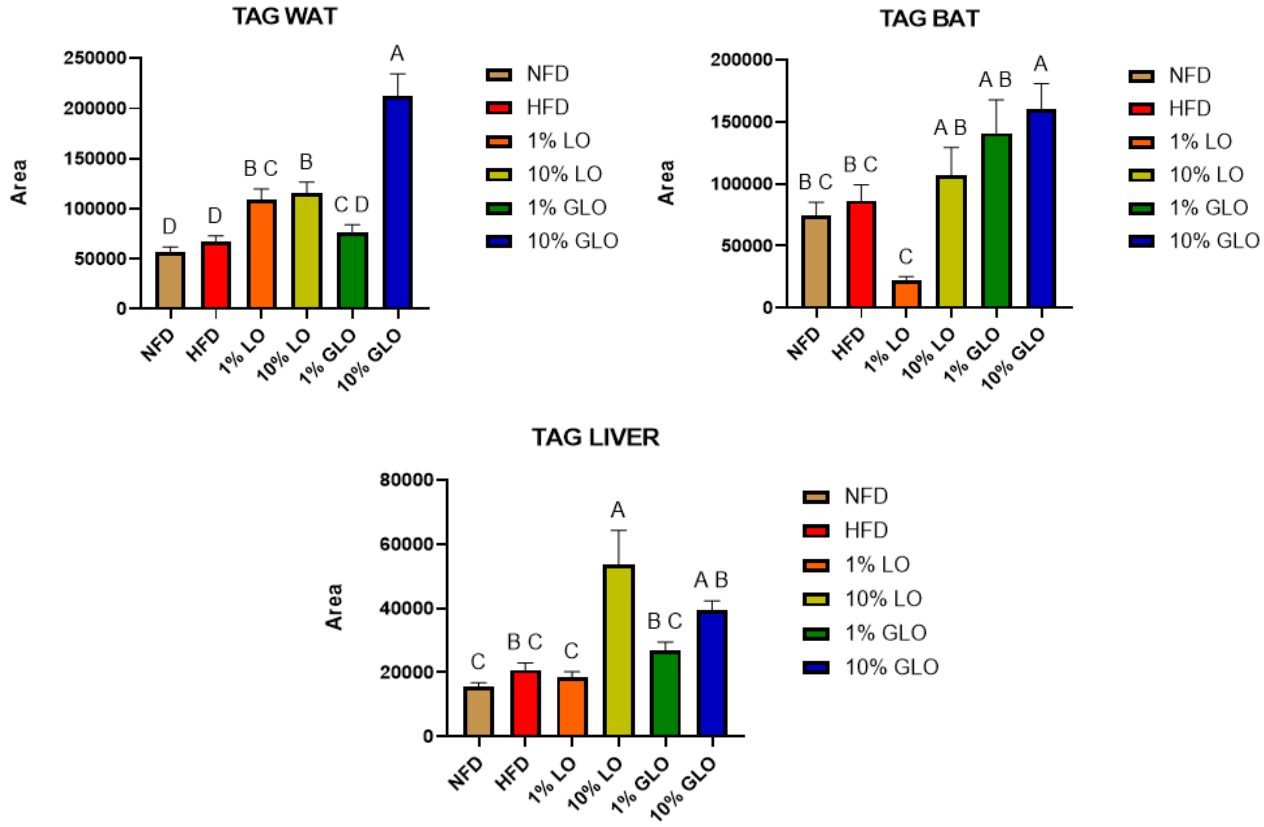

Figure 10: Relative distribution (Area) of total detected TAG in WAT, BAT, & liver of C57BL/6 wild-type mice. Data are presented as mean ± SEM (n>9). Statistical significance was determined using one-way ANOVA followed by Tukey's multiple comparison test. Groups labeled with different letters are significantly different ($p < 0.05$).

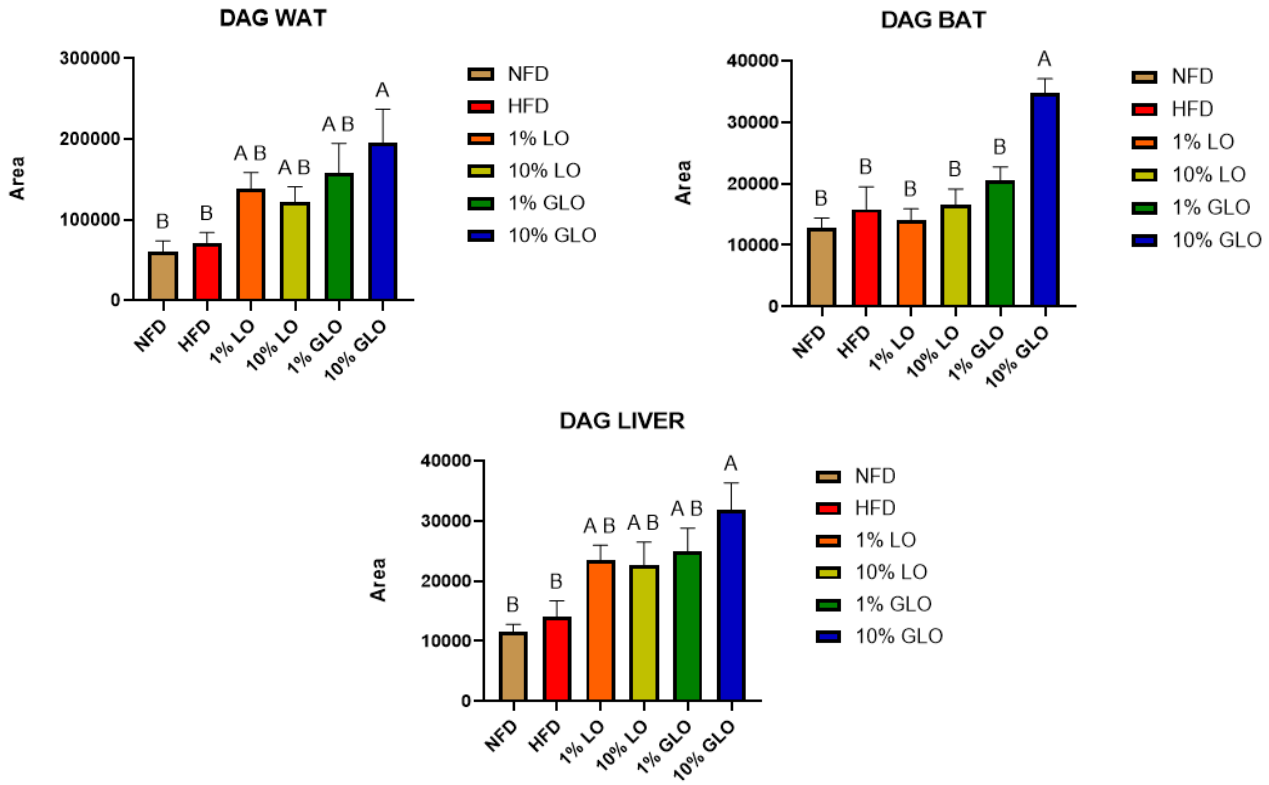

Figure 11: Relative distribution (Area) of total detected DAG in WAT, BAT, & liver of C57BL/6 wild-type mice. Data are presented as mean ± SEM (n>9). Statistical significance was determined using one-way ANOVA followed by Tukey's multiple comparison test. Groups labeled with different letters are significantly different ($p < 0.05$).

As expected, TAGs were the predominating lipid class in the primary organ of energy storage (WAT), although BAT has a comparable distribution (see figure 10). While NFD and HFD treatments indicated statistically similar TAG levels, linseed oil supplemented diets crucially altered the TAG content. Particularly, 10% GLO marked the highest TAG accumulation, significantly to all other groups, followed by the 10% LO supplementation. 1% Treatments showed intermediate levels which are higher than NFD and HFD but lower than the 10% groups. Thus, the linseed oil supplementation increased the TAG storage relative to the other two diets. DAG followed a similar pattern, with slightly different significances, but again 10% GLO indicated the greatest elevation of the DAG content. While DAG levels were significantly decreased in NFD and HFD compared to 10% GLO, the other three groups showed no statistical significance (see figure 11). These groups moderately elevated DAG, suggesting that even a smaller dose of linseed oil supplementation might alter the DAG distribution or rather composition. Interestingly, the graphs propose both an increased TAG accumulation and a simultaneous upregulation of β-oxidation. At first glance, this observation seems to be surprising, as

enhanced β-oxidation is typically associated with reduced lipid storage. However, the pattern shown may indicate a dynamic lipid turnover, where an elevated TAG content reflects an increased substrate availability for β-oxidation. This aligns with a study from X. X. Yu et al., (2002) in which a simultaneous upregulation of glucose uptake, *de novo* fatty acid synthesis and β-oxidation during cold exposure was observed. Although their study did not specifically assess the coordinated upregulation of TAG levels and fatty acid oxidation, the simultaneous stimulation of lipid breakdown and synthesis highlighted the capacity of BAT to store and oxidize lipids concurrently.

Unlike WAT, BAT is specialized on energy expenditure, thermogenic capacity and containing high mitochondria density and smaller lipid droplets (Cannon & Nedergaard, 2004). Aligning with our results the lipid composition of BAT is slightly different with phospholipids being the predominating form of lipids and a lower lipid storage in form of TAG and DAG. For instance, in BAT PE and PC were higher than in WAT under the same diet, whereas interestingly PI was higher in WAT than in BAT. TAG was comparatively lower. Except PI, these results concur with previous lipidomic analyses showing BAT is enriched in membrane lipids in comparison to WAT (Leiria & Tseng, 2020). In our study HFD marked a trend of elevated TAG area compared to NFD, consistent with increased lipid deposition. However, this increase did not reach statistical significance. While TAG levels were lowest in the 1% LO group, both 10% LO and 1% GLO showed an intermediate TAG pool. However, 10% GLO represented the highest TAG accumulation. DAG did not dramatically differ among groups, except the 10% GLO treatment, which significantly elevated DAG levels compared to the other groups. The availability of ALA promoted lipid oxidation in BAT rather than contributing to DAG accumulation. Biochemically, omega-3 PUFAs can activate brown fat metabolism and mitochondrial activity, thereby promoting the utilization of fatty acids for heat production rather than storage. This aligns with our observations. Moreover, maintaining BAT function is crucial as active BAT plays a key role in facilitating TAG clearance from circulation and contributes to vascular lipoprotein homeostasis (Bartelt et al., 2011; Fernández-Galilea et al., 2020).

Liver TAG showed the lowest total area of all tissues aligning with the fact that an excessive lipid accumulation in the liver is associated with nonalcoholic fatty liver disease coupled with insulin resistance and type 2 diabetes mellitus (Nagle et al., 2009). The HFD

group showed higher values than NFD and 1% LO, although no significance could be detected. Interestingly, 10% LO had the biggest impact on the TAG accumulation, followed by 10% GLO and 1% GLO. Similar patterns could be observed in DAG liver, except this time 10% GLO indicated the strongest effect compared to the significantly lower NFD and HFD. The three other groups only showed intermediate impacts without any significance. Nagle et al., (2009) suggested that shunting excess fatty acids into TAG is an adaptive strategy that protects cells from lipotoxic intermediates. Thus, the high PUFA amount in 10% LO in liver, appears to sequester surplus ALA into TAG. However, chronic TAG storage can promote insulin resistance. Noteworthy, the 10% GLO diet mitigated the TAG accumulation relative to 10% LO. The accumulation of DAG likely reflects enhanced lipid turnover and membrane biosynthesis as it is an intermediate in TAG synthesis and responsible for phospholipid remodeling. In addition, DAG acts as a second messenger that activates protein kinase C isoforms, but nonetheless chronic elevation has been linked to insulin resistance. Therefore, DAG accumulation may signal both active lipid remodeling and a potential metabolic deficit (Verrier et al., 2004).

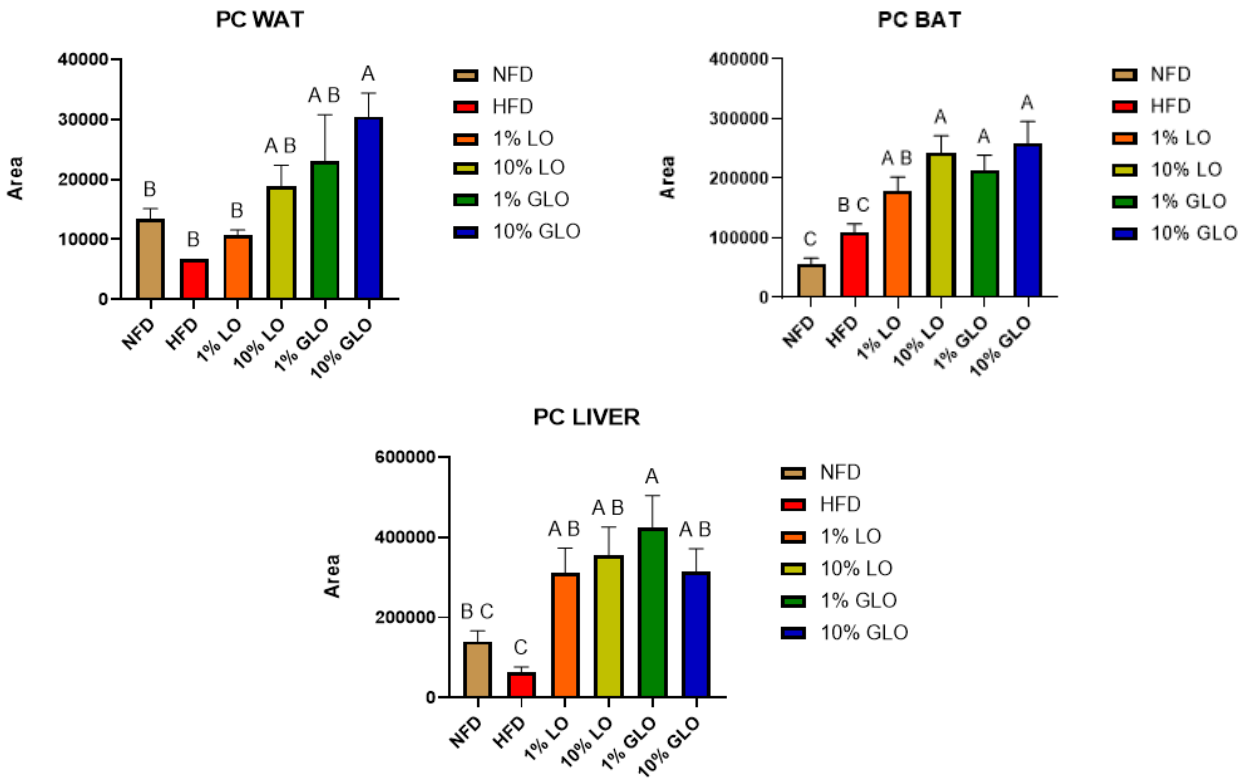

Figure 12: Relative distribution (Area) of total detected PC in WAT, BAT, & liver of C57BL/6 wild-type mice. Data are presented as mean ± SEM (n>9). Statistical significance was determined using one-way ANOVA followed by Tukey's multiple comparison test. Groups labeled with different letters are significantly different ($p < 0.05$).

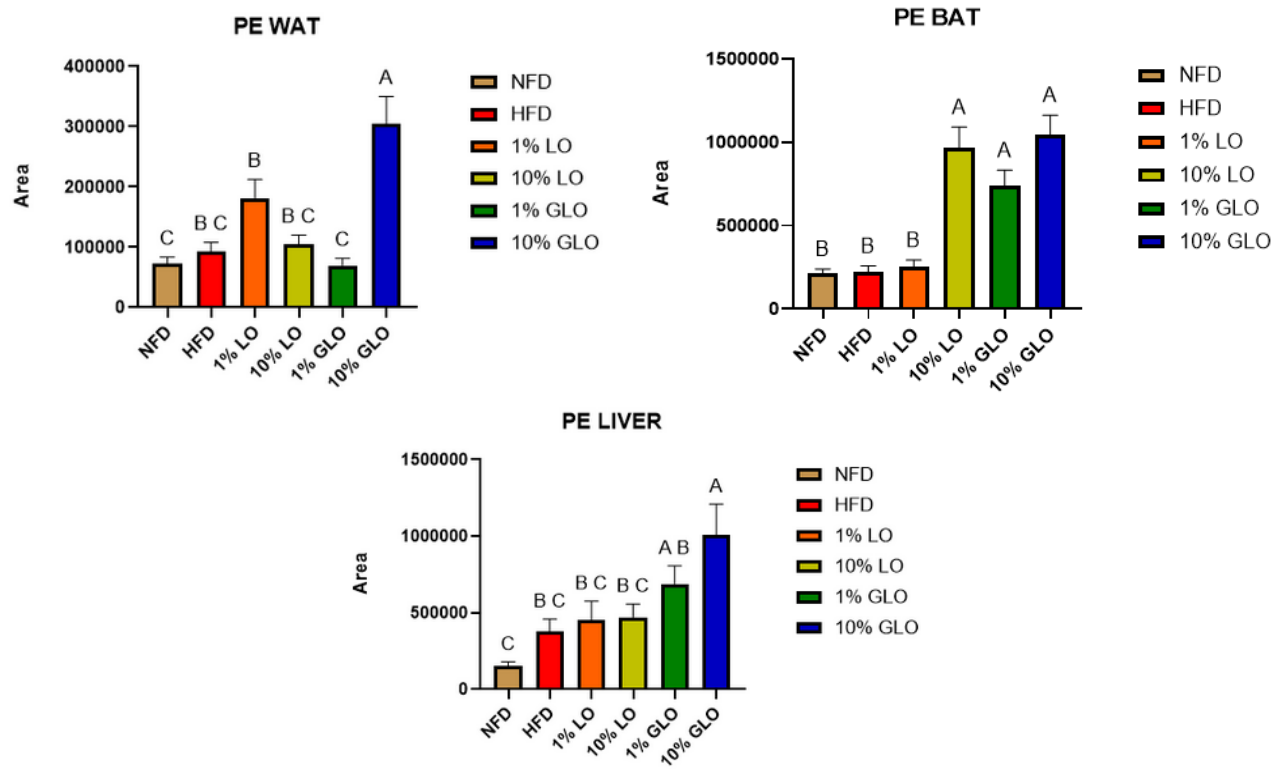

Figure 13: Relative distribution (Area) of total detected PE in WAT, BAT, & liver of C57BL/6 wild-type mice. Data are presented as mean ± SEM (n>9). Statistical significance was determined using one-way ANOVA followed by Tukey's multiple comparison test. Groups labeled with different letters are significantly different ($p < 0.05$).

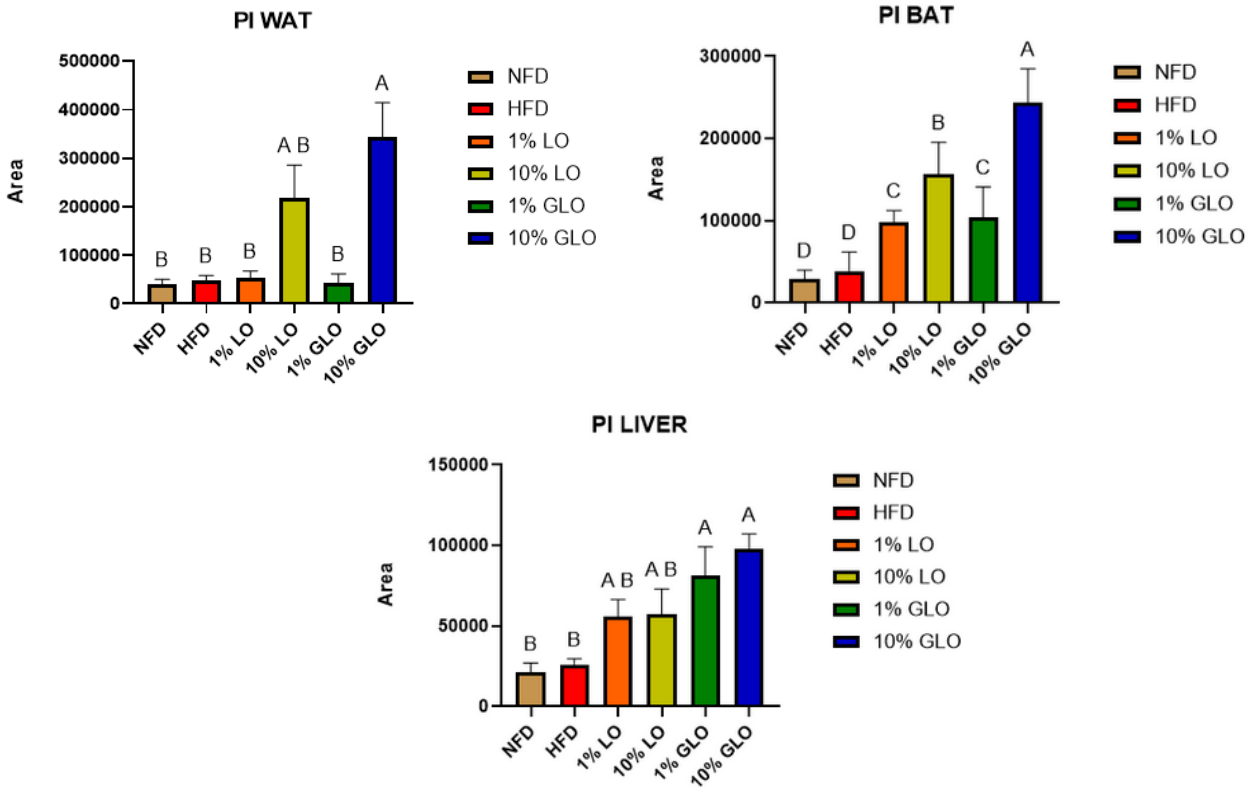

Figure 14: Relative distribution (Area) of total detected PI in WAT, BAT, & liver of C57BL/6 wild-type mice. Data are presented as mean ± SEM (n>9). Statistical significance was determined using one-way ANOVA followed by Tukey's multiple comparison test. Groups labeled with different letters are significantly different ($p < 0.05$).

The linseed oil supplementation also had an impact on the phospholipid composition of WAT. While PC and PE are key components of cell membranes, PI is a minor yet important signaling lipid. NFD, HFD and interestingly 1% LO had the lowest PC levels. Diets with higher LO content or rather GLO increased the PC level, with 10% GLO being significantly above the first three diets (see figure 12). PE area was lowest in NFD, 1% GLO and 10% LO, indicating minimal differences. Interestingly, 1% LO resulted in a marked increase in PE levels and again 10% GLO showed the highest PE content (see figure 13). In comparison to PE and PC, PI showed a quite different distribution, as the two 10% supplementation groups were visually higher, with the 10% GLO group being again significant to the other four treatments (see figure 14). The coordinated increase in phospholipid levels with linseed oil supplementation suggests enhanced membrane lipid synthesis or remodeling in adipocytes, which enlarge with more TAG and therefore require extra phospholipids for expanding lipid droplet surfaces and cellular membranes (Leiria & Tseng, 2020).

The phospholipid classes in BAT remained relatively high across all groups, reflecting the tissue's need for membrane integrity and mitochondrial membranes. Throughout all classes NFD remained at the lowest compared to the other groups. HFD showed a slight increase in phospholipid levels, but no significance could be seen. Supplementation with 1% LO already increased PC levels significantly compared to NFD, while 10% LO, 1% GLO and 10% GLO reached the highest PC values. PE levels were significantly higher in the same groups as in PC. PI accumulates the most in the 10% GLO group, followed by intermediate levels at 10% LO and 1% GLO, which are all significant compared to NFD and HFD. This strengthens the assumption of membrane remodeling and mitochondrial biogenesis, as PE and PC are abundant in membranes and PI is important for lipid signaling. By providing ALA through the supplementation with linseed, it can enhance the unsaturation of phospholipids in BAT, potentially improving membrane fluidity (Di Paolo & De Camilli, 2006; Shabalina et al., 2013; Van Meer et al., 2008).

In summary phospholipids in liver showed a relatively high area, whereby PC, PE and PI were elevated by LO supplementation especially by the germinated seeds. PE and PI showed very similar patterns whereas PC had a slightly different beam distribution due to the high accumulation in the 1% GLO group. The boost in phospholipids mostly

facilitated membrane expansion and VLDL-mediated lipid export, which are beneficial adaptations in the context of high-fat intake. To better understand how individual lipid species behave under different dietary treatments and across tissues, a subsequent targeted lipidomic analysis was performed. This approach enables a more precise quantification of key compounds and supports the untargeted findings with higher analytical resolution. These findings align with studies from H. Han et al., (2017)- and Nagle et al., (2009) where enrichment of hepatic phospholipids and improved phospholipid: TAG ratios are hallmarks of reduced steatosis. One outcome of the study from H. Han et al., (2017) was that dietary supplementation with linseed alleviated western-type-diet induced nonalcoholic fatty liver disease by improving hepatic lipid homeostasis and reduction in oxidative stress as well as suppression of inflammatory responses.

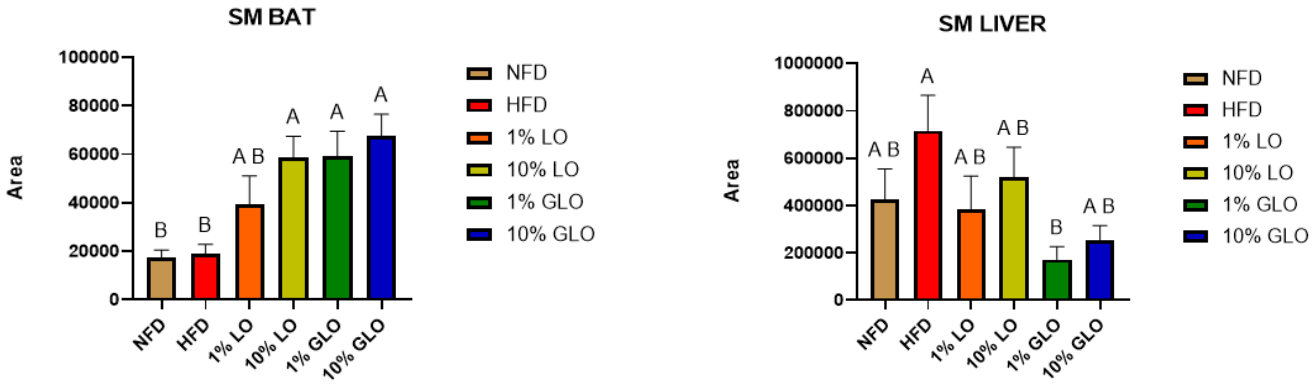

Figure 15: Relative distribution (Area) of total detected SM in WAT, BAT, & liver of C57BL/6 wild-type mice. Data are presented as mean ± SEM (n>9). Statistical significance was determined using one-way ANOVA followed by Tukey's multiple comparison test. Groups labeled with different letters are significantly different ($p < 0.05$).

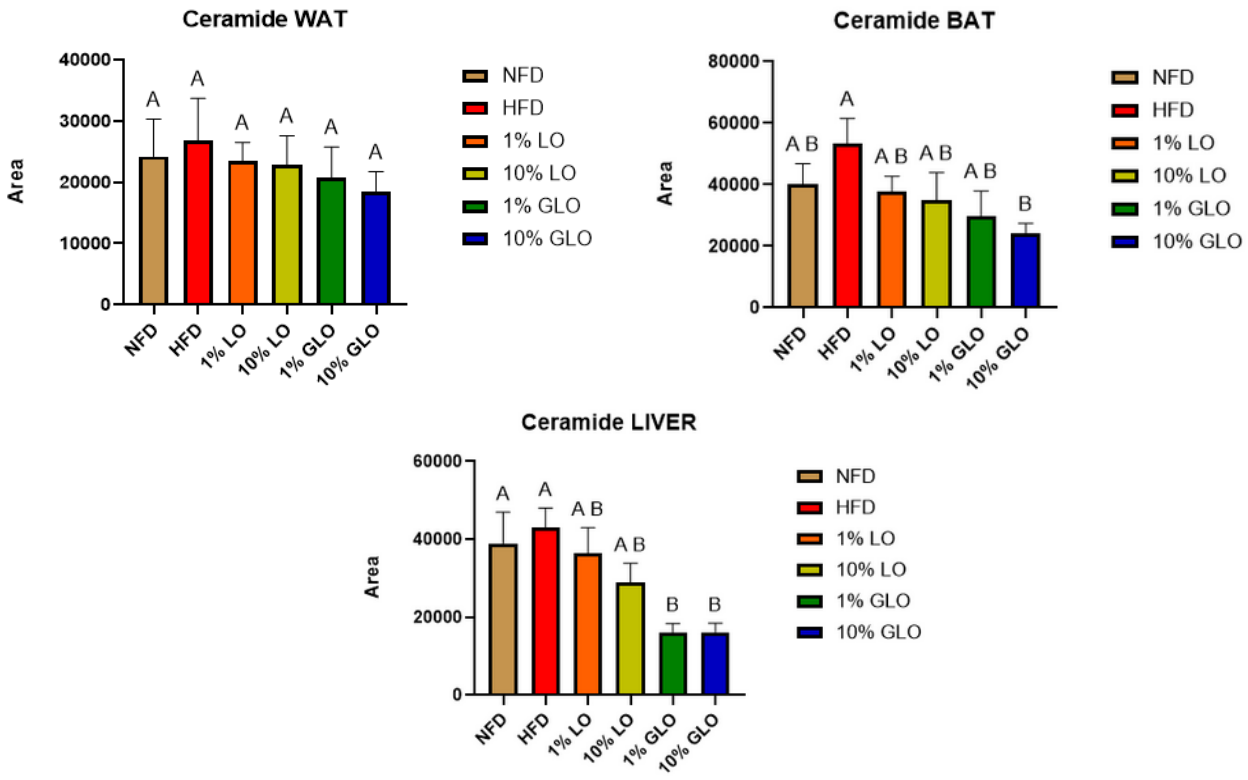

Figure 16: Relative distribution (Area) of total detected ceramide in WAT, BAT, & liver of C57BL/6 wild-type mice. Data are presented as mean ± SEM (n>9). Statistical significance was determined using one-way ANOVA followed by Tukey's multiple comparison test. Groups labeled with different letters are significantly different ($p < 0.05$).

Unlike the other lipids, the ceramide levels in WAT were stable across all diets (see figure 16). Surprisingly, neither HFD nor linseed interventions significantly altered the WAT ceramide content, which is interesting as ceramides often accumulate with obesity and high fat intake (Kolak et al., 2007). We suggest that either the HFD-induced ceramide rise was counteracted by the linseed oil's metabolic effects, especially in its germinated version, yielding comparable ceramide levels, or that the ceramide metabolism was buffered or already elevated, also in NFD (Herchi et al., 2015). Not only a decrease in ceramide but also an unchanged pool is a positive sign, even when storing more TAG, as there is no additional lipotoxic ceramide buildup, which is positive due to the known negative impact on insulin signaling in adipocytes and pro-inflammatory effects (Leiria & Tseng, 2020). Noteworthy, no SM data for WAT was reported due to insufficient identification, which aligns with the already low SM content in WAT (see figure 15). Furthermore, it meets the expectation that white fat cells have less membranes relative to stored fat, and thus low measurable sphingolipids.

In BAT SM was quantifiable unlike in WAT, with 10% GLO showing the highest values, next to 1% GLO and 10% LO. 1% LO marked intermediate effects without any statistical significance to NFD and HFD. Dietary treatments also produced distinct changes in BAT ceramide content. The HFD group displayed the highest ceramide pool in BAT, in contrast to the 10% GLO diet, which yields the lowest ceramide accumulation. The remaining groups showed intermediate ceramide concentrations. SM and ceramides are closely linked within the sphingolipid pathway. SM serves as a structural membrane lipid, while ceramide is a bioactive lipid that promotes insulin resistance and inflammation. The shift indicated in the graphs above, suggest a beneficial effect, as higher SM supports membrane integrity and signaling, while a reduction in ceramide levels alleviate lipotoxic stress and improve insulin sensitivity. But nonetheless this distribution should be interpreted with caution as SM is a precursor of ceramide and a high accumulation of this phospholipid might also be an indicator for a high ceramide turnover rate. (Albeituni & Stiban, 2019; Slotte, 2013; Y. Zhao et al., 2024).

In comparison to BAT, SM and ceramides showed a very similar distribution in liver, which might be favorable for positive metabolic activity. In both graphs HFD had the greatest peak, whereas GLO marked visually lower beams. This reduction is metabolically important as ceramides and SMs are not just markers of lipid imbalance, but they also actively contribute to liver and metabolic pathology. In accordance with our data LO and especially GLO likely increased health outcomes due to improved hepatic insulin resistance and steatosis (Dong et al., 2017; X. Yu et al., 2018). These outcomes are also strengthened by the low ceramide pool and by the anti-inflammatory membrane profile. Overall, our data underscores beneficial effects of LO and GLO as they counteract the sphingolipid / ceramide related lipotoxicity of HFD. In SM the 1% GLO group was sufficient enough to normalize the pool, highlighting how even a low dose of a bioactive rich GLO can influence harmful lipid pathways.

To sum it up, a supplementation with LO and GLO, especially in its higher dosed form, substantially altered the WAT lipidome by increasing the storage lipid fraction, specified as TAG and DAG, and expanding the phospholipid pool without worsening the ceramide accumulation, resulting in a metabolically favorable impact of LO and especially GLO. Extra dietary fats, rich in ALA, were most likely channeled into adipose TAG stores instead

of leading to an extensive lipid spillover, aligning with prior results that have shown that an omega-3 PUFA intake promotes healthy adipose expansion, which resulted in smaller adipocyte size, leading to more but yet less hypertrophic fat cells alongside significantly lower inflammatory markers in fat (Baranowski et al., 2012). This concurs with our findings, as the supplementation in WAT, although containing more TAG, did not show an increase in ceramides. By providing PUFAs, GLO and LO may enhance the adipocyte`s capacity to form polyunsaturated phospholipids and TAG, thereby buffering excess fatty acids into inert storage, which is metabolically beneficial as it prevents lipotoxic intermediate build-up in non-adipose organs (Leiria & Tseng, 2020). In addition, 10% supplementation caused far greater alterations than 1% and germination further amplified certain responses, especially due to the enriched antioxidants and bioactive components. (Pointner et al., 2024).

The preservation of a high phospholipid profile coupled with low TAG and DAG in BAT with LO and GLO has notable biological implications. Active BAT requires plenty of membrane lipids and less fat droplet load to function optimally. Our results suggest that LO, particularly at a 10% concentration, contributed to the maintenance of BAT in a more metabolically active thermogenic state. By limiting the TAG accumulation through omega-3 fatty acids, especially when a conversion into EPA and DHA was possible, LO may have prevented the HFD-induced decline in BAT activity, aligning with literature that reports mitigation of HFD effects by enhancing oxidative metabolism in BAT (Smorenburg et al., 2025; Van Meer et al., 2008). Improvements like a decline in ceramide and an increase in TAG might favorably modulate BAT, as the metabolically active state consumes more fatty acids and glucose, contributing to the overall energy expenditure and insulin sensitivity (Dátilo et al., 2018). Moreover, the 10% GLO group showed the greatest trends in maintaining a lipid balance, suggesting that the additional nutrients such as antioxidants and vitamins from germination further support the oxidative capacity. Higher Tocopherol content might protect lipids from oxidative damage during thermogenesis, thereby sustaining mitochondrial function (Pointner et al., 2024). Overall, LO, particularly GLO supplementation aided to prevent BAT from becoming an energy storing tissue and kept it towards an energy burning tissue.

4.3 Targeted Metabolomics

This section provides a quantitative analysis of how different dietary treatments influences tissue specific distribution of selected acylcarnitines. The results were investigated in the context of lipid metabolism, mitochondrial function and fatty acid oxidation or rather the transport of fatty acids. Consequently, this study focused primarily on carnitine species, which were the most consistently quantifiable and biologically informative metabolite group in the present context.

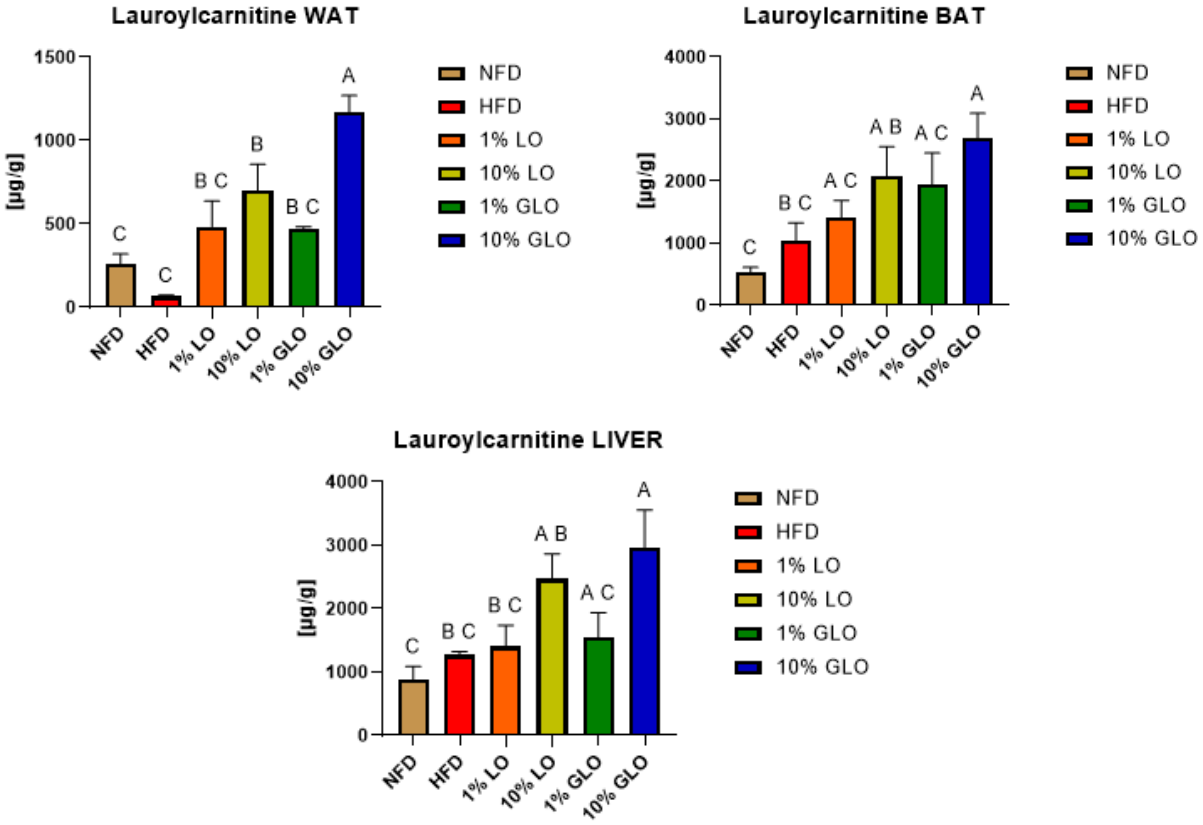

Figure 17: Absolute distribution (µg/g) of total detected lauroylcarnitine in WAT, BAT, & liver of C57BL/6 wild-type mice. Data are presented as mean ± SEM (n>9). Statistical significance was determined using one-way ANOVA followed by Tukey's multiple comparison test. Groups labeled with different letters are significantly different ($p < 0.05$).

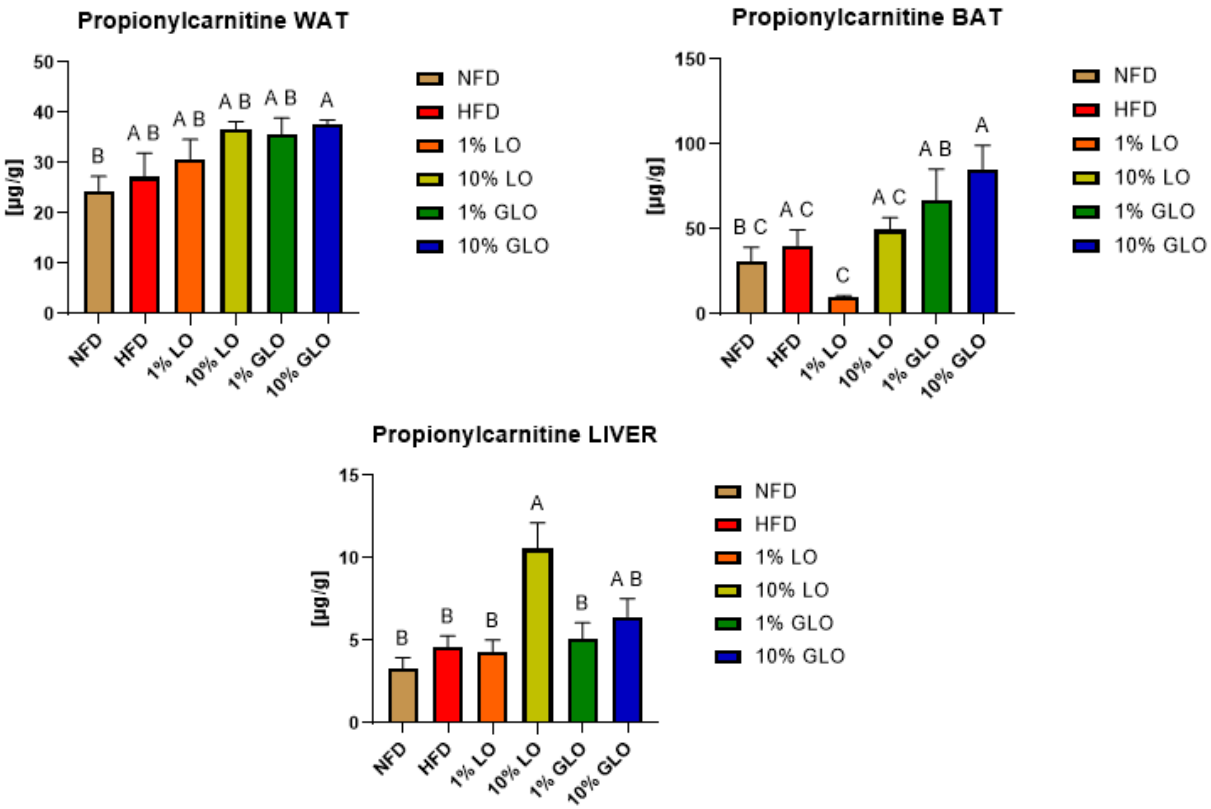

Figure 18: Absolute distribution (µg/g) of total detected propionylcarnitine in WAT, BAT, & liver of C57BL/6 wild-type mice. Data are presented as mean ± SEM (n>9). Statistical significance was determined using one-way ANOVA followed by Tukey's multiple comparison test. Groups labeled with different letters are significantly different ($p < 0.05$).

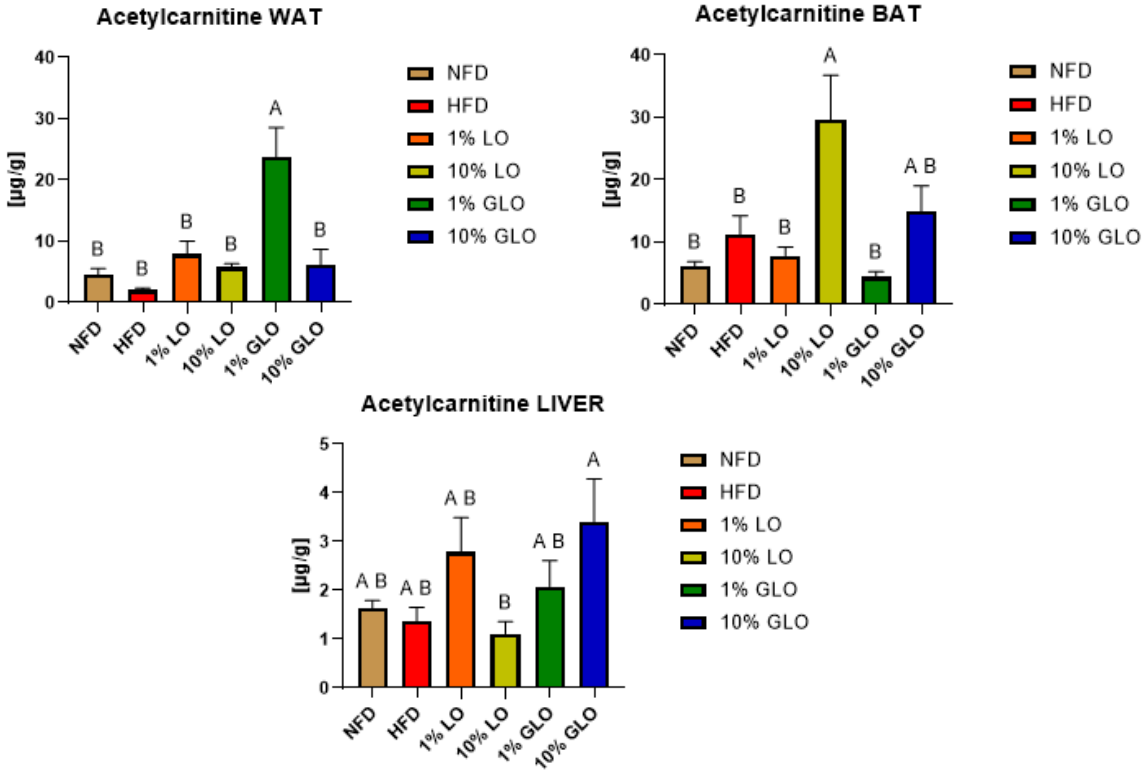

Figure 19: Absolute distribution (µg/g) of total detected acetylcarnitine in WAT, BAT, & liver of C57BL/6 wild-type mice. Data are presented as mean ± SEM (n>9). Statistical significance was determined using one-way ANOVA followed by Tukey's multiple comparison test. Groups labeled with different letters are significantly different ($p < 0.05$).

BAT showed consistently high carnitine content throughout all dietary treatments, which is very consistent with its dominant role in mitochondrial metabolism and fatty acid oxidation (Cannon & Nedergaard, 2004) (see figure 17-19). The high carnitine content in BAT was already evident in the untargeted metabolomics analysis, underlining BAT's high mitochondrial activity even before targeted validation. WAT had an intermediate pool of carnitines and liver had the lowest concentration of acetylcarnitine and propionylcarnitine. According to the graphs, the LO and GLO groups showed higher values compared to NFD and HFD. One interesting finding was the high concentrations of lauroylcarnitine, also known as dodecanoylcarnitine. In a study from Simcox et al., (2017) it has been shown that acylcarnitine levels in liver increase within one hour during cold exposure. In WAT both 10% LO and 10% GLO significantly raised lauroylcarnitine in comparison to NFD and HFD. BAT and liver showed a similar distribution as all omega-3 enriched diets increased the acylcarnitine level (see figure 17). Across all three tissues, it can be seen that the 1% supplementation group had less impact on the accumulation than the 10% groups. Together, these patterns strengthen the assumption that LO and GLO enhanced the medium/long chain fatty acid transport into the mitochondria. Omega-3 PUFAs, especially ALA are known to activate PPARα and increase the entry into mitochondria via CPT1 (Popeijus et al., 2014). Propionylcarnitine showed a little more subtle changes, especially when it comes to WAT, where 10% GLO again marks the highest beam, but only statistically significant to NFD. Surprisingly, in the high mitochondrial dense tissue BAT, 1% LO indicated the lowest accumulation, whereas the other supplementation groups are visually higher than NFD and HFD, particularly 1% GLO and 10% GLO increased propionylcarnitine, marking once again the positive effects of germination. In liver the distribution shows a little maintenance throughout the graph, with 10% LO being significantly higher than all groups except 10% GLO (see figure 18). Interestingly, acetylcarnitine did not follow a linear dose response to GLO supplementation. Overall, the linseed oil groups once again had the greatest impact on carnitine accumulation. While in WAT 1% GLO was significantly dominant, in BAT 10% LO showed the highest values with a statistical significance compared to all groups except 10% GLO. In liver 10% GLO represented the greatest rise in carnitine levels (see figure 19). Due to the discrepancies in regard to the dose dependent treatment, it might be that this pattern may reflect a metabolic threshold, where moderate stimulation of β-

oxidation leads to acetyl-CoA accumulation that is buffered into acetylcarnitine and therefore regulating energy flow and preventing from energetic imbalance (Davies et al., 2016).

To sum it up, GLO had the biggest impact and showed the largest increases in the investigated acylcarnitines. In almost every case, the 10% GLO group was significantly different from NFD and HFD, whereas HFD barely increased the carnitine level above the NFD threshold. For instance, lauroylcarnitine remained high in GLO groups throughout all tissues. Our results suggest that the germination of the oil mediated additional bioactivity beyond the known effects of omega-3 PUFAs. Moreover, Popeijus et al., (2014) showed that ALA drives the PPARα transactivation and CPT1 expression, whereas Lemas et al., (2012) found that omega-3 PUFAs can increase hepatic CPT1-mediated β-oxidation. Furthermore, elevated carnitine levels are consistent with increased mitochondrial uptake of fatty acids, as carnitine shuttles transport long-chain acyl groups into the mitochondria for β-oxidation. Particularly the intense rise of lauroylcarnitine after the GLO supplementation suggests an upregulation of CPT1 and CPT2, which subsequently allows a greater long chain acyl group entrance into the matrix (Cannon & Nedergaard, 2004). Besides the already mentioned facts, germination enhances the content of antioxidative and bioactive compounds in linseed oil, which might prevent mitochondrial lipid peroxidation and promote oxidative stability (Pointner et al., 2024). These effects may thus affect sustained β-oxidation within the GLO treatments. Noteworthy, the observed increase in tissue acylcarnitine concentrations most likely reflects a positive metabolic adaption rather than a pathological accumulation. While elevated plasma acylcarnitines are also associated with incomplete β-oxidation in metabolic disorders like type 2 diabetes and obesity, the current pattern in combination with the dietary treatments are expected to improve oxidation. The consistent upregulation of acylcarnitines, especially lauroylcarnitine, in the 10% GLO group represents a robust and reproducible dietary effect. The accumulation of the medium/long-chain fatty acid lauroylcarnitine and acetylcarnitine, suggests an improved mitochondrial fatty acid throughput (Cannon & Nedergaard, 2004; Koves et al., 2008). Therefore, our results support the interpretation that the specific acylcarnitine profile with its shifts represents a beneficial metabolic activity by enhancing β-oxidation due to

the modulation of carnitine metabolism and mitochondrial transport via the GLO supplementation.

4.4 Targeted Lipidomics

Lipidomic profiling was performed using a targeted approach, to quantify individual lipid species in metabolically active tissue throughout several dietary treatments. Given the key role of lipid species distribution in regulating membrane function, signaling pathways and lipotoxic stress, this approach provides insights into how the dietary interventions modulate tissue specific lipid homeostasis. In particular lipid subclasses out of TAG, DAG, PC, PE, PI, SM and ceramide were examined due to their established relevance in metabolic regulation.

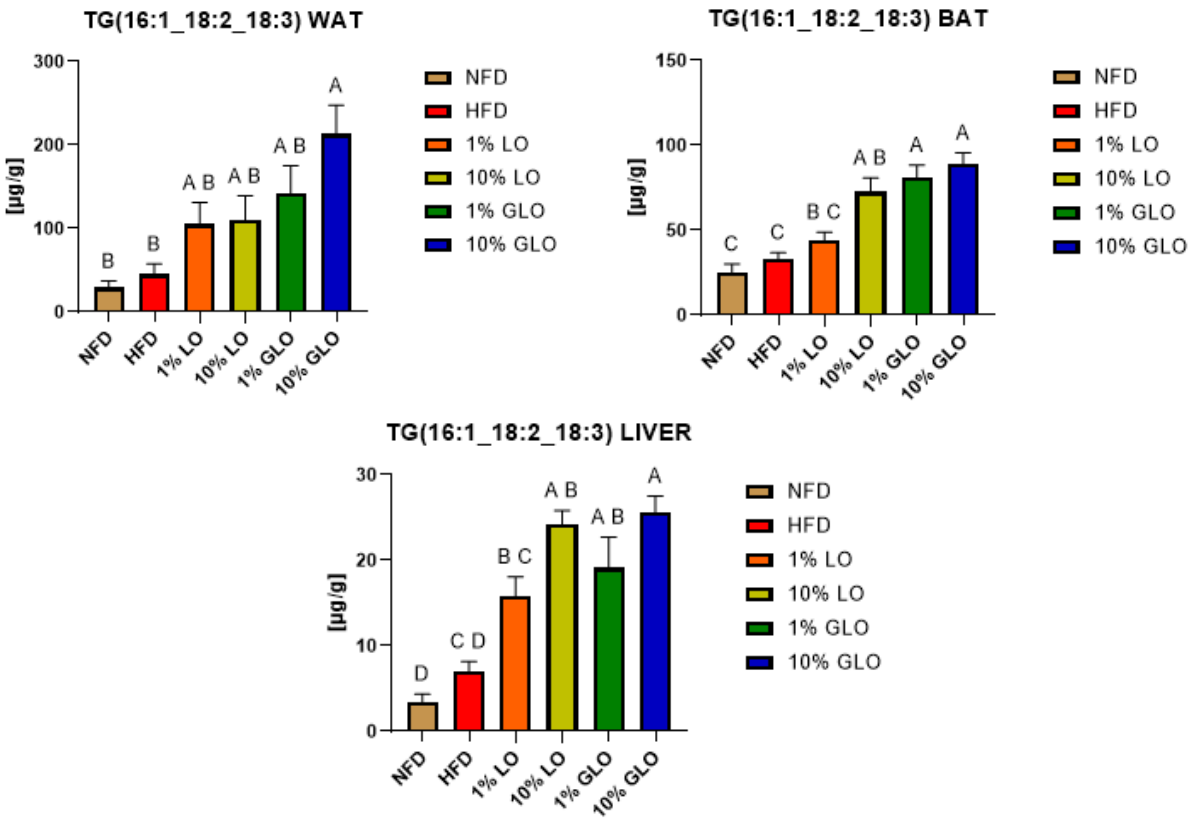

Figure 20: Absolute distribution (µg/g) of total detected 3-[hexadec-9-enoyloxy]-2-[octadeca-9,12-dienoyloxy]propyl-octadeca-6,9,12-trienoate (TG(16:1_18:2_18:3)) in WAT, BAT, & liver of C57BL/6 wild-type mice. Data are presented as mean ± SEM (n>9). Statistical significance was determined using one-way ANOVA followed by Tukey's multiple comparison test. Groups labeled with different letters are significantly different ($p < 0.05$).

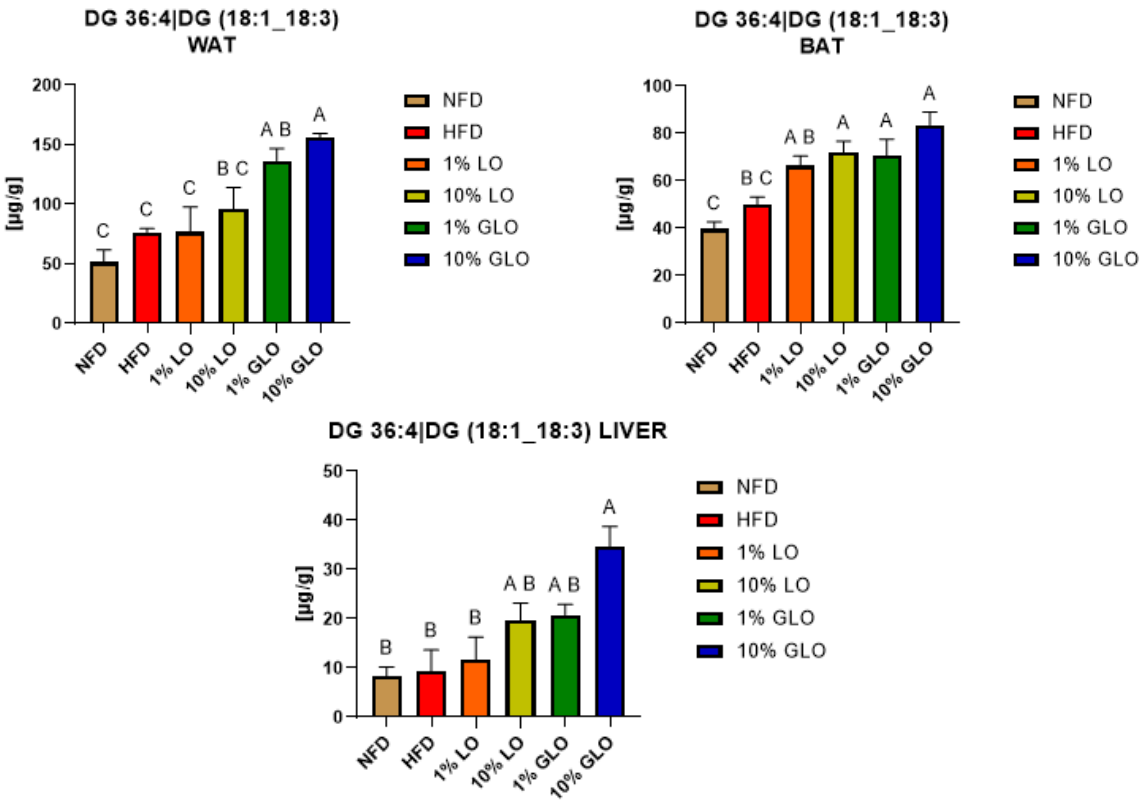

Figure 21: Absolute distribution (µg/g) of total detected 1-hydroxy-3-[octadec-9-enoyloxy]propan-2-yl-octadeca-9,12,15-trienoate (DG 36:4|DG (18:1_18:3) in WAT, BAT, & liver of C57BL/6 wild-type mice. Data are presented as mean ± SEM (n>9). Statistical significance was determined using one-way ANOVA followed by Tukey's multiple comparison test. Groups labeled with different letters are significantly different ($p < 0.05$).

One of the several identified lipid species was 3-[hexadec-9-enoyloxy]-2-[-octadeca-9,12-dienoyloxy]propyl-octadeca-6,9,12-trienoate, which is shortly known as TG(16:1_18:2_18:3), composed of palmitoleic, linoleic and α-linolenic acid. The concentrations rise consistently within the supplemented groups, whereby across all three tissues the 10% GLO group showed the highest impact. In WAT and BAT 1% GLO showed the second highest accumulation of TG(16:1_18:2_18:3). Levels of this lipid species were significantly lower in NFD and HFD across all three tissue types (see figure 20). The concentrations are biologically plausible as WAT is the primary organ for lipid storage, whereas BAT has a high turnover rate and liver is generally low in TAG and DAG (Cannon & Nedergaard, 2004; Heinonen et al., 2020; Trefts et al., 2017). The fatty acid pattern reflects an improved inclusion of dietary unsaturated fatty acids into adipose storage lipids. The certain accumulation of ALA in WAT of GLO supplemented mice, represented by TG(16:1_18:2_18:3), suggests that GLO provides abundant omega-3 precursors that are efficiently deposited in adipocytes, which is favorable as the

enhancement or rather enrichment of PUFAs may improve lipid storage capacity and fluidity of lipid droplets, leading to a prevention of excessive saturated fat deposition (Zhang et al., 2023). Furthermore 16:1 is a lipokine associated with beneficial effects on metabolic health, due to the fact that elevated levels may indicate improved adipocyte function, which is strengthened by the study of Cao et al., (2008). In addition, dietary treatments with linseed oil, especially linseed oil from germinated seeds, have been shown to increase adiponectin release from WAT and upregulation of β-oxidation. Adiponectin is thought to stand in relation to obesity prevention (Seike et al., 2024). Therefore, higher adiponectin and fatty acid oxidation in WAT limits undesired fat accumulation, leading to the assumption that our results with a GLO induced enrichment with unsaturated TAGs, together with previous reports suggest a shift towards a metabolically healthier pattern of adipose tissue expansion. The presence of 16:1 and 18:3 in BAT TAG of GLO fed mice suggests an improved lipid turnover or rather an enhanced uptake of essential fatty acids. This corresponds to more readily oxidizable substrate in brown fat, as unsaturated fatty acids are preferred for mitochondrial β-oxidation (Cannon & Nedergaard, 2004). Moreover, ALA can be endogenously converted into EPA and DHA leading to an incorporation into phospholipids, thereby potentially enhancing mitochondrial membrane integrity and thermogenic activity (Takić et al., 2024). Seike et al., (2024) suggested that UCP-1, which is highly expressed by LO and activated by adiponectin and omega-3 PUFAs, contributes to obesity prevention and induction of thermogenesis in BAT. It is plausible that the GLO and LO treatment promoted fatty acid oxidation by upregulating UCP-1 and mitochondrial abundance in BAT, potentially driven by increased adiponectin levels. Among all measured species TG(16:1_18:2_18:3) was relatively low in HFD, although it was expected that HFD leads to substantial TAG deposition in liver. The rise in the supplemented groups indicated positive effects, as there might be higher hepatic content of ALA and less saturated lipids. Importantly, the concentrations were lower than in adipose tissue. Another critical factor is hepatic DAG, in this case 1-hydroxy-3-[octadec-9-enoyloxy]propan-2-yl-octadeca-9,12,15-trienoate, shortly known as DG 36:4|DG (18:1_18:3). On the one hand an accumulation of DAG is a likely driver of insulin resistance and on the other hand the adiponectin elevation by LO can exert positive effects on liver, as hepatic receptors like the adiponectin receptor 2 activate AMPK and increases fatty acid oxidation while

simultaneously inhibiting *de novo* lipogenesis (Wang et al., 2016). Our data suggests that LO and GLO treatments increase unsaturated DAG species in adipose tissue. A study from Perdomo et al., (2015) mentioned that this species can have protective effects against saturated fat induced insulin resistance, due to the included monounsaturated oleic acid. Nevertheless, the rise in DAG still means that alterations take place, whether they are negative or positive cannot be excluded yet. While oleic acid or ALA may be metabolically beneficial, the overall elevated DAG pool could still impact signaling pathways. A study from Bergman et al., (2012) indicated that only saturated DAG in membranes are related to insulin resistance. Future studies of this DAG constellation in adipose tissue will be important to clarify functional consequences.

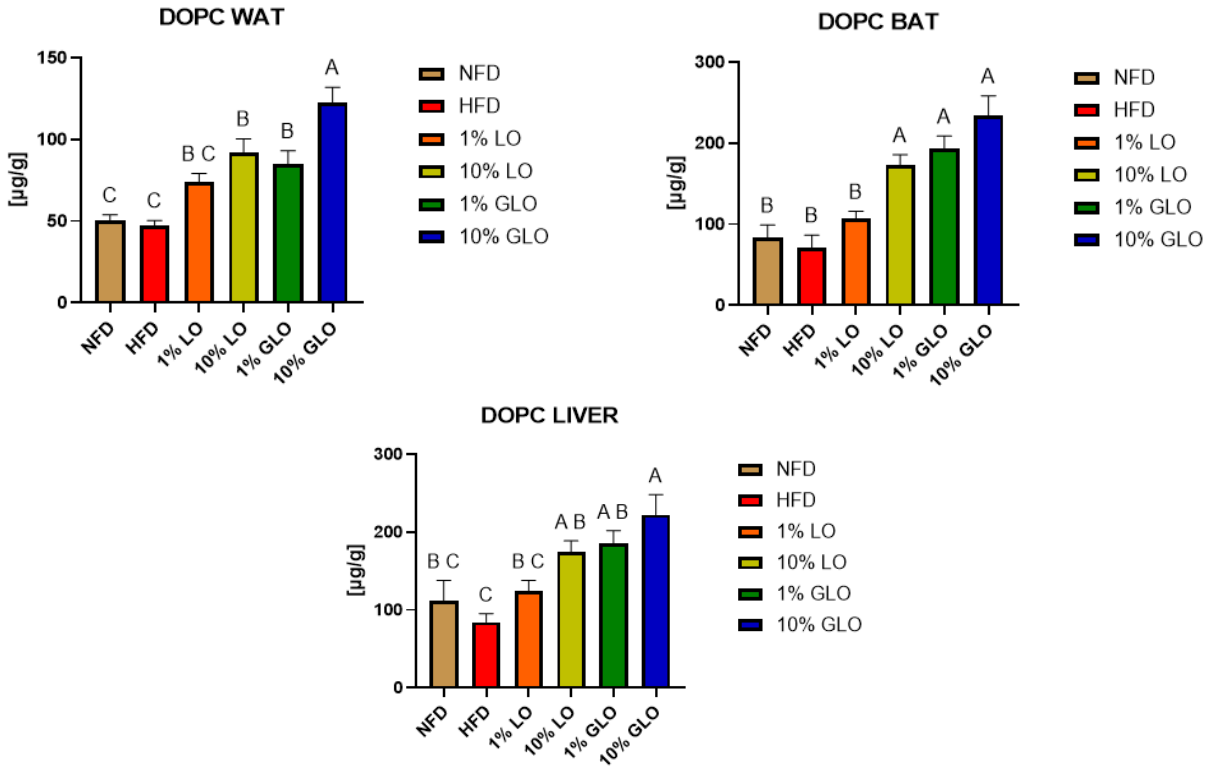

Figure 22: Absolute distribution (µg/g) of total detected 1,2-Dioleoyl-sn-glycero-3-phosphocholine (DOPC) in WAT, BAT, & liver of C57BL/6 wild-type mice. Data are presented as mean ± SEM (n>9). Statistical significance was determined using one-way ANOVA followed by Tukey's multiple comparison test. Groups labeled with different letters are significantly different ($p < 0.05$).

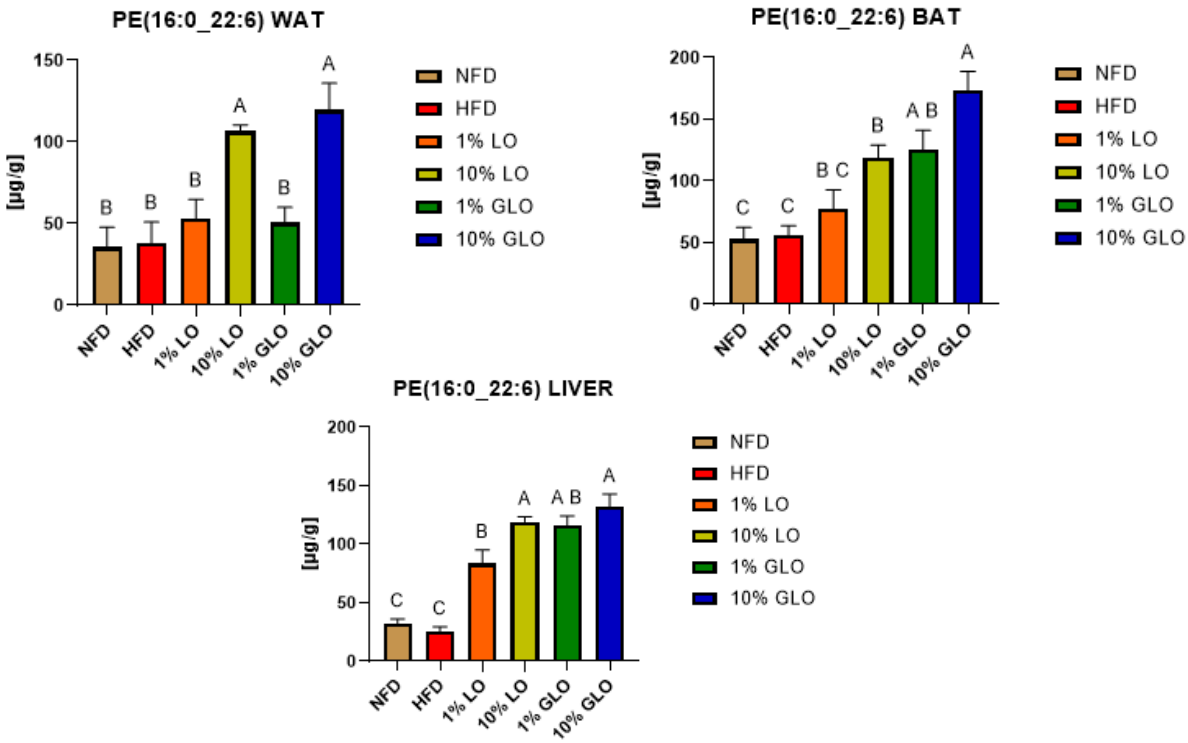

Figure 23: Absolute distribution (µg/g) of total detected 1-Palmitoyl-2-docosahexanoyl-sn-glycero-3-phosphoethanolamine (PE(16:0_22:6)) in WAT, BAT, & liver of C57BL/6 wild-type mice. Data are presented as mean ± SEM (n>9). Statistical significance was determined using one-way ANOVA followed by Tukey's multiple comparison test. Groups labeled with different letters are significantly different (p < 0.05).

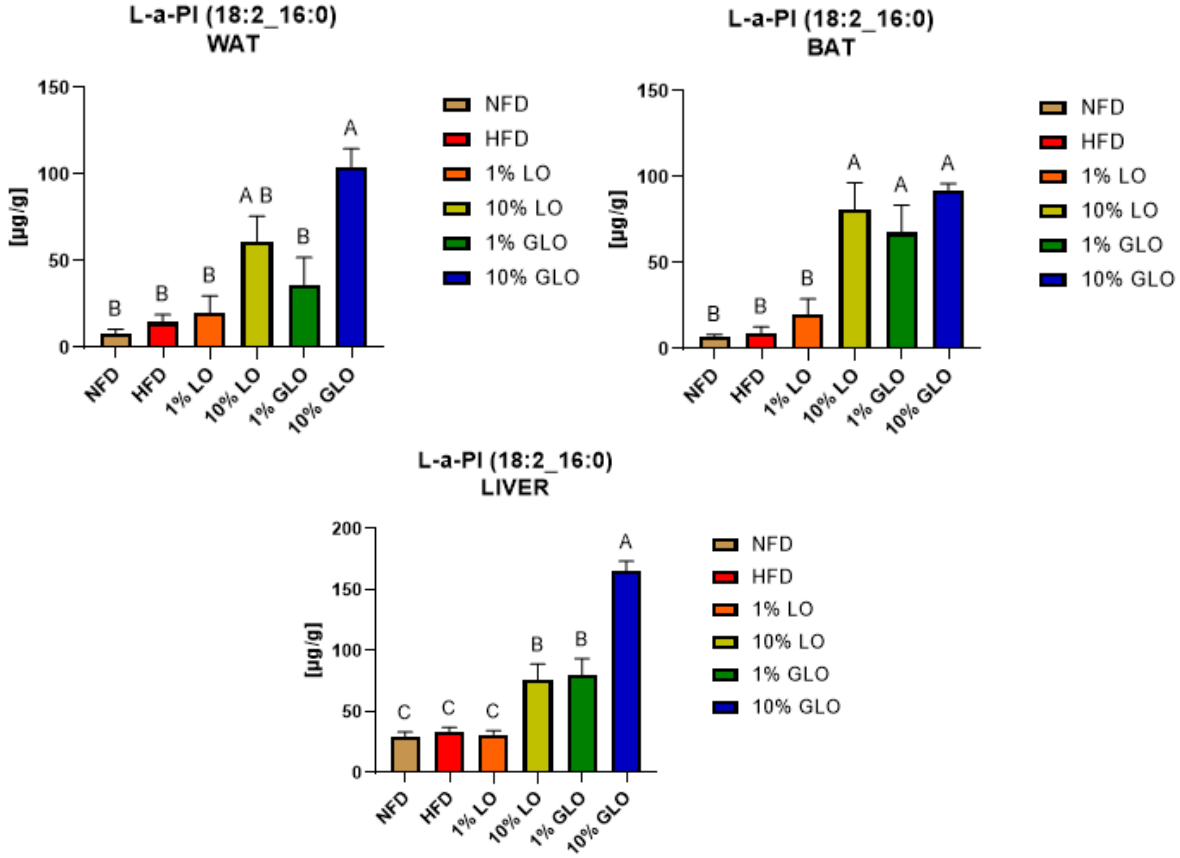

Figure 24: Absolute distribution (µg/g) of total detected 1-hexadecanoyl-2-(octadecadienoyl)-sn-glycero-3-phospho-D-myo-inositol (L-a-PI (18:2_16:0)) in WAT, BAT, & liver of C57BL/6 wild-type mice. Data are presented as mean ± SEM (n>9). Statistical significance was determined using one-way ANOVA followed by Tukey's multiple comparison test. Groups labeled with different letters are significantly different (p < 0.05).

The phospholipid distribution hints at a favorable adaptation, especially PC species that contain unsaturated fatty acids, such as 1,2-Dioleoyl-sn-glycero-3-phosphocholine, known as DOPC, which also has an 18:1 constellation. PCs like these form highly fluid bilayers, which allows greater lateral mobility and conformational flexibility of embedded proteins. Diets rich in saturated fat drive the *de novo* lipogenesis and incorporation of saturated acyl chains into membrane PCs, reducing membrane fluidity (O'Leary et al., 2018; Pilon, 2016). Shirouchi et al., (2007) has shown that PC enriched with omega 3-PUFAs significantly reduced the weight of WAT and hepatic lipid levels in rats, therefore it led to the enhancement in the activities of carnitine palmitoyltransferase and peroxisomal β-oxidation. Moreover, this diet reduced glucose levels and increased adiponectin levels. These results demonstrate that a specific PC composition can modulate tissue lipidomes and suggest that a diet rich in oleic acid would raise DOPC levels in cell membranes, thereby promoting a more fluid bilayer. Similarly, 1-palmitoyl-2-docosahexanoyl-sn-glycero-3-phosphoethanolamine, also known as PE(16:0_22:6), which contains palmitic acid and DHA, significantly increased in the 10% LO and 10% GLO groups. This suggests that some ALA from LO was converted to DHA and incorporated into PE. DHA is known to improve electron transport chain efficiency and ATP production when integrated into mitochondrial phospholipids. The presence of DHA in adipose lipids in GLO fed mice aligns with improved mitochondrial biogenesis and respiration in adipocytes, which concurs with increased mitochondrial content in WAT that typically leads to a browning effect or rather a brown like adipose phenotype (Fernández-Galilea et al., 2020; Smith, 2024). In addition, DHA is essential for maintaining normal brain function in adults and growth of infant's brains. Deficiency of DHA is associated with problems in learning and moreover it has positive impacts on diseases like hypertension, diabetes mellitus, arthritis and myocardial infarction (Horrocks & Yeo, 1999). Finally, figure 24 shows the distribution of 1-hexadecanoyl-2-(octadecadienoyl)-sn-glycero-3-phospho-D-myo-inositol, which is also known as L-α-PI(18:2_16:0). Diets rich in PUFAs tend to maintain PI(18:2_16:0) levels in adipose tissue. Our results showed that 10% LO and both GLO groups preserved PI(18:2_16:0), which may limit its desaturation to arachidonic acid 20:4, which acts as a precursor of pro-inflammatory eicosanoids. Literature suggests that an increase in linoleic acid does not necessarily raise tissue arachidonate levels but rather maintains a non-inflammatory

PUFA profile in membrane lipids (Rett & Whelan, 2011). In summary, GLO helps balancing the phospholipid profile in WAT, counteracting HFD induced membrane saturation. A reduction in PI (18:2) availability in adipose tissue was associated with an impaired PI3K/Akt signal path, systemic insulin resistance and alterations in lipid metabolism (Massey et al., 2023). The phospholipid content in BAT in LO diets, especially in the 10% GLO group, was significantly higher compared to the phospholipid levels in NFD and HFD. This rise in unsaturated phospholipids in BAT could facilitate more dynamic mitochondrial membranes and efficient use of UCP-1, as the mitochondria in BAT relies on fluid membranes for proper coupling and uncoupling processes. Furthermore, a high content of unsaturated fatty acids and PE is essential for optimal function, which aligns with the increase DHA content after the LO and GLO treatments, which likely improved mitochondrial oxidative capacity (Shabalina et al., 2013; Smith, 2024). DHA in hepatic PE was significantly increased by 10% GLO in comparison to NFD, HFD and interestingly to 1% LO. DHA in liver promotes multiple protective effects, such as the inhibition of lipogenesis via the suppression of SREBP-1c, which occurs via the inhibition of the proteolytic activation of this full-length protein. This suppression is mediated by AMPK phosphorylation of serine 365. In addition, DHA also downregulates mechanistic Target of Rapamycin Complex 1-ribosomal protein S6 kinase beta-1 (mTORC1-p70S6K) signaling, a pathway involved in cellular growth and lipid biosynthesis, further contributing to the anti-lipogenic effects of DHA (Deng et al., 2015). In our context, it likely led to enhanced β-oxidation, as the increased DHA content helps disposing fatty acids that would otherwise form TAG droplets. This interpretation is consistent with findings from related studies. For instance, Wang et al., (2016) demonstrated that LO, rich in ALA, alleviated alcoholic fatty liver disease in mice by activating AMPK and improving hepatic fatty acid oxidation. This, together with suppression in SREBP-1, due to PUFAs, strengthens the favorable distribution of our dietary treatments (Sekiya,2003).

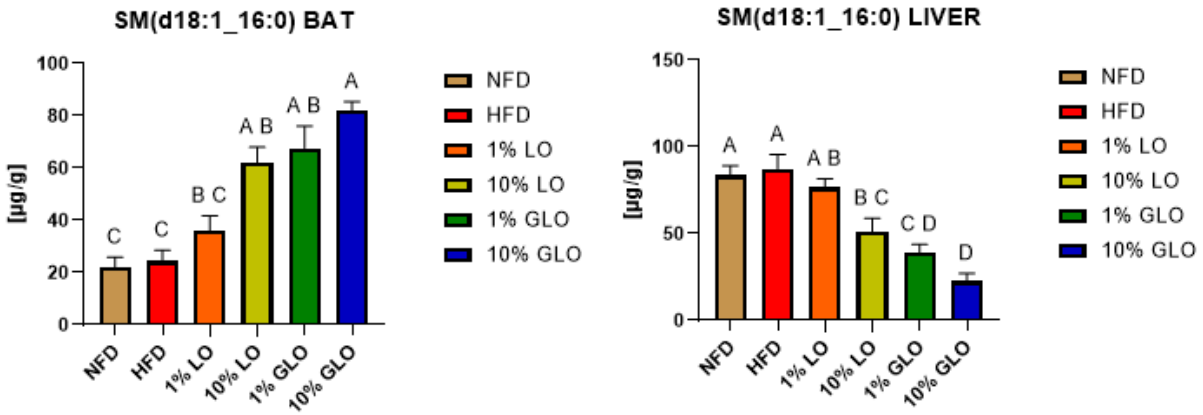

Figure 25: Absolute distribution (µg/g) of total detected {[2-hexadecanamido-3-hydroxyoctadec-4-en-1-yl]oxy} [2-(trimethylazaniumyl)ethoxy] phosphinic acid (SM(d18:1_16:0)) in WAT, BAT, & liver of C57BL/6 wild-type mice. Data are presented as mean ± SEM (n>9). Statistical significance was determined using one-way ANOVA followed by Tukey's multiple comparison test. Groups labeled with different letters are significantly different ($p < 0.05$).

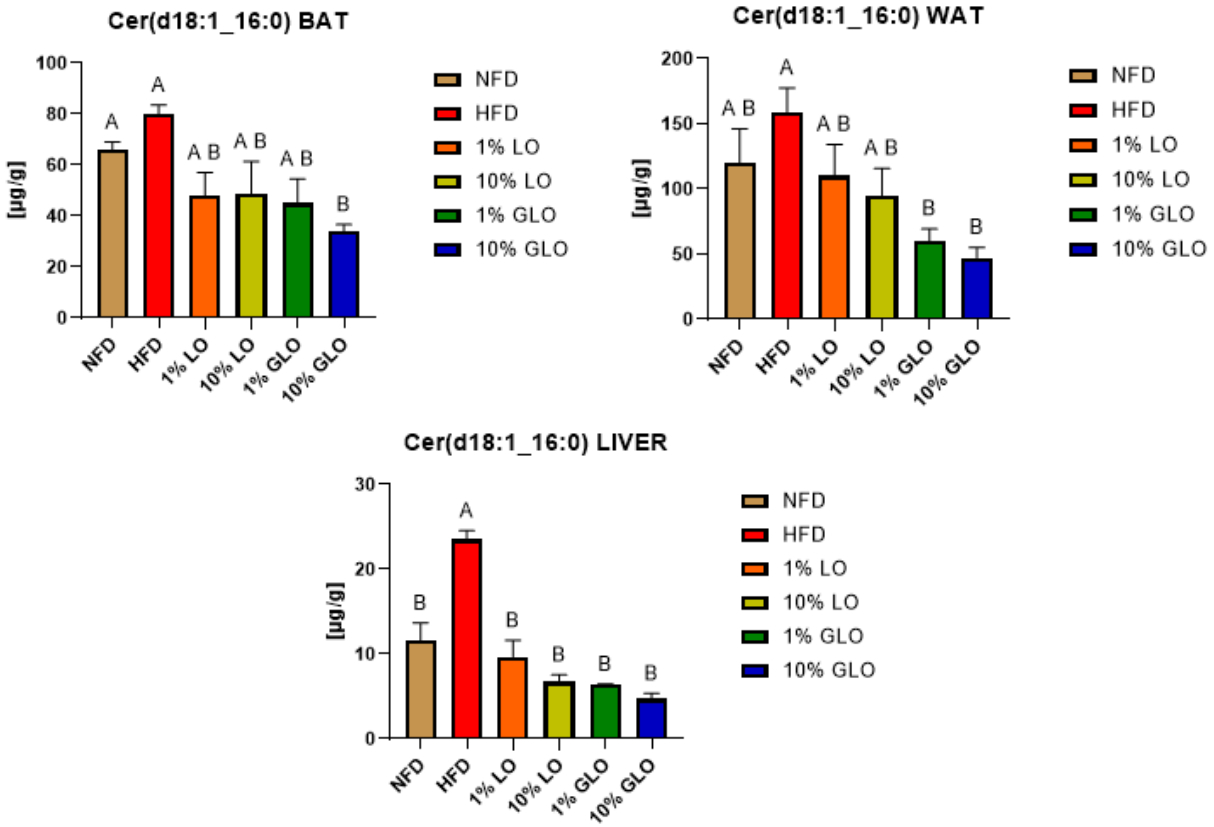

Figure 26: Absolute distribution (µg/g) of total detected N-Palmitoylsphingosine (Cer(d18:1_16:0)) in WAT, BAT, & liver of C57BL/6 wild-type mice. Data are presented as mean ± SEM (n>9). Statistical significance was determined using one-way ANOVA followed by Tukey's multiple comparison test. Groups labeled with different letters are significantly different ($p < 0.05$).

The sphingolipid analysis revealed tissue-specific responses to dietary intervention. As mentioned in section 4.2 no graph was inserted of SM in WAT, likely due to low basal SM turnover or detection limits in mature adipocytes. Therefore {[2-hexadecanamido-3-hydroxyoctadec-4-en-1-yl]oxy}[2(trimethylazaniumyl)ethoxy]phosphinic acid, also known as SM(d18:1_16:0) could not be detected in WAT. But in BAT, a steady rise can be noted, whereby the SM(d18:1_16:0) content in the 10% GLO group is significantly higher than NFD, HFD and 1% LO, whereas 10% LO and 1% GLO showed a significant increase in comparison to NFD and HFD. Liver indicated the complete opposite, with a significant increase of SM(d18:1_16:0) levels in NFD, HFD and 1% LO in comparison to 1% GLO and 10% GLO, whereas no significance could be observed between 10% LO, 1% GLO or rather 1% GLO and 10% GLO (see figure 25). In regards of N-palmitoylsphingosine, also known as Cer(d18:1_16:0), all tissues showed the same pattern, especially in liver a strong significance could be observed. WAT showed the highest concentration and liver the lowest (see figure 26). High intake of saturated fat drives *de novo* ceramide synthesis in insulin sensitive tissues. For instance, lard infused rats showed increased ceramide levels in muscle and liver, which caused insulin resistance, whereas blocking the serine palmitoyl transferase, an enzyme which favors palmitoyl-CoA as a substrate, prevented both ceramide accumulation and glucose intolerance (Holland & Summers, 2008). SM contributes to membrane structure by influencing the membrane shaping and facilitating lipid raft formation, especially in tissues with high mitochondrial content (Slotte, 2013). Importantly, ceramide in BAT was still significantly reduced under GLO, suggesting that the SM increase did not transform into lipotoxic ceramide accumulation, but may instead support membrane stability. In liver, both ceramide and SM were elevated under HFD. In comparison to LO, GLO treatment had stronger reducing effects on Cer(d18:1_16:0) and SM(d18:1_16:0), likely due to the higher content of antioxidant phytochemicals (Zhang et al., 2023). The abundance of ALA in GLO and LO groups also might suppress the *de novo* ceramide synthesis, due to the fact that it is an 18C PUFA, which is a poor substrate for the highly selective enzyme serine palmitoyl transferase that exhibits a strong preference for saturated fatty acyl-CoAs with a chain length of 15-17C. The reaction rate is primarily determined by the availability of free fatty acid substrates, which explains why saturated, but not unsaturated fatty acids act as a promoter for the sphingolipid synthesis (Holland & Summers, 2008). Supplementation

with LO, particularly when germination occurred, increases the EPA and DHA content, as well as resolvins such as RvE1-E2, RvD2, RvD5- D6 (E/D series resolvins), which correlate with anti-inflammatory cytokines, like interleukins 4 and 10 (IL-4 and IL-10), as well as arginase 1, and reduced pro-inflammatory substances (Bashir et al., 2019). Furthermore, omega-3 rich diets tend to rise adiponectin, a compound that promotes insulin sensitivity and cell survival and decreases inflammation. Adiponectin potentially activates a ceramidase activity, which catalyzes the conversion of ceramides into sphingosine and subsequently into sphingosine-1-phosphate. This adiponectin-ceramidase pathways, mediated through adiponectin receptor 1 and 2 (AdiPoR1 and AdipoR2), with AMPK dependent signaling, effectively enhances ceramide degradation in liver. Accordingly, GLO promotes the breakdown of Cer(d18:1_16:0) and complements its inhibitory effects on ceramide synthesis by increasing the adiponectin pool and providing antioxidant support (Holland et al., 2011).

In summary these literature inputs are supported by our data, which demonstrates that GLO supplementation not only reduced ceramide accumulation across WAT, BAT and liver but also significantly improved the overall tissue lipid profile, which was characterized by lower lipotoxic species and enhanced incorporation of metabolically favorable lipids.

5 Conclusion

In conclusion, this study is the first to date, which provides a comprehensive analysis of a supplementation with linseed oil from germinated seeds (GLO), combining high-resolution untargeted and targeted metabolomics and lipidomics across metabolically active tissues. Through this “omics” approach, we captured a broad spectrum of lipid classes and metabolites. Taking these findings into consideration, we subsequently quantified selected key compounds with targeted LC-MS using appropriate reference standards. This strategy enabled us to identify tissue specific shifts in lipid metabolism and mitochondrial function with high analytical precision. Moreover, GLO, especially 10% GLO induced favorable changes in mitochondrial β-oxidation and lipid remodeling. These effects were particularly pronounced in high dose treatments. In WAT, GLO supplementation remodels lipids storage by enriching adipose depots with omega-3

PUFAs and reducing lipotoxic species, reflecting a healthier lipid profile and improved metabolic flexibility. When it comes to GLO, in BAT, an elevation of markers of fatty acid catabolism and thermogenesis, including shifts in acylcarnitine concentrations consistent with intensified β-oxidation activity could be observed. Similarly, GLO supplementation led to a decrease in hepatic lipotoxic intermediates such as ceramides, while concurrently increasing polyunsaturated phospholipid species like PE(16:0_22:6) or DOPC. These shifts reflect enhanced hepatic lipid homeostasis and mitochondrial membrane integrity (Van Meer et al., 2008; Wang et al., 2016). Collectively, these findings strongly support both proposed hypotheses. Our outcomes confirm that GLO enhances mitochondrial β-oxidation by modulating carnitine metabolism and improving fatty acid transport efficiency. Evidence for this includes the observed upregulation of the carnitine shuttle system. Dietary treatment with GLO led to higher free carnitine availability and a favorable acylcarnitine profile, signifying greater efficiency in mitochondrial import and oxidation of fatty acids (Popeijus et al., 2014). Moreover, the results confirm that GLO significantly alters the tissue lipidome by facilitating the incorporation of unsaturated fatty acids into storage lipids and adjusting key pathways of lipid remodeling processes that support mitochondrial integrity. Increased content of unsaturated lipid species such as TG(16:1_18:2_18:3), membrane phospholipids and decreased ceramide levels point towards improved mitochondrial activity and reduced lipotoxic stress. These changes are partially mediated by higher adiponectin performance, which has been shown to activate ceramide enzymes that subsequently degrade ceramide and further improve insulin sensitivity (Holland et al., 2011).

In summary GLO acts as a potent modulator of systemic lipid metabolism by enhancing mitochondrial β-oxidation and promoting favorable lipid remodeling in adipose tissue and liver. In addition, the results clearly demonstrate distinct advantages of GLO compared to LO. Across several lipid species, GLO induced more pronounced and consistent effects. These benefits are likely attributable to the enhanced bioactive compound profile generated through germination. While 10% GLO supplementation showed the strongest alterations in lipid and carnitine profiles, some favorable changes were already observable at a 1% supplementation. This suggests that a GLO supplementation with even lower doses may be sufficient to trigger beneficial metabolic responses. By simultaneously stimulating carnitine-mediated β-oxidation and improving

lipid storage and membrane composition, GLO contributes to the enhancement of lipid homeostasis and improvement of metabolic flexibility. Therefore, both hypotheses proposed in this study can be affirmed based on the presented data. Moreover, GLO supplementation may represent a promising nutritional strategy, particularly for counteracting metabolic impairments of HFD. Future studies are necessary to confirm these findings in long term models and to focus on translational validation, mechanistic pathways and maybe to evaluate the durability of GLO induced lipidomic and metabolic adaptations and their implications for chronic disease prevention.

6 Zusammenfassung

Der Lipidstoffwechsel ist für die zelluläre Energiehomöostase von entscheidender Bedeutung, wobei die β-Oxidation als wichtiger Weg für den Abbau von Fettsäuren dient (Hisanaga et al., 2004). Darüber hinaus sind Lipide für verschiedene physiologische Prozesse unerlässlich, darunter Thermoregulation, Energiespeicherung, Immunregulation und Membransynthese (Cannon & Nedergaard, 2004; Yoon et al., 2021). Leinöl, insbesondere aus gekeimten Leinsamen, enthält zahlreiche bioaktive Verbindungen wie PUFAs, Polyphenole, Tocopherole und Antioxidantien, was zu einer erhöhten antioxidativen Aktivität und oxidativen Stabilität führt (Pointner et al., 2024). Das Ziel dieser Arbeit ist es, die Auswirkungen einer Supplementierung mit Leinöl, insbesondere aus gekeimten Leinsamen, auf Lipid- und Metabolitprofile zu analysieren, da die allgemeinen ernährungsphysiologischen Eigenschaften von Leinsamen zwar bekannt sind, die spezifischen Auswirkungen auf Lipidstoffwechselwege jedoch noch nicht vollständig untersucht wurden. Daher schließt diese Studie eine wichtige Lücke und bietet neue Perspektiven für Ernährungsinterventionen, die metabolische Gesundheit und die potenziellen Anwendungen von gekeimtem Leinsamenöl. Mit Hilfe von nicht zielgerichteten und zielgerichteten Ansätzen wurden metabolische Veränderungen in BAT, WAT und Leber untersucht. Diese Gewebe wurden aufgrund ihrer individuellen Auswirkungen auf den Lipidstoffwechsel ausgewählt, wie z. B. Thermoregulation (BAT), überschüssige Energiespeicherung (WAT) und die Interaktion mit Fettgewebe (Leber) (Cannon & Nedergaard, 2004; Heinonen et al., 2020; Trefts et al., 2017) Die Supplementierung mit LO und GLO führte zu einer günstigen Remodellierung des lipidomischen Profils, einschließlich einer Anreicherung mit Phospholipiden und einer Verringerung der Ceramide sowie zu Veränderungen in der Fettsäurezusammensetzung. Darüber hinaus wurde ein Anstieg der Acylcarnitine beobachtet. Besonderes Augenmerk wurde auf mehrere Metabolite wie Carnitine und Lipidklassen wie TAG, GPs und SM gelegt. Außerdem wurden verschiedene Konzentrationen der Diäten verglichen. Unsere Studie zeigte, dass LO, insbesondere aus gekeimtem Leinsamen, Veränderungen im Fettstoffwechsel in BAT, WAT und Leber induzierte. Erhöhte Acylcarnitin-Konzentrationen in BAT, insbesondere in der GLO-Gruppe, spiegelten eine verstärkte β-Oxidation und thermogene Kapazität wider, während GLO die Einlagerung von Omega-

3-Fettsäuren-reichen TAGs erhöhte und gleichzeitig lipotoxische Spezies wie Ceramide reduzierte, was auf ein metabolisch günstiges Lipid- und Metabolitprofil hindeutet. Die Anreicherung von mehrfach ungesättigten Phospholipiden in der Leber, darunter DHA-haltige Spezies wie PE(16:0_22:6), sowie eine Verringerung schädlicher Zwischenprodukte wie Cer(d18:1_16:0) stärkten das Lipidprofil. Eine Supplementierung mit LO und GLO, insbesondere in höherer Dosierung, veränderte das WAT-Lipidom erheblich, indem sie den Anteil der Speicherlipide erhöhte und den Phospholipidpool erweiterte, ohne die Ceramidakkumulation zu verstärken, was zu einer metabolisch günstigen Wirkung von LO und insbesondere GLO führte. Insgesamt deuten diese Veränderungen auf eine verbesserte Lipidhomöostase, einen verstärkten Fettsäuretransport in die Mitochondrien und eine verbesserte metabolische Flexibilität bei LO- und GLO- supplementierten Mäusen hin.

7 Abstract

Lipid metabolism is essential for cellular energy homeostasis with β-oxidation serving as an important pathway for the breakdown of fatty acids (Hisanaga et al., 2004). Moreover, lipids are essential for various metabolic mechanisms as they are involved in thermoregulation, energy storage, immunoregulatory responses, membrane synthesis and many more (Cannon & Nedergaard, 2004; Yoon et al., 2021). Linseed oil, especially from germinated linseed, contains lots of bioactive compounds such as PUFAs, polyphenols, tocopherols and antioxidants, resulting in an increased antioxidant activity and oxidative stability (Pointner et al., 2024). This thesis aims to analyze the effects of supplementation with linseed oil, particularly from germinated linseeds, on lipid and metabolite profiles, as the general nutritional properties of linseed are well known, but the specific impact on metabolic and lipidomic pathways has not yet fully been investigated. Therefore, this study fills a critical gap, offering new perspectives on dietary interventions, metabolic health and the potential applications of germinated linseed oil. With the help of untargeted and targeted approaches, metabolic alterations were examined throughout BAT, WAT and liver. These tissues were chosen based on their individual effects on lipid metabolism, such as thermoregulation (BAT), excess energy storage (WAT) and the interaction with adipose tissue (liver) (Cannon & Nedergaard, 2004; Heinonen et al., 2020; Trefts et al., 2017). Notably, supplementation with LO and GLO led to a favorable lipidomic remodeling, such as the enrichment with phospholipids and a reduction in ceramides, as well as alterations in the fatty acid composition. In addition, an increase in acylcarnitines was observed. Special emphasis was placed on several metabolites like carnitines and lipid classes such as TAG, GPs and SM. In addition, different levels of dietary supplementations were compared. Our study showed that LO, particularly from germinated linseeds, induced alterations in lipid metabolism across BAT, WAT and liver. Elevated acylcarnitine concentrations in BAT, especially in the GLO group, reflected enhanced β-oxidation and thermogenic capacity, whereas GLO increased the incorporation of omega-3 fatty acid rich TAGs, while reducing lipotoxic species such as ceramides, indicating a metabolically favorable lipid and metabolite profile. The hepatic enrichment of polyunsaturated phospholipids, including DHA containing species like PE(16:0_22:6), alongside a decrease in harmful intermediates,

such as Cer(d18:1_16:0), strengthened the lipid profile. A supplementation with LO and GLO, especially in its higher dosed form, substantially altered the WAT lipidome by increasing the storage lipid fraction and expanding the phospholipid pool without worsening the ceramide accumulation, resulting in a metabolically favorable impact of LO and especially GLO. Overall, these changes suggest enhanced lipid homeostasis, greater mitochondrial fatty acid transport and improved metabolic flexibility in LO- and GLO- supplemented mice.

8 Bibliography

Adeva-Andany, M. M., Carneiro-Freire, N., Seco-Filgueira, M., Fernández-Fernández, C., & Mouriño-Bayolo, D. (2019). Mitochondrial β-oxidation of saturated fatty acids in humans. *Mitochondrion*, *46*, 73–90. https://doi.org/10.1016/j.mito.2018.02.009

Albeituni, S., & Stiban, J. (2019). Roles of Ceramides and Other Sphingolipids in Immune Cell Function and Inflammation. In K. V. Honn & D. C. Zeldin (Hrsg.), *The Role of Bioactive Lipids in Cancer, Inflammation and Related Diseases* (Bd. 1161, S. 169–191). Springer International Publishing. https://doi.org/10.1007/978-3-030-21735-8_15

Baranowski, M., Enns, J., Blewett, H., Yakandawala, U., Zahradka, P., & Taylor, C. G. (2012). Dietary flaxseed oil reduces adipocyte size, adipose monocyte chemoattractant protein-1 levels and T-cell infiltration in obese, insulin-resistant rats. *Cytokine*, *59*(2), 382–391. https://doi.org/10.1016/j.cyto.2012.04.004

Bartelt, A., Bruns, O. T., Reimer, R., Hohenberg, H., Ittrich, H., Peldschus, K., Kaul, M. G., Tromsdorf, U. I., Weller, H., Waurisch, C., Eychmüller, A., Gordts, P. L. S. M., Rinninger, F., Bruegelmann, K., Freund, B., Nielsen, P., Merkel, M., & Heeren, J. (2011). Brown adipose tissue activity controls triglyceride clearance. *Nature Medicine*, *17*(2), 200–205. https://doi.org/10.1038/nm.2297

Bashir, S., Sharma, Y., Jairajpuri, D., Rashid, F., Nematullah, Md., & Khan, F. (2019). Alteration of adipose tissue immune cell milieu towards the suppression of inflammation in high fat diet fed mice by flaxseed oil supplementation. *PLOS ONE*, *14*(10), e0223070. https://doi.org/10.1371/journal.pone.0223070

Becker, S., Kortz, L., Helmschrodt, C., Thiery, J., & Ceglarek, U. (2012). LC–MS-based metabolomics in the clinical laboratory. *Journal of Chromatography B*, *883–884*, 68–75. https://doi.org/10.1016/j.jchromb.2011.10.018

Beckonert, O., Keun, H. C., Ebbels, T. M. D., Bundy, J., Holmes, E., Lindon, J. C., & Nicholson, J. K. (2007). Metabolic profiling, metabolomic and metabonomic procedures for NMR

spectroscopy of urine, plasma, serum and tissue extracts. *Nature Protocols*, *2*(11), 2692–2703. https://doi.org/10.1038/nprot.2007.376

Bergman, B. C., Hunerdosse, D. M., Kerege, A., Playdon, M. C., & Perreault, L. (2012). Localisation and composition of skeletal muscle diacylglycerol predicts insulin resistance in humans. *Diabetologia*, *55*(4), 1140–1150. https://doi.org/10.1007/s00125-011-2419-7

Bligh, E. G., & Dyer, W. J. (1959). A RAPID METHOD OF TOTAL LIPID EXTRACTION AND PURIFICATION. *Canadian Journal of Biochemistry and Physiology*, *37*(8), 911–917. https://doi.org/10.1139/o59-099

Brejchova, J., Brejchova, K., & Kuda, O. (2024). Metabolic Pathways of Acylcarnitine Synthesis. *Physiological Research*, *73*(S1), S153–S163. https://doi.org/10.33549/physiolres.935261

Bujak, R., Struck-Lewicka, W., Markuszewski, M. J., & Kaliszan, R. (2015). Metabolomics for laboratory diagnostics. *Journal of Pharmaceutical and Biomedical Analysis*, *113*, 108–120. https://doi.org/10.1016/j.jpba.2014.12.017

Buré, C., Cacas, J.-L., Mongrand, S., & Schmitter, J.-M. (2014). Characterization of glycosyl inositol phosphoryl ceramides from plants and fungi by mass spectrometry. *Analytical and Bioanalytical Chemistry*, *406*(4), 995–1010. https://doi.org/10.1007/s00216-013-7130-8

Byrdwell, W. C. (2001). Atmospheric pressure chemical ionization mass spectrometry for analysis of lipids. *Lipids*, *36*(4), 327–346. https://doi.org/10.1007/s11745-001-0725-5

Cáceres, P. J., Peñas, E., Martinez-Villaluenga, C., Amigo, L., & Frias, J. (2017). Enhancement of biologically active compounds in germinated brown rice and the effect of sun-drying. *Journal of Cereal Science*, *73*, 1–9. https://doi.org/10.1016/j.jcs.2016.11.001

Campos, J. R., Severino, P., Ferreira, C. S., Zielinska, A., Santini, A., Souto, S. B., & Souto, E. B. (2019). Linseed Essential Oil – Source of Lipids as Active Ingredients for Pharmaceuticals and Nutraceuticals. *Current Medicinal Chemistry*, *26*(24), 4537–4558. https://doi.org/10.2174/0929867325666181031105603

Cannon, B., & Nedergaard, J. (2004). Brown Adipose Tissue: Function and Physiological Significance. *Physiological Reviews*, *84*(1), 277–359. https://doi.org/10.1152/physrev.00015.2003

Cao, H., Gerhold, K., Mayers, J. R., Wiest, M. M., Watkins, S. M., & Hotamisligil, G. S. (2008). Identification of a Lipokine, a Lipid Hormone Linking Adipose Tissue to Systemic Metabolism. *Cell*, *134*(6), 933–944. https://doi.org/10.1016/j.cell.2008.07.048

Carrasco, S., & Mérida, I. (2007). Diacylglycerol, when simplicity becomes complex. *Trends in Biochemical Sciences*, *32*(1), 27–36. https://doi.org/10.1016/j.tibs.2006.11.004

Castro-Gómez, P., Garcia-Serrano, A., Visioli, F., & Fontecha, J. (2015). Relevance of dietary glycerophospholipids and sphingolipids to human health. *Prostaglandins, Leukotrienes and Essential Fatty Acids*, *101*, 41–51. https://doi.org/10.1016/j.plefa.2015.07.004

Checa, A., Bedia, C., & Jaumot, J. (2015). Lipidomic data analysis: Tutorial, practical guidelines and applications. *Analytica Chimica Acta*, *885*, 1–16. https://doi.org/10.1016/j.aca.2015.02.068

Dambrova, M., Makrecka-Kuka, M., Kuka, J., Vilskersts, R., Nordberg, D., Attwood, M. M., Smesny, S., Sen, Z. D., Guo, A. C., Oler, E., Tian, S., Zheng, J., Wishart, D. S., Liepinsh, E., & Schiöth, H. B. (2022). Acylcarnitines: Nomenclature, Biomarkers, Therapeutic Potential, Drug Targets, and Clinical Trials. *Pharmacological Reviews*, *74*(3), 506–551. https://doi.org/10.1124/pharmrev.121.000408

Dátilo, M. N., Sant'Ana, M. R., Formigari, G. P., Rodrigues, P. B., De Moura, L. P., Da Silva, A. S. R., Ropelle, E. R., Pauli, J. R., & Cintra, D. E. (2018). Omega-3 from Flaxseed Oil Protects Obese Mice Against Diabetic Retinopathy Through GPR120 Receptor. *Scientific Reports*, *8*(1), 14318. https://doi.org/10.1038/s41598-018-32553-5

Davies, M. N., Kjalarsdottir, L., Thompson, J. W., Dubois, L. G., Stevens, R. D., Ilkayeva, O. R., Brosnan, M. J., Rolph, T. P., Grimsrud, P. A., & Muoio, D. M. (2016). The Acetyl Group Buffering Action of Carnitine Acetyltransferase Offsets Macronutrient-Induced Lysine Acetylation of Mitochondrial Proteins. *Cell Reports*, *14*(2), 243–254. https://doi.org/10.1016/j.celrep.2015.12.030

Deng, X., Dong, Q., Bridges, D., Raghow, R., Park, E. A., & Elam, M. B. (2015). Docosahexaenoic acid inhibits proteolytic processing of sterol regulatory element-binding protein-1c (SREBP-1c) via activation of AMP-activated kinase. *Biochimica et Biophysica Acta (BBA) - Molecular and Cell Biology of Lipids*, *1851*(12), 1521–1529. https://doi.org/10.1016/j.bbalip.2015.08.007

Di Paolo, G., & De Camilli, P. (2006). Phosphoinositides in cell regulation and membrane dynamics. *Nature*, *443*(7112), 651–657. https://doi.org/10.1038/nature05185

Donato, P., Dugo, P., & Mondello, L. (2013). Separation of Lipids. In *Liquid Chromatography* (S. 203–248). Elsevier. https://doi.org/10.1016/B978-0-12-415806-1.00009-7

Dong, Y., Zhang, X., Sun, L., Zhang, S., Liu, B., Liu, H., Wang, X., & Jiang, C. (2017). Omega-3 PUFA ameliorates hyperhomocysteinemia-induced hepatic steatosis in mice by inhibiting hepatic ceramide synthesis. *Acta Pharmacologica Sinica*, *38*(12), 1601–1610. https://doi.org/10.1038/aps.2017.127

Duarte, S., Shah, M. A., & Sanches Silva, A. (2025). Flaxseed in Diet: A Comprehensive Look at Pros and Cons. *Molecules*, *30*(6), 1335. https://doi.org/10.3390/molecules30061335

Eggers, L. F., & Schwudke, D. (2016). Liquid Extraction: Folch. In M. R. Wenk (Hrsg.), *Encyclopedia of Lipidomics* (S. 1–6). Springer Netherlands. https://doi.org/10.1007/978-94-007-7864-1_89-1

Ellis, D. I., Dunn, W. B., Griffin, J. L., Allwood, J. W., & Goodacre, R. (2007). Metabolic Fingerprinting As A Diagnostic Tool. *Pharmacogenomics*, *8*(9), 1243–1266. https://doi.org/10.2217/14622416.8.9.1243

Esser, V., Brown, N. F., Cowan, A. T., Foster, D. W., & McGarry, J. D. (1996). Expression of a cDNA Isolated from Rat Brown Adipose Tissue and Heart Identifies the Product as the Muscle Isoform of Carnitine Palmitoyltransferase I (M-CPT I). *Journal of Biological Chemistry*, *271*(12), 6972–6977. https://doi.org/10.1074/jbc.271.12.6972

Farag, M. A., Elimam, D. M., & Afifi, S. M. (2021). Outgoing and potential trends of the omega-3 rich linseed oil quality characteristics and rancidity management: A comprehensive review for

maximizing its food and nutraceutical applications. *Trends in Food Science & Technology*, *114*, 292–309. https://doi.org/10.1016/j.tifs.2021.05.041

Fernández-Galilea, M., Félix-Soriano, E., Colón-Mesa, I., Escoté, X., & Moreno-Aliaga, M. J. (2020). Omega-3 fatty acids as regulators of brown/beige adipose tissue: From mechanisms to therapeutic potential. *Journal of Physiology and Biochemistry*, *76*(2), 251–267. https://doi.org/10.1007/s13105-019-00720-5

Ferré, P., & Foufelle, F. (2007). SREBP-1c Transcription Factor and Lipid Homeostasis: Clinical Perspective. *Hormone Research in Paediatrics*, *68*(2), 72–82. https://doi.org/10.1159/000100426

Ferreira, G. C., & McKenna, M. C. (2017a). L-Carnitine and Acetyl-l-carnitine Roles and Neuroprotection in Developing Brain. *Neurochemical Research*, *42*(6), 1661–1675. https://doi.org/10.1007/s11064-017-2288-7

Ferreira, G. C., & McKenna, M. C. (2017b). L-Carnitine and Acetyl-l-carnitine Roles and Neuroprotection in Developing Brain. *Neurochemical Research*, *42*(6), 1661–1675. https://doi.org/10.1007/s11064-017-2288-7

Fiehn, O. (2001). Combining genomics, metabolome analysis, and biochemical modelling to understand metabolic networks. *Comparative and Functional Genomics*, *2*(3), 155–168. https://doi.org/10.1002/cfg.82

Folch, J., Lees, M., & Stanley, G. H. S. (1957). A SIMPLE METHOD FOR THE ISOLATION AND PURIFICATION OF TOTAL LIPIDES FROM ANIMAL TISSUES. *Journal of Biological Chemistry*, *226*(1), 497–509. https://doi.org/10.1016/S0021-9258(18)64849-5

Giesbertz, P., Ecker, J., Haag, A., Spanier, B., & Daniel, H. (2015). An LC-MS/MS method to quantify acylcarnitine species including isomeric and odd-numbered forms in plasma and tissues. *Journal of Lipid Research*, *56*(10), 2029–2039. https://doi.org/10.1194/jlr.D061721

Gnoni, A., Longo, S., Gnoni, G. V., & Giudetti, A. M. (2020). Carnitine in Human Muscle Bioenergetics: Can Carnitine Supplementation Improve Physical Exercise? *Molecules (Basel, Switzerland)*, *25*(1), 182. https://doi.org/10.3390/molecules25010182

Gowda, G. N., Zhang, S., Gu, H., Asiago, V., Shanaiah, N., & Raftery, D. (2008). Metabolomics-based methods for early disease diagnostics. *Expert Review of Molecular Diagnostics*, *8*(5), 617–633. https://doi.org/10.1586/14737159.8.5.617

Gucciardi, A., Pirillo, P., Di Gangi, I. M., Naturale, M., & Giordano, G. (2012). A rapid UPLC–MS/MS method for simultaneous separation of 48 acylcarnitines in dried blood spots and plasma useful as a second-tier test for expanded newborn screening. *Analytical and Bioanalytical Chemistry*, *404*(3), 741–751. https://doi.org/10.1007/s00216-012-6194-1

Han, H., Qiu, F., Zhao, H., Tang, H., Li, X., & Shi, D. (2017). Dietary Flaxseed Oil Prevents Western-Type Diet-Induced Nonalcoholic Fatty Liver Disease in Apolipoprotein-E Knockout Mice. *Oxidative Medicine and Cellular Longevity*, *2017*(1), 3256241. https://doi.org/10.1155/2017/3256241

Han, X., Yang, K., & Gross, R. W. (2012). Multi-dimensional mass spectrometry-based shotgun lipidomics and novel strategies for lipidomic analyses. *Mass Spectrometry Reviews*, *31*(1), 134–178. https://doi.org/10.1002/mas.20342

Hasin, Y., Seldin, M., & Lusis, A. (2017). Multi-omics approaches to disease. *Genome Biology*, *18*(1), 83. https://doi.org/10.1186/s13059-017-1215-1

Heiles, S. (2021). Advanced tandem mass spectrometry in metabolomics and lipidomics—Methods and applications. *Analytical and Bioanalytical Chemistry*, *413*(24), 5927–5948. https://doi.org/10.1007/s00216-021-03425-1

Heinonen, S., Jokinen, R., Rissanen, A., & Pietiläinen, K. H. (2020). White adipose tissue mitochondrial metabolism in health and in obesity. *Obesity Reviews*, *21*(2), e12958. https://doi.org/10.1111/obr.12958

Herchi, W., Arr^|^aacute;ez-Rom^|^aacute;n, D., Trabelsi, H., Bouali, I., Boukhchina, S., Kallel, H., Segura-Carretero, A., & Fern^|^aacute;ndez-Gutierrez, A. (2014). Phenolic Compounds in

Flaxseed: A Review of Their Properties and Analytical Methods. An Overview of the Last Decade. *Journal of Oleo Science*, *63*(1), 7–14. https://doi.org/10.5650/jos.ess13135

Herchi, W., Bahashwan, S., Sebei, K., Ben Saleh, H., Kallel, H., & Boukhchina, S. (2015). Effects of germination on chemical composition and antioxidant activity of flaxseed (Linum usitatissimum L) oil. *Grasas y Aceites*, *66*(1), e057. https://doi.org/10.3989/gya.0463141

Hisanaga, Y., Ago, H., Nakagawa, N., Hamada, K., Ida, K., Yamamoto, M., Hori, T., Arii, Y., Sugahara, M., Kuramitsu, S., Yokoyama, S., & Miyano, M. (2004). Structural Basis of the Substrate-specific Two-step Catalysis of Long Chain Fatty Acyl-CoA Synthetase Dimer. *Journal of Biological Chemistry*, *279*(30), 31717–31726. https://doi.org/10.1074/jbc.M400100200

Ho, C. S., Lam, C. W. K., Chan, M. H. M., Cheung, R. C. K., Law, L. K., Lit, L. C. W., Ng, K. F., Suen, M. W. M., & Tai, H. L. (2003). Electrospray ionisation mass spectrometry: Principles and clinical applications. *The Clinical Biochemist. Reviews*, *24*(1), 3–12.

Holland, W. L., Miller, R. A., Wang, Z. V., Sun, K., Barth, B. M., Bui, H. H., Davis, K. E., Bikman, B. T., Halberg, N., Rutkowski, J. M., Wade, M. R., Tenorio, V. M., Kuo, M.-S., Brozinick, J. T., Zhang, B. B., Birnbaum, M. J., Summers, S. A., & Scherer, P. E. (2011). Receptor-mediated activation of ceramidase activity initiates the pleiotropic actions of adiponectin. *Nature Medicine*, *17*(1), 55–63. https://doi.org/10.1038/nm.2277

Holland, W. L., & Summers, S. A. (2008). Sphingolipids, Insulin Resistance, and Metabolic Disease: New Insights from in Vivo Manipulation of Sphingolipid Metabolism. *Endocrine Reviews*, *29*(4), 381–402. https://doi.org/10.1210/er.2007-0025

Hoppel, C. (2003). The role of carnitine in normal and altered fatty acid metabolism. *American Journal of Kidney Diseases*, *41*, S4–S12. https://doi.org/10.1016/S0272-6386(03)00112-4

Horning, E. C., & Horning, M. G. (1971). Metabolic Profiles: Gas-Phase Methods for Analysis of Metabolites. *Clinical Chemistry*, *17*(8), 802–809. https://doi.org/10.1093/clinchem/17.8.802

Horrocks, L. A., & Yeo, Y. K. (1999). HEALTH BENEFITS OF DOCOSAHEXAENOIC ACID (DHA). *Pharmacological Research*, *40*(3), 211–225. https://doi.org/10.1006/phrs.1999.0495

Huang, Q., Tan, Y., Yin, P., Ye, G., Gao, P., Lu, X., Wang, H., & Xu, G. (2013). Metabolic Characterization of Hepatocellular Carcinoma Using Nontargeted Tissue Metabolomics. *Cancer Research*, *73*(16), 4992–5002. https://doi.org/10.1158/0008-5472.CAN-13-0308

Huitema, K., Van Den Dikkenberg, J., Brouwers, J. F. H. M., & Holthuis, J. C. M. (2004). Identification of a family of animal sphingomyelin synthases. *The EMBO Journal*, *23*(1), 33–44. https://doi.org/10.1038/sj.emboj.7600034

Iqbal, J., & Hussain, M. M. (2009). Intestinal lipid absorption. *American Journal of Physiology-Endocrinology and Metabolism*, *296*(6), E1183–E1194. https://doi.org/10.1152/ajpendo.90899.2008

Junot, C., Fenaille, F., Colsch, B., & Bécher, F. (2014). High resolution mass spectrometry based techniques at the crossroads of metabolic pathways. *Mass Spectrometry Reviews*, *33*(6), 471–500. https://doi.org/10.1002/mas.21401

Kang, J., Park, J., Park, W. Y., Jiao, W., Lee, S., Jung, Y., Youn, D.-H., Song, G., Cho, S. Y., Kim, W. Y., Park, J. Y., Ahn, K. S., Kwak, H.-J., & Um, J.-Y. (2020). A phytoestrogen secoisolariciresinol diglucoside induces browning of white adipose tissue and activates non-shivering thermogenesis through AMPK pathway. *Pharmacological Research*, *158*, 104852. https://doi.org/10.1016/j.phrs.2020.104852

Kennedy, E. P. (1957). Metabolism of Lipides. *Annual Review of Biochemistry*, *26*(1), 119–148. https://doi.org/10.1146/annurev.bi.26.070157.001003

Kind, T., Wohlgemuth, G., Lee, D. Y., Lu, Y., Palazoglu, M., Shahbaz, S., & Fiehn, O. (2009). FiehnLib: Mass Spectral and Retention Index Libraries for Metabolomics Based on Quadrupole and Time-of-Flight Gas Chromatography/Mass Spectrometry. *Analytical Chemistry*, *81*(24), 10038–10048. https://doi.org/10.1021/ac9019522

Koeth, R. A., Wang, Z., Levison, B. S., Buffa, J. A., Org, E., Sheehy, B. T., Britt, E. B., Fu, X., Wu, Y., Li, L., Smith, J. D., DiDonato, J. A., Chen, J., Li, H., Wu, G. D., Lewis, J. D., Warrier, M., Brown, J. M., Krauss, R. M., … Hazen, S. L. (2013). Intestinal microbiota metabolism of l-carnitine, a nutrient

in red meat, promotes atherosclerosis. *Nature Medicine*, *19*(5), 576–585. https://doi.org/10.1038/nm.3145

Kolak, M., Westerbacka, J., Velagapudi, V. R., Wågsäter, D., Yetukuri, L., Makkonen, J., Rissanen, A., Häkkinen, A.-M., Lindell, M., Bergholm, R., Hamsten, A., Eriksson, P., Fisher, R. M., Orešič, M., & Yki-Järvinen, H. (2007). Adipose Tissue Inflammation and Increased Ceramide Content Characterize Subjects With High Liver Fat Content Independent of Obesity. *Diabetes*, *56*(8), 1960–1968. https://doi.org/10.2337/db07-0111

Koves, T. R., Ussher, J. R., Noland, R. C., Slentz, D., Mosedale, M., Ilkayeva, O., Bain, J., Stevens, R., Dyck, J. R. B., Newgard, C. B., Lopaschuk, G. D., & Muoio, D. M. (2008). Mitochondrial Overload and Incomplete Fatty Acid Oxidation Contribute to Skeletal Muscle Insulin Resistance. *Cell Metabolism*, *7*(1), 45–56. https://doi.org/10.1016/j.cmet.2007.10.013

Lehner, R., & Kuksis, A. (1996). Biosynthesis of triacylglycerols. *Progress in Lipid Research*, *35*(2), 169–201. https://doi.org/10.1016/0163-7827(96)00005-7

Leiria, L. O., & Tseng, Y.-H. (2020). Lipidomics of brown and white adipose tissue: Implications for energy metabolism. *Biochimica et Biophysica Acta (BBA) - Molecular and Cell Biology of Lipids*, *1865*(10), 158788. https://doi.org/10.1016/j.bbalip.2020.158788

Lemas, D. J., Wiener, H. W., O'Brien, D. M., Hopkins, S., Stanhope, K. L., Havel, P. J., Allison, D. B., Fernandez, J. R., Tiwari, H. K., & Boyer, B. B. (2012). Genetic polymorphisms in carnitine palmitoyltransferase 1A gene are associated with variation in body composition and fasting lipid traits in Yup'ik Eskimos. *Journal of Lipid Research*, *53*(1), 175–184. https://doi.org/10.1194/jlr.P018952

Lenihan-Geels, G., Bishop, K., & Ferguson, L. (2013). Alternative Sources of Omega-3 Fats: Can We Find a Sustainable Substitute for Fish? *Nutrients*, *5*(4), 1301–1315. https://doi.org/10.3390/nu5041301

Li, Z., Peng, S., Chen, X., Zhu, Y., Zou, L., Liu, W., & Liu, C. (2018). Pluronics modified liposomes for curcumin encapsulation: Sustained release, stability and bioaccessibility. *Food Research International*, *108*, 246–253. https://doi.org/10.1016/j.foodres.2018.03.048

Lindon, J. C., & Nicholson, J. K. (2008). Spectroscopic and Statistical Techniques for Information Recovery in Metabonomics and Metabolomics. *Annual Review of Analytical Chemistry*, *1*(1), 45–69. https://doi.org/10.1146/annurev.anchem.1.031207.113026

Liu, H., Hu, X., Li, Z., Fa, K., Gong, H., Ma, K., Liao, M., Li, P., Webster, J. R. P., Petkov, J. T., Thomas, R. K., & Ren Lu, J. (2021). Surface adsorption and solution aggregation of a novel lauroyl-l-carnitine surfactant. *Journal of Colloid and Interface Science*, *591*, 106–114. https://doi.org/10.1016/j.jcis.2021.01.106

Lligona-Trulla, L., Arduini, A., Aldaghlas, T. A., Calvani, M., & Kelleher, J. K. (1997). Acetyl-L-carnitine flux to lipids in cells estimated using isotopomer spectral analysis. *Journal of Lipid Research*, *38*(7), 1454–1462.

Longo, N., Frigeni, M., & Pasquali, M. (2016). Carnitine transport and fatty acid oxidation. *Biochimica et Biophysica Acta (BBA) - Molecular Cell Research*, *1863*(10), 2422–2435. https://doi.org/10.1016/j.bbamcr.2016.01.023

Madsen, K. L., Preisler, N., Rasmussen, J., Hedermann, G., Olesen, J. H., Lund, A. M., & Vissing, J. (2018). L-Carnitine Improves Skeletal Muscle Fat Oxidation in Primary Carnitine Deficiency. *The Journal of Clinical Endocrinology & Metabolism*, *103*(12), 4580–4588. https://doi.org/10.1210/jc.2018-00953

Malaguarnera, M. (2012). Carnitine derivatives: Clinical usefulness. *Current Opinion in Gastroenterology*, *28*(2), 166–176. https://doi.org/10.1097/MOG.0b013e3283505a3b

Mapelli, V., Olsson, L., & Nielsen, J. (2008). Metabolic footprinting in microbiology: Methods and applications in functional genomics and biotechnology. *Trends in Biotechnology*, *26*(9), 490–497. https://doi.org/10.1016/j.tibtech.2008.05.008

Mashek, D. G., Bornfeldt, K. E., Coleman, R. A., Berger, J., Bernlohr, D. A., Black, P., DiRusso, C. C., Farber, S. A., Guo, W., Hashimoto, N., Khodiyar, V., Kuypers, F. A., Maltais, L. J., Nebert, D. W., Renieri, A., Schaffer, J. E., Stahl, A., Watkins, P. A., Vasiliou, V., & Yamamoto, T. T. (2004). Revised nomenclature for the mammalian long-chain acyl-CoA synthetase gene family. *Journal of Lipid Research*, *45*(10), 1958–1961. https://doi.org/10.1194/jlr.E400002-JLR200

Massey, W. J., Varadharajan, V., Banerjee, R., Brown, A. L., Horak, A. J., Hohe, R. C., Jung, B. M., Qiu, Y., Chan, E. R., Pan, C., Zhang, R., Allende, D. S., Willard, B., Cheng, F., Lusis, A. J., & Brown, J. M. (2023). MBOAT7-driven lysophosphatidylinositol acylation in adipocytes contributes to systemic glucose homeostasis. *Journal of Lipid Research*, *64*(4), 100349. https://doi.org/10.1016/j.jlr.2023.100349

Masyita, A., Mustika Sari, R., Dwi Astuti, A., Yasir, B., Rahma Rumata, N., Emran, T. B., Nainu, F., & Simal-Gandara, J. (2022). Terpenes and terpenoids as main bioactive compounds of essential oils, their roles in human health and potential application as natural food preservatives. *Food Chemistry: X*, *13*, 100217. https://doi.org/10.1016/j.fochx.2022.100217

Morato, N. M., & Cooks, R. G. (2023). Desorption Electrospray Ionization Mass Spectrometry: 20 Years. *Accounts of Chemical Research*, *56*(18), 2526–2536. https://doi.org/10.1021/acs.accounts.3c00382

Nagle, C. A., Klett, E. L., & Coleman, R. A. (2009a). Hepatic triacylglycerol accumulation and insulin resistance. *Journal of Lipid Research*, *50 Suppl*(Suppl), S74-79. https://doi.org/10.1194/jlr.R800053-JLR200

Nagle, C. A., Klett, E. L., & Coleman, R. A. (2009b). Hepatic triacylglycerol accumulation and insulin resistance. *Journal of Lipid Research*, *50 Suppl*(Suppl), S74-79. https://doi.org/10.1194/jlr.R800053-JLR200

Nanjundan, M., & Possmayer, F. (2003). Pulmonary phosphatidic acid phosphatase and lipid phosphate phosphohydrolase. *American Journal of Physiology-Lung Cellular and Molecular Physiology*, *284*(1), L1–L23. https://doi.org/10.1152/ajplung.00029.2002

Nicholson, J. K., Lindon, J. C., & Holmes, E. (1999). „Metabonomics“: Understanding the metabolic responses of living systems to pathophysiological stimuli via multivariate statistical analysis of biological NMR spectroscopic data. *Xenobiotica*, *29*(11), 1181–1189. https://doi.org/10.1080/004982599238047

Oh, H., Park, C. H., & Jun, D. W. (2022). Impact of l-Carnitine Supplementation on Liver Enzyme Normalization in Patients with Chronic Liver Disease: A Meta-Analysis of Randomized Trials. *Journal of Personalized Medicine*, *12*(7), 1053. https://doi.org/10.3390/jpm12071053

Ohsaki, Y., Cheng, J., Suzuki, M., Shinohara, Y., Fujita, A., & Fujimoto, T. (2009). Biogenesis of cytoplasmic lipid droplets: From the lipid ester globule in the membrane to the visible structure. *Biochimica et Biophysica Acta (BBA) - Molecular and Cell Biology of Lipids*, *1791*(6), 399–407. https://doi.org/10.1016/j.bbalip.2008.10.002

O'Leary, E. I., Jiang, Z., Strub, M.-P., & Lee, J. C. (2018). Effects of phosphatidylcholine membrane fluidity on the conformation and aggregation of N-terminally acetylated α-synuclein. *The Journal of Biological Chemistry*, *293*(28), 11195–11205. https://doi.org/10.1074/jbc.RA118.002780

Omer, E., & Chiodi, C. (2024). Fat digestion and absorption: Normal physiology and pathophysiology of malabsorption, including diagnostic testing. *Nutrition in Clinical Practice*, *39*(S1). https://doi.org/10.1002/ncp.11130

Paglia, G., Kliman, M., Claude, E., Geromanos, S., & Astarita, G. (2015). Applications of ion-mobility mass spectrometry for lipid analysis. *Analytical and Bioanalytical Chemistry*, *407*(17), 4995–5007. https://doi.org/10.1007/s00216-015-8664-8

Pauling, L., Robinson, A. B., Teranishi, R., & Cary, P. (1971). Quantitative Analysis of Urine Vapor and Breath by Gas-Liquid Partition Chromatography. *Proceedings of the National Academy of Sciences*, *68*(10), 2374–2376. https://doi.org/10.1073/pnas.68.10.2374

Pekala, J., Patkowska-Sokola, B., Bodkowski, R., Jamroz, D., Nowakowski, P., Lochynski, S., & Librowski, T. (2011). L-Carnitine—Metabolic Functions and Meaning in Humans Life. *Current Drug Metabolism*, *12*(7), 667–678. https://doi.org/10.2174/138920011796504536

Perdomo, L., Beneit, N., Otero, Y. F., Escribano, Ó., Díaz-Castroverde, S., Gómez-Hernández, A., & Benito, M. (2015). Protective role of oleic acid against cardiovascular insulin resistance and in the early and late cellular atherosclerotic process. *Cardiovascular Diabetology*, *14*(1). https://doi.org/10.1186/s12933-015-0237-9

Pignitter, M., Grosshagauer, S., & Somoza, V. (2019). Stability of Vitamin E in Foods. In P. Weber, M. Birringer, J. B. Blumberg, M. Eggersdorfer, & J. Frank (Hrsg.), *Vitamin E in Human Health* (S. 215–232). Springer International Publishing. https://doi.org/10.1007/978-3-030-05315-4_16

Pilon, M. (2016). Revisiting the membrane-centric view of diabetes. *Lipids in Health and Disease*, *15*(1). https://doi.org/10.1186/s12944-016-0342-0

Plumb, R. S. (2023, Oktober). *Application of Neutral Loss and Precursor Ion Scanning by Tandem Quadrupole Mass Spectrometry to Monitor for Drug Metabolites in in vivo and in vitro Samples*. Waters Corporation. https://www.waters.com/nextgen/us/en/library/application-notes/2023/application-of-neutral-loss-and-precursor-ion-scanning-by-tandem-quadrupole-mass-spectrometry-to-monitor-for-drug-metabolites-in-in-vivo-and-in-vitro-samples.html?srsltid=AfmBOoosRfiGnX26AMpqIALz8yaG7goem-urLj7NA11j3i65w22iak7P

Pointner, T., Rauh, K., Auñon-Lopez, A., Kostadinović Veličkovska, S., Mitrev, S., Arsov, E., & Pignitter, M. (2024). Comprehensive analysis of oxidative stability and nutritional values of germinated linseed and sunflower seed oil. *Food Chemistry*, *454*, 139790. https://doi.org/10.1016/j.foodchem.2024.139790

Popeijus, H. E., Van Otterdijk, S. D., Van Der Krieken, S. E., Konings, M., Serbonij, K., Plat, J., & Mensink, R. P. (2014). Fatty acid chain length and saturation influences PPARα transcriptional activation and repression in HepG2 cells. *Molecular Nutrition & Food Research*, *58*(12), 2342–2349. https://doi.org/10.1002/mnfr.201400314

Prescha, A., Grajzer, M., Dedyk, M., & Grajeta, H. (2014). The Antioxidant Activity and Oxidative Stability of Cold-Pressed Oils. *Journal of the American Oil Chemists' Society*, *91*(8), 1291–1301. https://doi.org/10.1007/s11746-014-2479-1

Rett, B. S., & Whelan, J. (2011). Increasing dietary linoleic acid does not increase tissue arachidonic acid content in adults consuming Western-type diets: A systematic review. *Nutrition & Metabolism*, *8*(1), 36. https://doi.org/10.1186/1743-7075-8-36

Scafidi, S., Fiskum, G., Lindauer, S. L., Bamford, P., Shi, D., Hopkins, I., & McKenna, M. C. (2010). Metabolism of acetyl-l-carnitine for energy and neurotransmitter synthesis in the immature rat brain. *Journal of Neurochemistry*, *114*(3), 820–831. https://doi.org/10.1111/j.1471-4159.2010.06807.x

Schooneman, M. G., Vaz, F. M., Houten, S. M., & Soeters, M. R. (2013). Acylcarnitines. *Diabetes*, *62*(1), 1–8. https://doi.org/10.2337/db12-0466

Seike, M., Ashida, H., & Yamashita, Y. (2024). Dietary flaxseed oil induces production of adiponectin in visceral fat and prevents obesity in mice. *Nutrition Research*, *121*, 16–27. https://doi.org/10.1016/j.nutres.2023.11.004

Shabalina, I. G., Petrovic, N., de Jong, J. M. A., Kalinovich, A. V., Cannon, B., & Nedergaard, J. (2013). UCP1 in Brite/Beige Adipose Tissue Mitochondria Is Functionally Thermogenic. *Cell Reports*, *5*(5), 1196–1203. https://doi.org/10.1016/j.celrep.2013.10.044

Shahidi, F., & Ambigaipalan, P. (2018). Omega-3 Polyunsaturated Fatty Acids and Their Health Benefits. *Annual Review of Food Science and Technology*, *9*(1), 345–381. https://doi.org/10.1146/annurev-food-111317-095850

Shim, Y. Y., Gui, B., Arnison, P. G., Wang, Y., & Reaney, M. J. T. (2014). Flaxseed (Linum usitatissimum L.) bioactive compounds and peptide nomenclature: A review. *Trends in Food Science & Technology*, *38*(1), 5–20. https://doi.org/10.1016/j.tifs.2014.03.011

Shirouchi, B., Nagao, K., Inoue, N., Ohkubo, T., Hibino, H., & Yanagita, T. (2007). Effect of Dietary Omega 3 Phosphatidylcholine on Obesity-Related Disorders in Obese Otsuka Long-Evans

Tokushima Fatty Rats. *Journal of Agricultural and Food Chemistry*, *55*(17), 7170–7176. https://doi.org/10.1021/jf071225x

Simcox, J., Geoghegan, G., Maschek, J. A., Bensard, C. L., Pasquali, M., Miao, R., Lee, S., Jiang, L., Huck, I., Kershaw, E. E., Donato, A. J., Apte, U., Longo, N., Rutter, J., Schreiber, R., Zechner, R., Cox, J., & Villanueva, C. J. (2017). Global Analysis of Plasma Lipids Identifies Liver-Derived Acylcarnitines as a Fuel Source for Brown Fat Thermogenesis. *Cell Metabolism*, *26*(3), 509-522.e6. https://doi.org/10.1016/j.cmet.2017.08.006

Skurk, T., Alberti-Huber, C., Herder, C., & Hauner, H. (2007). Relationship between Adipocyte Size and Adipokine Expression and Secretion. *The Journal of Clinical Endocrinology & Metabolism*, *92*(3), 1023–1033. https://doi.org/10.1210/jc.2006-1055

Slotte, J. P. (2013). Biological functions of sphingomyelins. *Progress in Lipid Research*, *52*(4), 424–437. https://doi.org/10.1016/j.plipres.2013.05.001

Smith, M. (2024). Omega-3 Fatty Acids and Mitochondrial Function: Implications for Metabolic Health. *J Clin Nutr Metab 8:2.* https://doi.org/DOI: 10.35841/JCNM.1000142

Smorenburg, J. N., Hodun, K., McTavish, P. V., Wang, C., Pinheiro, M. A., Wells, K. R. D., Brunt, K. R., Nakamura, M. T., Chabowski, A., & Mutch, D. M. (2025). EPA/DHA but Not ALA Reduces Visceral Adiposity and Adipocyte Size in High Fat Diet-Induced Obese Delta-6 Desaturase Knockout Mice. *Molecular Nutrition & Food Research*, *69*(2), e202400721. https://doi.org/10.1002/mnfr.202400721

Spagou, K., Tsoukali, H., Raikos, N., Gika, H., Wilson, I. D., & Theodoridis, G. (2010). Hydrophilic interaction chromatography coupled to MS for metabonomic/metabolomic studies. *Journal of Separation Science*, *33*(6–7), 716–727. https://doi.org/10.1002/jssc.200900803

Tada, N., & Yoshida, H. (2003). Diacylglycerol on lipid metabolism: *Current Opinion in Lipidology*, *14*(1), 29–33. https://doi.org/10.1097/00041433-200302000-00006

Takić, M., Ranković, S., Girek, Z., Pavlović, S., Jovanović, P., Jovanović, V., & Šarac, I. (2024). Current Insights into the Effects of Dietary α-Linolenic Acid Focusing on Alterations of Polyunsaturated

Fatty Acid Profiles in Metabolic Syndrome. *International Journal of Molecular Sciences*, *25*(9), 4909. https://doi.org/10.3390/ijms25094909

Tang, Z., Ying, R.-F., Lv, B.-F., Yang, L.-H., Xu, Z., Yan, L.-Q., Bu, J.-Z., & Wei, Y.-S. (2021). Flaxseed oil: Extraction, health benefits and products. *Quality Assurance and Safety of Crops & Foods*, *13*(1), 1–19. https://doi.org/10.15586/qas.v13i1.783

Trayhurn, P., & Beattie, J. H. (2001). Physiological role of adipose tissue: White adipose tissue as an endocrine and secretory organ. *Proceedings of the Nutrition Society*, *60*(3), 329–339. https://doi.org/10.1079/PNS200194

Trefts, E., Gannon, M., & Wasserman, D. H. (2017). The liver. *Current Biology*, *27*(21), R1147–R1151. https://doi.org/10.1016/j.cub.2017.09.019

Tsuji, A. (2005). Small molecular drug transfer across the blood-brain barrier via carrier-mediated transport systems. *NeuroRX*, *2*(1), 54–62. https://doi.org/10.1602/neurorx.2.1.54

Universidad de Barcelona. (2016). Omega-3 fatty acids stimulate brown adipose tissue metabolism. *Science daily*. www.sciencedaily.com/releases/2016/11/161121112311.htm

Valsecchi, M., Mauri, L., Casellato, R., Prioni, S., Loberto, N., Prinetti, A., Chigorno, V., & Sonnino, S. (2007). Ceramide and sphingomyelin species of fibroblasts and neurons in culture. *Journal of Lipid Research*, *48*(2), 417–424. https://doi.org/10.1194/jlr.M600344-JLR200

Van Meer, G., Voelker, D. R., & Feigenson, G. W. (2008). Membrane lipids: Where they are and how they behave. *Nature Reviews Molecular Cell Biology*, *9*(2), 112–124. https://doi.org/10.1038/nrm2330

Vanella, A., Russo, A., Acquaviva, R., Campisi, A., Di Giacomo, C., Sorrenti, V., & Barcellona, M. L. (2000). L-Propionyl-carnitine as superoxide scavenger, antioxidant, and DNA cleavage protector. *Cell Biology and Toxicology*, *16*(2), 99–104. https://doi.org/10.1023/A:1007638025856

Verrier, E., Wang, L., Wadham, C., Albanese, N., Hahn, C., Gamble, J. R., Chatterjee, V. K. K., Vadas, M. A., & Xia, P. (2004). PPARγ Agonists Ameliorate Endothelial Cell Activation via Inhibition of

Diacylglycerol–Protein Kinase C Signaling Pathway: Role of Diacylglycerol Kinase. *Circulation Research*, *94*(11), 1515–1522. https://doi.org/10.1161/01.RES.0000130527.92537.06

Wang, M., Zhang, X.-J., Feng, K., He, C., Li, P., Hu, Y.-J., Su, H., & Wan, J.-B. (2016). Dietary α-linolenic acid-rich flaxseed oil prevents against alcoholic hepatic steatosis via ameliorating lipid homeostasis at adipose tissue-liver axis in mice. *Scientific Reports*, *6*(1). https://doi.org/10.1038/srep26826

Wiseman, L. R., & Brogden, R. N. (1998). Propionyl-L-Carnitine: *Drugs & Aging*, *12*(3), 243–248. https://doi.org/10.2165/00002512-199812030-00006

Wronska, A., & Kmiec, Z. (2012). Structural and biochemical characteristics of various white adipose tissue depots. *Acta Physiologica*, *205*(2), 194–208. https://doi.org/10.1111/j.1748-1716.2012.02409.x

Xia, T., Mostafa, N., Bhat, B. G., Florant, G. L., & Coleman, R. A. (1993). Selective retention of essential fatty acids: The role of hepatic monoacylglycerol acyltransferase. *American Journal of Physiology-Regulatory, Integrative and Comparative Physiology*, *265*(2), R414–R419. https://doi.org/10.1152/ajpregu.1993.265.2.R414

Xu, C., & Shanklin, J. (2016). Triacylglycerol Metabolism, Function, and Accumulation in Plant Vegetative Tissues. *Annual Review of Plant Biology*, *67*(1), 179–206. https://doi.org/10.1146/annurev-arplant-043015-111641

Xu, E., Chen, C., Fu, J., Zhu, L., Shu, J., Jin, M., Wang, Y., & Zong, X. (2021). Dietary fatty acids in gut health: Absorption, metabolism and function. *Animal Nutrition*, *7*(4), 1337–1344. https://doi.org/10.1016/j.aninu.2021.09.010

Yang, J., Wen, C., Duan, Y., Deng, Q., Peng, D., Zhang, H., & Ma, H. (2021). The composition, extraction, analysis, bioactivities, bioavailability and applications in food system of flaxseed (Linum usitatissimum L.) oil: A review. *Trends in Food Science & Technology*, *118*, 252–260. https://doi.org/10.1016/j.tifs.2021.09.025

Yang, K., & Han, X. (2016). Lipidomics: Techniques, Applications, and Outcomes Related to Biomedical Sciences. *Trends in Biochemical Sciences*, *41*(11), 954–969. https://doi.org/10.1016/j.tibs.2016.08.010

Yen, C.-L. E., Stone, S. J., Koliwad, S., Harris, C., & Farese, R. V. (2008). Thematic review series: Glycerolipids. DGAT enzymes and triacylglycerol biosynthesis. *Journal of Lipid Research*, *49*(11), 2283–2301. https://doi.org/10.1194/jlr.R800018-JLR200

Yoon, H., Shaw, J. L., Haigis, M. C., & Greka, A. (2021). Lipid metabolism in sickness and in health: Emerging regulators of lipotoxicity. *Molecular Cell*, *81*(18), 3708–3730. https://doi.org/10.1016/j.molcel.2021.08.027

Yu, X., Deng, Q., Tang, Y., Xiao, L., Liu, L., Yao, P., Tang, H., & Dong, X. (2018). Flaxseed Oil Attenuates Hepatic Steatosis and Insulin Resistance in Mice by Rescuing the Adaption to ER Stress. *Journal of Agricultural and Food Chemistry*, *66*(41), 10729–10740. https://doi.org/10.1021/acs.jafc.8b03906

Yu, X. X., Lewin, D. A., Forrest, W., & Adams, S. H. (2002). Cold elicits the simultaneous induction of fatty acid synthesis and β-oxidation in murine brown adipose tissue: Prediction from differential gene expression and confirmation in vivo. *The FASEB Journal*, *16*(2), 155–168. https://doi.org/10.1096/fj.01-0568com

Zaima, N., Hayasaka, T., Goto-Inoue, N., & Setou, M. (2010). Matrix-assisted laser desorption/ionization imaging mass spectrometry. *International Journal of Molecular Sciences*, *11*(12), 5040–5055. https://doi.org/10.3390/ijms11125040

Zhang, X., Zhang, Y., Sun, P., Su, W., Qu, Z., Dong, Y., Du, S., & Yu, X. (2023). Effect of germination pretreatment on the physicochemical properties and lipid concomitants of flaxseed oil. *RSC Advances*, *13*(5), 3306–3316. https://doi.org/10.1039/D2RA07458C

Zhao, Y., Zhao, H., Li, L., Yu, S., Liu, M., & Jiang, L. (2024). Ceramide on the road to insulin resistance and immunometabolic disorders in transition dairy cows: Driver or passenger? *Frontiers in Immunology*, *14*, 1321597. https://doi.org/10.3389/fimmu.2023.1321597

Zhao, Y.-Y., Wu, S.-P., Liu, S., Zhang, Y., & Lin, R.-C. (2014). Ultra-performance liquid chromatography–mass spectrometry as a sensitive and powerful technology in lipidomic applications. *Chemico-Biological Interactions*, *220*, 181–192. https://doi.org/10.1016/j.cbi.2014.06.029

Zhou, J., Hou, H.-T., Song, Y., Zhou, X.-L., Chen, H.-X., Zhang, L.-L., Xue, H.-M., Yang, Q., & He, G.-W. (2024). Metabolomics Analysis Identifies Differential Metabolites as Biomarkers for Acute Myocardial Infarction. *Biomolecules*, *14*(5), 532. https://doi.org/10.3390/biom14050532

9 Appendix

Table 8: Feature overview and most abundant matched metabolites

ID	m/z	RT	Area	Frag. scans	Frag. m/z	Spectral match	Cosine similarity	Adduct
14639	204.1238	4.57	1.3E6	34	60.0806 / 85.0286	Acetylcarnitine - 40.0 eV	0.883	M+H
15938	204.1227	5.00	1.3E6	2		Acetylcarnitine - 70.00 eV	0.954	M+H
13566	160.1330	3.83	4.1E5	14	55.0539 / 60.0808 / 101.0602	L-CARNITINE	0.828	M+H
9392	260.1870	1.84	2.7E5	8	85.0284 / 145.0496	Hexanoyl-L-Carnitine	0.860	[M+H]+
9	162.1121	0.24	9.3E4	8		(R)-carnitine	0.899	2M-2H+Na
93	162.1125	0.26	3.5E4	2	60.0801 / 162.1117 / 85.0282	Carnitine	0.957	2M-2H+Na
18359	248.1130	7.00	3.3E4	22	60.0811 / 85.0285 / 248.1151	O-malonylcarnitine	0.752	[M+H]+
93	162.1125	0.26	3.4E4	2	60.0805 / 85.0283 / 103.0385	(-) -L-Carnitine - 40.0 eV	0.961	M+H
13169	232.1540	3.38	2.8E4	14	85.0282 / 173.0809	LAUROYLCARNITINE	0.888	M+H
12565	146.1176	2.94	2.5E4	10	87.0443 / 60.0807	DEOXYCARNITINE	0.885	[M+H]+
13645	218.1384	3.91	2.2E4	10	85.0283	PROPIONYLCARNITINE	0.912	[M+H]+
21191	104.1068	10.91	2.4E6	4	60.0805 / 104.1069	Choline	0.854	M+H
763	280.2635	0.61	6.5E4	14	69.0697 / 109.1006 / 83.0853	Roccellaric acid	0.844	M+H
857	256.2632	0.86	4.5E4	16	256.2634	Palmitamide	0.748	M+H
51	118.0861	0.25	3.1E4	6	58.0649 / 59.0726 / 118.0858	Betaine	0.934	M+H
3110	567.5819	3.02	1.8E4	8	284.2948	Octadecanamide	0.796	M+H
219	123.0552	0.28	1.5E4	2	80.0494 / 123.0556	NICOTINAMIDE	0.944	[M+H]+
3806	388.3421	5.02	1.1E4	2	71.0852 / 129.0545	Hexanedioic acid, bis(2-ethylhexyl) ester	0.892	M+H
3887	675.6763	5.08	1.0E4	2	338.3419	13-Docosenamide	0.814	2M+H
134	288.2896	1.46	1.0E4	4	288.2897 /106.0857	Lauryldiethanolamine|2-[dodecyl(2-hydroxyethyl)amino]ethanol	0.806	M+H
2704	511.5195	1.00	7.2E3	2	256.2630	Amylamine-C11:0	0.749	2M+H

Table 9: Feature overview and most abundant matched lipid classes

ID	m/z	RT	Area	Frag. scans	Frag. m/z	Spectral match	Cosine similarity	Adduct
13948	846.7606	6.94	7.8E6	10	549.4879 / 575.5024 / 573.4876	TG(16:0/16:1/18:2)	0.755	M+NH4
14858	876.8031	7.10	7.2E5	12	577.5191 / 603.5351	TG(16:0/18:1/18:1)	0.751	M+NH4
5937	902.8181	7.09	7.0E5	8	603.5356	TG(18:1/18:1/18:1)	0.806	M+NH4
5848	900.8026	7.05	6.0E5	8	601.5170 / 900.7980 / 603.5327	TG(18:1/18:1/18:2)	0.780	M+NH4
5428	874.7871	7.06	5.7E5	8	601.5192 / 575.5018 / 577.5179	TG(16:1/18:1/18:1)	0.817	M+NH4
6198	906.8475	7.30	5.0E5	12	605.5463 / 607.5629	TG(18:0/18:0/18:1)	0.785	M+NH4
2760	786.6011	6.01	4.6E5	6	184.0729 / 786.5987	1-Palmitoyl-2-myristoyl-sn-glycero-3-PC	0.962	M+H
14852	524.3712	4.69	4.0E5	12	104.1070 / 184.0731 / 524.3685	Lyso-PC (16:0)	0.867	M+H
2671	730.5384	5.54	3.7E5	4	184.0739	1-(9Z-Octadecenoyl)-2-tetradecanoyl-sn-glycero-3-phosphocholine	0.955	M+H
7145	788.6170	6.11	3.4E5	8	184.0731 / 788.6154	1-Hexadecanoyl-2-octadecadienoyl-sn-glycero-3-phosphocholine	0.888	
4880	848.7731	6.99	3.2E5	8	575.5048 / 848.7692 / 549.4886	2-((heptadec-9-enoyl)oxy)-3-(palmitoyloxy) propyl octadec-11-enoate	0.838	M+H
2394	806.5712	5.73	3.0E5	8	184.0731 / 806.5687	Palmitoyl sphingomyelin	0.937	M+H
14532	868.7539	6.78	3.0E5	4	573.4949 / 597.4944 / 868.7942	TG(16:1/18:2/18:3)	0.732	M+NH4
3146	740.5231	5.66	2.9E5	2	71.0851 / 313.2739 / 599.5074	1-Octadecanoyl-2-(5Z,8Z,11Z,14Z-eicosatetraenoyl)-sn-glycero-3-	0.828	M+H

						phosphoethanolamine		
16200	904.8290	7.27	2.8E5	4	605.5468 / 904.8242 / 603.5310	TAG (16:0/18:1/20:1)/TAG (18:0/18:1/18:1)	0.800	M+NH4
14300	822.7556	6.99	2.4E5	6	523.4692 / 549.4871 / 577.5158	TG(16:0_16:0_16:1) - 2.3-bis(hexadecanoyloxy)propyl-hexadec-9-enoate	0.799	M+NH4
11683	756.5537	2.60	2.4E5	8	184.0728 / 756.5520	1,2-dioleoyl-sn-glycero-3-PC	0.928	M+H
942	563.5515	1.23	2.4E5	56	282.2789	cis-Vaccenic acid	0.798	M+H
5926	850.7889	7.07	2.4E5	8	577.5212 / 551.5065	TAG (16:0/16:0/18:1)	0.882	M+NH4
6580	962.9102	7.55	2.3E5	2	577.5192 / 663.6261 / 689.6449	3-(heptadecanoyloxy)-2-(stearoyloxy)propyl oleate	0.812	M+H
4417	682.5991	6.53	2.1E5	6	383.3145 / 409.3302 / 577.5177	1-(hexadecanoyloxy)-3-hydroxypropan-2-yl-octadec-9-enoate	0.849	M+H
5717	898.7902	6.96	1.9E5	4	599.5057 / 603.5355 / 601.5199	TG(18:1/18:2/18:2)	0.773	M+NH4
646	522.3553	0.46	1.4E5	16	184.0742 / 522.3560	PAF C-16	0.875	M+H
5229	733.5573	5.77	1.1E5	4	184.0731 / 733.5566	1-Myristoyl-2-palmitoyl-sn-glycero-3-phosphocholine	0.892	M+H
11660	757.5567	3.82	1.1E5	4	86.0965 / 184.0735	1,2-Dipalmitoleoyl-sn-glycero-3-phosphocholine	0.863	M+H
8438	608.5260	6.12	1.1E5	4	601.5192 / 575.5018 / 577.5179	DAG (16:0/18:3)	0.817	M+NH4
9802	636.5569	6.25	1.0E5	4	337.2746 / 339.2905 / 601.5205	1-Linoleoyl-2-oleoyl-rac-glycerol	0.731	M+H
4157	832.5839	2.30	9.6E4	6	184.0730 / 832.5806	1-Octadecanoyl-2-octadecenoyl-sn-glycero-3-phosphocholine	0.886	M+H
3019	904.5909	5.72	9.5E4	4	627.5333	L-a-phosphatidyli	0.832	M+H

						nositol (18:2/16:0)		
17371	932.8629	7.33	9.0E4	6	633.5830 / 603.5349 / 932.8678	TG(18:1/18:1/20:0)	0.728	M+NH4
2654	834.6009	5.9	8.8E4	4	184.0733 / 834. 5993	Palmitoyleicosapentaenoyl phosphatidylcholine	0.966	M+H
14211	764.6878	6.73	7.9E4	2	491.4145 / 467.4134 / 575.5114	TG(12:0/14:0/18:2)	0.744	M+NH4
3900	813.6845	6.20	7.6E4	2	184.0735 / 813.6817	SM(d18:1/24:1)	0.834	[M+H]+
5883	888.8037	7.05	7.5E4	2	589.5175 / 888.7994 / 591.5358	TG(17:1/18:1/18:1)	0.777	M+NH4
2875	762.6008	6.07	7.1E4	4	184.0741	1-Oleoyl-2-palmitoyl-sn-glycero-3-phosphocholine	0.950	M+H
6511	809.5885	5.79	7.0E4	2	184.0730 / 760.5833	PC(P-16:0/20:5)	0.902	M+H
2952	814.6323	6.12	6.9E4	6	184.0740 / 785. 5894	1-Stearoyl-2-linoleoyl-sn-glycero-3-phosphocholine	0.929	M+H
5866	934.8787	7.44	6.6E4	6	577.5203 / 633.5822 / 635.5966	TG(18:0/18:1/20:0)	0.779	M+NH4
2510	809.6867	5.80	6.3E4	2	184.0737 / 809.5898	PC(16:0/16:0)	0.805	M+H
3602	454.2922	1.72	6.2E4	4	62.0595 / 313.2746	1-Palmitoyl-2-hydroxy-sn-glycero-3-phosphoethanolamine	0.885	M+H
3217	731.6052	5.86	5.7E4	4	184.0721	1-Hexadecyl-2-(9Z-octadecenoyl)-sn-glycero-3-phosphocholine	0.959	M+H
3527	752.5585	6.08	5.4E4	4	361.2749 / 392.2911	PE(P-18:0/20:4)	0.731	M+H
5565	892.9276	7.27	5.2E4	2	591.5335 / 577.5177 / 605.5464	TG(17:0/18:0/18:1)	0.798	M+NH4
5872	960.8646	7.44	4.9E4	6	661.6143 / 603.5321 / 603.5407	TG(18:1/18:1/22:0)	0.722	M+NH4
3560	728.5591	6.11	4.2E4	4	337.2727 / 392.2912	PE(P-18:0/18:2	0.766	M+H
3187	716.5212	5.85	2.8E4	2	575.5021 / 716.5226	1-Hexadecanoyl-2-(9Z-octadecenoyl)	0.875	M+H

						-sn-glycero-3-phosphoethanolamine		
3650	634.5405	6.13	2.7E4	2	339.2891 / 599.5007 / 335.2552	DAG (18:1/18:3)/ DAG (18:2/18:2)	0.753	M+NH4
1203	310.3107	3.89	2.6E4	8	57.0692 / 83.0851 / 97.1008	cis-13-Eicosenoic acid	0.724	M+H
5805	864.8334	7.40	2.1E4	2	383.3158 / 551.5046	2,3-di(hexadecanoyloxy)propyl-octadec-9-enoate	0.748	M+H
6952	582.5091	6.09	1.9E4	2	337.2719 / 285.2422 / 547.4683	DAG (14:0/18:2)	0.762	M+H
4909	650.6440	6.55	1.9E4	2	264.2670 / 632.6336	Ceramide (18:1/16:0)	0.877	M+H
2542	268.2634	0.76	1.6E4	4	69.0700 / 83.0852 / 100.0757	Methyl hexadec-9-enoate	0.746	M+H
3477	338.3417	5.12	1.4E4	4	69.0698 / 114.0905 / 57.0694	16-Hydroxyhexadecanoic acid	0.803	M+H
2189	520.3388	5.12	1.3E4	12	184.0742 / 104.1068 / 520.3391	1-Stearoyl-2-myristoyl-sn-glycero-3-phosphocholine	0.874	M+H
2383	778.5380	5.27	1.0E4	2	184.0736 / 778.5364	1-Hexadecanoyl-2-(9Z-octadecenoyl)-sn-glycero-3-phosphocholine	0.939	M+H
4662	701.5590	5.43	1.0E4	4	184.0732 / 701.5526	Sphingomyelin	0.845	M+H
3887	675.6763	5.08	1.0E4	2	338.3419	13-Docosenamide	0.814	2M+H
2530	754.5376	5.43	8.3E3	2	184.0732 / 754.5377	Arachidonoylthio-PC	0.878	M+H
2875	282.2797	1.11	1.3E6	78	57.0697 / 69.0699	Elaidic acid	0.775	M+H

Table 10: Tissue masses of BAT, WAT and liver / 25.9

25.09	Liver	WAT	BAT
705	28.5 mg	24.1 mg	14.9 + 25.0 mg
727	26.2 mg	23.3 mg	10.4 + 16.5 mg
728	29.4 mg	26.9 mg	20.0 mg
729	27.0 mg	24.7 mg	11.6 + 5.1 mg
730	27.6 mg	23.5 mg	14.4 mg
731	26.8 mg	29.9 mg	8.0 mg
732	28.1 mg	30.8 mg	23.5 mg
733	26.0 mg	25.0 mg	11.0 mg
734	27.2 mg	22.3 mg	14.3 mg
735	28.3 mg	28.6 mg	22.9 mg
745	25.9 mg	30.0 mg	23.0 mg
752	24.5 mg	29.6 mg	12.5 + 5.5 mg
753	22.4 mg	24.8 mg	10.7 mg
765	29.1 mg	26.4 mg	19.5 + 9.8 mg
766	20.2 mg	27.9 mg	9.6 mg
767	21.8 mg	29.0 mg	10.2 + 11.6 mg
768	21.5 mg	25.0 mg	9.4 + 5.7 mg
817	27.9 mg	27.3 mg	10.7 mg
818	28.4 mg	31.5 mg	8.1 mg
832	23.8 mg		9.6 + 4.8 mg
833	24.0 mg	25.4 mg	13.2 mg
834	21.2 mg	12.4 mg	24.0 mg

Table 11:Tissue masses of BAT, WAT and liver / 26.9

26.09	Liver	WAT	BAT
706	25.2 mg	22.8 mg	26.4 mg
717	23.8 mg	23.6 mg	29.2 mg
718			
719	22.4 mg	26.8 mg	17.9 + 19.2 mg
720	24.2 mg	22.2 mg	25.3 mg
758	28.3 mg	27.0 mg	19.2 + 16.2 mg
759	35.7 mg	33.7 mg	21.2 mg
760	20.7 mg	26.3 mg	20.1 mg
761	21.3 mg	22.0 mg	16.5 + 22.0 mg
778	33.1 mg	23.9 mg	20.0 mg
779	20.3 mg	29.2 mg	9.7 mg
780	20.1 mg	23.7 mg	13.5 mg
781	25.9 mg	25.7 mg	18.5 mg
782	31.8 mg	22.5 mg	10.5 + 11.8 mg
783	22.5 mg	28.4 mg	10.6 mg
790	25.1 mg	21.9 mg	8.6 mg
791	25.5 mg	24.3 mg	14.1 mg
792	31.6 mg	25.5 mg	21.6 mg
793	23.3 mg	29.0 mg	9.7 mg
800	24.9 mg	23.2 mg	13.2 mg
801	23.7 mg	28.1 mg	14.8 mg
819	27.1 mg	27.5 mg	12.0 mg

Table 12: Tissue masses of BAT, WAT and liver / 28.9

28.09	Liver	WAT	BAT
653	25.0 mg	31.3 mg	8.9 + 18.8 mg
654	31.8 mg	31.0 mg	23.3 mg
670	21.1 mg	32.0 mg	15.4 mg
671	23.3 mg	26.4 mg	10.5 + 11.5 mg
692	36.5 mg	20.4 mg	28.0 mg
693	29.7 mg	26.0 mg	12.7 mg
694	26.8 mg	29.0 mg	26.2 mg
794	23.2 mg	20.5 mg	15.7 + 4.0 mg
795	21.8 mg	28.0 mg	24.1 mg
796	20.8 mg	28.8 mg	15.4 + 8.6 mg
802	21.0 mg	28.4 mg	17.7 mg
803	30.7 mg	27.1 mg	17.7 mg
804	27.5 mg	24.9 mg	22.3 mg
809	25.5 mg	24.3 mg	15.8 + 9.5 mg
810	22.4 mg	29.8 mg	20.5 mg
811	24.2 mg	21.8 mg	13.8 + 6.5 mg
812	28.7 mg	32.0 mg	15.9 mg
841	27.7 mg	28.0 mg	12.7 mg
842	27.8 mg	32.5 mg	6.2 mg
843	24.3 mg	29.0 mg	12.2 mg
844	22.7 mg	23.7 mg	13.2 + 4.0 mg
845	22.1 mg	27.8 mg	7.1 mg

Table 13: MRM Transition List for Targeted Analysis (Organic)

Molecule Name	Precursor m/z	Product m/z	Product charge	Precursor Charge	Product adduct
1,2-dioleoyl-sn-glycero-3-phosphatidylcholine	756.60	184.1000	1	1	[M+H]+
1,2-dioleoyl-sn-glycero-3-phosphatidylcholine	756.60	756.6000	1	1	[M+H]+
1,2-Dipalmitoleoyl-sn-glycero-3-ph	757.60	86.1000	1	1	[M+H]+
1,2-Dipalmitoleoyl-sn-glycero-3-ph	757.60	184.1000	1	1	[M+H]+

13-Docosenamide	675.70	338.3000	1	1	[M+H]+
15:0:18:1 (d7) PE	710.559	710.559	1	1	[M+H]+
15:0-18:1 (d7) DAG	587.551	587.551	1	1	[M+H]+
15:0-18:1 (d7) PA	689.499	689.499	1	1	[M+H]+
15:0-18:1 (d7) PC	752.606	752.606	1	1	[M+H]+
15:0-18:1 (d7) PG	763.536	763.536	1	1	[M+H]+
15:0-18:1 (d7) PI	846.596	846.596	1	1	[M+H]+
15:0-18:1 (d7) PS	776.531	776.531	1	1	[M+H]+
15:0-18:1 (d7) TAG	811.765	811.765	1	1	[M+H]+
16-Hydroxyhexadecanoic acid	16.00	69.1000	1	1	[M+H]+
16-Hydroxyhexadecanoic acid	338.30	114.1000	1	1	[M+H]+
16-Hydroxyhexadecanoic acid	338.30	57.1000	1	1	[M+H]+
18:1-(d7) Cholesterolester	657.644	657.644	1	1	[M+H]+
18:1-(d7) Lyso PC	528.392	528.392	1	1	[M+H]+
18:1-(d7) Lyso PE	486.345	486.345	1	1	[M+H]+
1-9Z-Octadecenoyl-2-tetradecanoyl-sn-glycero-3-phopshocholine	730.50	184.1000	1	1	[M+H]+
1-Hexadecanoyl-2-9Z-octadecenoyl-sn-glycero-3-phosphocholine	778.50	184.1000	1	1	[M+H]+
1-Hexadecanoyl-2-9Z-octadecenoyl-sn-glycero-3-phosphocholine	778.50	778.5000	1	1	[M+H]+
1-Hexadecanoyl-2-9Z-octadecenoyl-sn-glycero-3-phosphoethanolamine	716.50	575.5000	1	1	[M+H]+
1-Hexadecanoyl-2-octadecadienoyl-sn-glycero-3-Phosphocholine	788.60	184.1000	1	1	[M+H]+
1-Hexadecanoyl-2-octadecadienoyl-sn-glycero-3-Phosphocholine	788.60	788.6000	1	1	[M+H]+
1-hexadecanoyloxy-3-hydroxypropan-2-yl-octadec-9-enoate	682.60	383.3000	1	1	[M+H]+

1-hexadecanoyloxy-3-hydroxypropan-2-yl-octadec-9-enoate	682.60	409.3000	1	1	[M+H]+
1-hexadecanoyloxy-3-hydroxypropan-2-yl-octadec-9-enoate	682.60	577.5000	1	1	[M+H]+
1-Hexadecyl-2-9Z-octadecenoyl-sn-glycero-3-phosphocholine	731.60	184.1000	1	1	[M+H]+
1-Linoleoyl-2-oleoyl-rac-glycerol	636.60	337.3000	1	1	[M+H]+
1-Linoleoyl-2-oleoyl-rac-glycerol	636.60	339.3000	1	1	[M+H]+
1-Linoleoyl-2-oleoyl-rac-glycerol	636.60	601.5000	1	1	[M+H]+
1-Myristoyl-2-palmitoyl-sn-glycero-3	733.60	184.1000	1	1	[M+H]+
1-Myristoyl-2-palmitoyl-sn-glycero-3	733.60	733.5000	1	1	[M+H]+
1-Octadecanoyl-2-5Z,8Z,11Z,14Z-eicosatetraenoyl-sn-glycero-3-phosphoethanolamine	740.50	71.1000	1	1	[M+H]+
1-Octadecanoyl-2-5Z,8Z,11Z,14Z-eicosatetraenoyl-sn-glycero-3-phosphoethanolamine	740.50	313.3000	1	1	[M+H]+
1-Octadecanoyl-2-5Z,8Z,11Z,14Z-eicosatetraenoyl-sn-glycero-3-phosphoethanolamine	740.50	599.5000	1	1	[M+H]+
1-Octadecanoyl-2-octadecenoyl-sn-glycero-3-phosphocholine	832.60	184.1000	1	1	[M+H]+
1-Octadecanoyl-2-octadecenoyl-sn-glycero-3-phosphocholine	832.60	832.6000	1	1	[M+H]+
1-Oleoyl-2-palmitoyl-sn-glycero-3-phosphocholine	762.60	184.1000	1	1	[M+H]+
1-Palmitoyl-2-hydrox-sn-glycero-	454.30	62.1000	1	1	[M+H]+
1-Palmitoyl-2-hydrox-sn-glycero-	454.30	313.3000	1	1	[M+H]+

1-Palmitoyl-2-myristoyl-sn-glycero-3-phopshocholine	786.60	184.1000	1	1	[M+H]+
1-Palmitoyl-2-myristoyl-sn-glycero-3-phopshocholine	786.60	786.5000	1	1	[M+H]+
1-Stearoyl-2-linoleoyl-sn-glycero-3-phosphocholine	814.60	184.1000	1	1	[M+H]+
1-Stearoyl-2-linoleoyl-sn-glycero-3-phosphocholine	814.60	785.6000	1	1	[M+H]+
1-Stearoyl-2-myristoyl-sn-glycero-3-phosphocholine	520.30	184.1000	1	1	[M+H]+
1-Stearoyl-2-myristoyl-sn-glycero-3-phosphocholine	520.30	104.1000	1	1	[M+H]+
2,3-di-hexadecanoyloxy-propyl-octadec-9-enoate	864.90	383.3000	1	1	[M+H]+
2,3-di-hexadecanoyloxy-propyl-octadec-9-enoate	864.90	551.5000	1	1	[M+H]+
2-heptadec-9-enoyl-oxy-3-palmitoyloxy-propyl-octadec-11-enoate	848.80	575.5000	1	1	[M+H]+
2-heptadec-9-enoyl-oxy-3-palmitoyloxy-propyl-octadec-11-enoate	848.80	848.8000	1	1	[M+H]+
2-heptadec-9-enoyl-oxy-3-palmitoyloxy-propyl-octadec-11-enoate	848.80	549.5000	1	1	[M+H]+
3-heptadecanoyloxy-2-stearoyloxy-propyl-oleate	962.90	577.5000	1	1	[M+H]+
3-heptadecanoyloxy-2-stearoyloxy-propyl-oleate	962.90	663.6000	1	1	[M+H]+
3-heptadecanoyloxy-2-stearoyloxy-propyl-oleate	962.90	689.6000	1	1	[M+H]+
Amylamine-C11:0	511.50	256.3000	1	1	[M+H]+
Arachidonoylthio-PC	754.50	184.1000	1	1	[M+H]+
Betaine	118.10	58.1000	1	1	[M+H]+
Betaine	118.10	59.1000	1	1	[M+H]+
Betaine	118.10	118.0000	1	1	[M+H]+
C18 (PLASMA) - 18:1 (d9) PC	780.670	780.670	1	1	[M+H]+
C18 (PLASMA) - 18:1 (d9) PE	738.620	738.620	1	1	[M+H]+

Ceramide_18:1/16:0	650.60	264.2000	1	1	[M+H]+
Ceramide_18:1/16:0	650.60	632.6000	1	1	[M+H]+
Choline	104.10	60.1000	1	1	[M+H]+
Choline	104.10	104.1000	1	1	[M+H]+
cis-13-Eicosenoic acid	310.30	57.1000	1	1	[M+H]+
cis-13-Eicosenoic acid	310.30	83.1000	1	1	[M+H]+
cis-13-Eicosenoic acid	310.30	97.1000	1	1	[M+H]+
cis-Vaccenic acid	563.60	282.3000	1	1	[M+H]+
d18:1-18:1 (d9) SM	737.640	737.640	1	1	[M+H]+
DAG_14:0/18:2	582.50	337.3000	1	1	[M+H]+
DAG_14:0/18:2	582.50	285.2000	1	1	[M+H]+
DAG_14:0/18:2	582.50	547.5000	1	1	[M+H]+
DAG_16:0/18:3	608.50	601.5000	1	1	[M+H]+
DAG_16:0/18:3	608.50	575.5000	1	1	[M+H]+
DAG_16:0/18:3	608.50	577.5000	1	1	[M+H]+
DAG_18:1/18:3	634.50	339.3000	1	1	[M+H]+
DAG_18:1/18:3	634.50	599.5000	1	1	[M+H]+
DAG_18:1/18:3	634.50	335.3000	1	1	[M+H]+
Elaidic acid	282.30	57.1000	1	1	[M+H]+
Elaidic acid	282.30	69.1000	1	1	[M+H]+
Hexanedioic acid,bis-2-ethylhexyl-ester	388.30	71.1000	1	1	[M+H]+
Hexanedioic acid,bis-2-ethylhexyl-ester	388.30	129.1000	1	1	[M+H]+
L-a-phosphatidylinositol_18:2/16:0	904.60	627.5000	1	1	[M+H]+
Lauryldiethanolamine	288.30	288.2000	1	1	[M+H]+
Lauryldiethanolamine	288.30	106.1000	1	1	[M+H]+
LysoPC_16:0	554.35	255.2330	1	1	[M+H]+
LysoPC_16:0	524.40	104.1000	1	1	[M+H]+
LysoPC_16:0	524.40	184.1000	1	1	[M+H]+
LysoPC_16:0	524.40	524.4000	1	1	[M+H]+
LysoPC_18:0	582.38	283.2640	1	1	[M+H]+
LysoPC_18:2	578.35	279.2330	1	1	[M+H]+
LysoPE_16:0	452.28	255.2330	1	1	[M+H]+
LysoPE_20:4	500.28	303.2330	1	1	[M+H]+
Methyl-hexadec-9-enoate	268.30	69.1000	1	1	[M+H]+
Methyl-hexadec-9-enoate	268.30	83.1000	1	1	[M+H]+
Methyl-hexadec-9-enoate	268.30	100.1000	1	1	[M+H]+
Nicotinamide	123.10	80.0000	1	1	[M+H]+
Nicotinamide	123.10	123.0000	1	1	[M+H]+
Octadecanamide	567.60	284.3000	1	1	[M+H]+
PAF C-16	522.40	184.1000	1	1	[M+H]+
PAF C-16	522.40	522.4000	1	1	[M+H]+
Palmitamide	256.30	256.2000	1	1	[M+H]+
Palmitoyl sphingomyelin	806.60	184.1000	1	1	[M+H]+
Palmitoyl sphingomyelin	806.60	806.5000	1	1	[M+H]+

Palmitoyleicosapentaenoylphosphatidylcholine	834.60	184.1000	1	1	[M+H]+
Palmitoyleicosapentaenoylphosphatidylcholine	834.60	834.5000	1	1	[M+H]+
PC_16:0/16:0	809.70	184.1000	1	1	[M+H]+
PC_16:0/16:0	809.70	809.6000	1	1	[M+H]+
PC_32:0	792.58	255.2330	1	1	[M+H]+
PC_34:1	818.59	309.2800	1	1	[M+H]+
PC_34:2	816.58	307.2640	1	1	[M+H]+
PC_P-16:0/20:5	809.60	184.1000	1	1	[M+H]+
PC_P-16:0/20:5	809.60	760.6000	1	1	[M+H]+
PE_16:0/20:2	742.54	307.2640	1	1	[M+H]+
PE_18:0/18:2	742.54	279.2330	1	1	[M+H]+
PE_36:1	744.56	309.2800	1	1	[M+H]+
PE_P-18:0/18:2	728.60	337.3000	1	1	[M+H]+
PE_P-18:0/18:2	728.60	392.3000	1	1	[M+H]+
PE_P-18:0/20:4	752.60	361.3000	1	1	[M+H]+
PE_P-18:0/20:4	752.60	392.3000	1	1	[M+H]+
Roccellaric acid	280.30	69.1000	1	1	[M+H]+
Roccellaric acid	280.30	109.1000	1	1	[M+H]+
Roccellaric acid	280.30	83.1000	1	1	[M+H]+
SM_18:1/24:1	813.70	184.1000	1	1	[M+H]+
SM_18:1/24:1	813.70	813.7000	1	1	[M+H]+
SM_38:1	759.60	100.0000	1	1	[M+H]+
SM_40:1	787.70	184.1000	1	1	[M+H]+
Sphingomyelin	701.60	184.1000	1	1	[M+H]+
Sphingomyelin	701.60	701.6000	1	1	[M+H]+
TAG_16:0/16:0/18:1	850.80	577.5000	1	1	[M+H]+
TAG_16:0/16:0/18:1	850.80	551.5000	1	1	[M+H]+
TAG_16:0/18:1/20:1	904.80	605.6000	1	1	[M+H]+
TAG_16:0/18:1/20:1	904.80	904.8000	1	1	[M+H]+
TAG_16:0/18:1/20:1	904.80	603.5000	1	1	[M+H]+
TG:12:0/14:0/18:2	764.70	491.4000	1	1	[M+H]+
TG:12:0/14:0/18:2	764.70	467.4000	1	1	[M+H]+
TG:12:0/14:0/18:2	764.70	575.5000	1	1	[M+H]+
TG_16:0/16:1/18:2	846.80	549.5000	1	1	[M+H]+
TG_16:0/16:1/18:2	846.80	575.5000	1	1	[M+H]+
TG_16:0/16:1/18:2	846.80	573.5000	1	1	[M+H]+
TG_16:0/18:1/18:1	876.80	577.5000	1	1	[M+H]+
TG_16:0/18:1/18:1	876.80	603.5000	1	1	[M+H]+
TG_16:0_16:0_16:1-2.3-bis-hexadecanoyloxy-propyl-hexadec-9-enoate	822.80	523.5000	1	1	[M+H]+
TG_16:0_16:0_16:1-2.3-bis-hexadecanoyloxy-propyl-hexadec-9-enoate	822.80	549.5000	1	1	[M+H]+
TG_16:0_16:0_16:1-2.3-bis-hexadecanoyloxy-	822.80	577.5000	1	1	[M+H]+

propyl-hexadec-9-enoate					
TG_16:1/18:1/18:1	874.80	601.5000	1	1	[M+H]+
TG_16:1/18:1/18:1	874.80	575.5000	1	1	[M+H]+
TG_16:1/18:1/18:1	874.80	577.5000	1	1	[M+H]+
TG_16:1/18:2/18:3	868.80	573.5000	1	1	[M+H]+
TG_16:1/18:2/18:3	868.80	597.5000	1	1	[M+H]+
TG_16:1/18:2/18:3	868.80	868.8000	1	1	[M+H]+
TG_17:0/18:0/18:1	892.90	591.5000	1	1	[M+H]+
TG_17:0/18:0/18:1	892.90	577.5000	1	1	[M+H]+
TG_17:0/18:0/18:1	892.90	605.0000	1	1	[M+H]+
TG_17:1/18:1/18:1	888.80	589.5000	1	1	[M+H]+
TG_17:1/18:1/18:1	888.80	888.7000	1	1	[M+H]+
TG_17:1/18:1/18:1	888.80	591.5000	1	1	[M+H]+
TG_18:0/18:0/18:1	906.90	605.5000	1	1	[M+H]+
TG_18:0/18:0/18:1	906.90	607.6000	1	1	[M+H]+
TG_18:0/18:1/20:0	934.80	577.5000	1	1	[M+H]+
TG_18:0/18:1/20:0	934.80	633.6000	1	1	[M+H]+
TG_18:0/18:1/20:0	934.80	635.6000	1	1	[M+H]+
TG_18:1/18:1/18:1	902.80	603.5000	1	1	[M+H]+
TG_18:1/18:1/18:2	900.80	601.5000	1	1	[M+H]+
TG_18:1/18:1/18:2	900.80	603.5000	1	1	[M+H]+
TG_18:1/18:1/18:2	900.80	900.8000	1	1	[M+H]+
TG_18:1/18:1/20:0	932.90	633.6000	1	1	[M+H]+
TG_18:1/18:1/20:0	932.90	603.5000	1	1	[M+H]+
TG_18:1/18:1/20:0	932.90	932.9000	1	1	[M+H]+
TG_18:1/18:1/20:0	960.80	661.6000	1	1	[M+H]+
TG_18:1/18:1/20:0	960.80	603.5000	1	1	[M+H]+
TG_18:1/18:1/20:0	960.80	603.5000	1	1	[M+H]+
TG_18:1/18:2/18:2	898.80	599.5000	1	1	[M+H]+
TG_18:1/18:2/18:2	898.80	603.5000	1	1	[M+H]+
TG_18:1/18:2/18:2	898.80	601.5000	1	1	[M+H]+
TG_52:2/FA14:0	876.80	631.6000	1	1	[M+H]+
TG_52:3/FA14:0	874.80	629.6000	1	1	[M+H]+
TG_54:4/FA16:0	900.80	627.5000	1	1	[M+H]+

Table 14: MRM Transition List for Targeted Analysis (Polar)

Molecule Name	**Precursor m/z**	**Product m/z**	**Product charge**	**Precursor Charge**	**Product adduct**
12:1-Carnitine	342.30	85.1000	1	1	[M+H]+
16:1-Carnitine	398.30	85.1	1	1	[M+H]+
Acetylcarnitine	204.10	85.1000	1	1	[M+H]+
Acetylcarnitine	204.10	60.1000	1	1	[M+H]+
alpha Linoeylcarnitine	422.30	85.1000	1	1	[M+H]+
Arachidonylcarnitine	448.30	85.1000	1	1	[M+H]+
Butylcarnitine	232.20	85.1000	1	1	[M+H]+
Carnitine	162.10	85.1000	1	1	[M+H]+
Carnitine	162.10	60.1000	1	1	[M+H]+

Decadienylcarnitine	312.20	85.1000	1	1	[M+H]+
Decanylcarnitine	316.20	85.1000	1	1	[M+H]+
Decenylcarnitine	314.20	85.1000	1	1	[M+H]+
Deoxycarnitine	146.10	87.0000	1	1	[M+H]+
Deoxycarnitine	146.10	60.1000	1	1	[M+H]+
DHA-Carnitine	472.30	85.1000	1	1	[M+H]+
Dodecanoylcarnitine	344.30	85.1000	1	1	[M+H]+
Eicosapentenylcarnitine	446.30	85.1000	1	1	[M+H]+
Hexadecadienylcarnitine	396.30	85.1000	1	1	[M+H]+
Hexanoylcarnitine	260.20	85.1000	1	1	[M+H]+
Hexanoylcarnitine	260.20	145.1000	1	1	[M+H]+
Isovalerylcarnitine	246.20	85.1000	1	1	[M+H]+
ISTD d3-Acetylcarnitine	207.10	85.1000	1	1	[M+H]+
ISTD d3-Carnitine	165.10	85.1000	1	1	[M+H]+
ISTD d3-Myristoylcarnitine	375.30	85.1000	1	1	[M+H]+
ISTD d3-Oleylcarnitine	429.40	85.1000	1	1	[M+H]+
Lauroylcarnitine	232.20	85.1000	1	1	[M+H]+
Lauroylcarnitine	232.20	173.1000	1	1	[M+H]+
Linoeylcarnitine	424.30	85.1000	1	1	[M+H]+
Myristoleylcarnitine	370.30	85.1000	1	1	[M+H]+
Myristoylcarnitine	372.30	85.1000	1	1	[M+H]+
Octanoylcarnitine	288.20	85.1000	1	1	[M+H]+
Octanoylcarnitine	288.20	229.1000	1	1	[M+H]+
Octenylcarnitine	286.20	85.1000	1	1	[M+H]+
Oleylcarnitine	426.40	85.1000	1	1	[M+H]+
O-malonylcarnitine	248.10	60.1000	1	1	[M+H]+
O-malonylcarnitine	248.10	85.1000	1	1	[M+H]+
Palmityl-Carnitine	400.30	85.1000	1	1	[M+H]+
Propionylcarnitine	218.10	85.1000	1	1	[M+H]+
Stearylcarnitine	428.40	85.1000	1	1	[M+H]+
Tetradecadienylcarnitine	368.30	85.1000	1	1	[M+H]+